HELSINKI UNIVERSITY OF TECHNOLOGY
Department of Engineering Physics and Mathematics

Janne Halme

Dye-sensitized nanostructured and organic photovoltaic cells: technical review and preliminary tests

Master's thesis submitted in partial fulfillment of the requirements for the degree of Master of Science in Technology

Espoo, February 12, 2002

Supervisor: Professor Peter Lund

Instructor: Professor Peter Lund

HELSINKI UNIVERSITY OF TECHNOLOGY ABSTRACT OF MASTER'S THESIS

Department of Engineering Physics and Mathematics

Author:	Janne Halme
Department:	Department of Engineering Physics and Mathematics
Major subject:	Engineering Physics - Advanced Energy Systems
Minor subject:	Systems and operations research
Title:	Dye-sensitized nanostructured and organic photovoltaic cells: technical review and preliminary tests
Title in Finnish:	Väriaineherkistetyt nanorakenteiset ja orgaaniset aurinkosähkökennot: tekninen kirjallisuuskatsaus ja alustavia kokeita
Chair:	Tfy-56, Advanced Energy Systems
Supervisor:	Professor Peter Lund
Instructor:	Professor Peter Lund

The solar electricity is presently a rapidly growing but often relatively expensive renewable energy form. Recently however, new molecular photovoltaic (PV) materials have been developed, which could enable a production of low-cost solar cells in the future.

The thesis begins with a discussion of the current status of the PV technology and a short introduction to the different PV technologies and to the basics of photovoltaics.

The dye-sensitized solar cell (DSSC) is an electrochemical solar cell where light absorption occurs by dye molecules attached to a nanostructured TiO_2 electrode. An introduction to the DSSC is given including a short description of the operating principle of the cell and a discussion of the physical and chemical processes behind it. A systematic literature review is done on the materials and most essential preparation methods of the standard DSSC.

The performance of the DSSC is reviewed in terms of the energy conversion efficiency and the long-term stability. The important directions of development are the transition from glass substrates to plastic foils and from batch processing to continuous processing as well as the use of solid state electrolytes. The glass-based DSSC technology is on the verge of commercialization and the manufacturing cost estimates for the technology are close to the projected costs of other PV technologies.

The purely organic solar cells are discussed individually beginning with the discussion of the fundamentals of organic photovoltaics and an introduction of different types of organic photovoltaic materials including semiconducting polymers, dyes, pigments and liquid crystalline materials. A review is done on the performance results of organic solar cells categorizing the cells by their device architecture. The development of the organic PV materials is still at an early stage and no clearly outperforming materials or cell structures have yet emerged.

Experimental results are reported including a demonstration of the dye-sensitization with a natural dye as well as a preparation and testing of a series of ruthenium-dye based DSSCs. An efficiency of 0.6% at about 600 W/m^2 solar illumination was obtained for the DSSCs in outdoor measurements.

Number of pages: 115

Key words: Solar cell, dye-sensitized solar cell, organic photovoltaic materials

Department fills:

Approved: **Library code:**

TEKNILLINEN KORKEAKOULU DIPLOMITYÖN TIIVISTELMÄ

Teknillisen fysiikan ja matematiikan osasto

Tekijä:	Janne Halme
Osasto:	Teknillisen fysiikan ja matematiikan osasto
Pääaine:	Teknillinen fysiikka - Energiateknologiat
Sivuaine:	Systeemi- ja operaatiotutkimus
Työn nimi:	Väriaineherkistetyt nanorakenteiset ja orgaaniset aurinkosähkökennot: tekninen kirjallisuuskatsaus ja alustavia kokeita
Title in English:	Dye-sensitized nanostructured and organic photovoltaic cells: technical review and preliminary tests
Professuuri:	Tfy-56, Energiateknologiat
Työn valvoja:	Professori Peter Lund
Työn ohjaaja:	Professori Peter Lund

Aurinkosähkö on tällä hetkellä nopeasti kasvava mutta usein verrattain kallis uusiutuva energiamuoto. Viime aikoina on kuitenkin kehitetty uusia molekulaarisia aurinkosähkömateriaaleja, jotka voivat mahdollistaa tulevaisuudessa halpojen aurinkosähkökennojen tuotannon.

Työn alussa käsitellään aurinkosähkön nykytilaa ja luodaan lyhyt katsaus eri aurinkosähköteknologioihin ja aurinkosähkön perusteisiin.

Väriaineherkistetty aurinkokenno (väriainekenno) on valosähkökemiallinen aurinkokenno, jossa valon absorptio tapahtuu nanorakenteisen TiO_2 -elektrodin pintaan kiinnittyneiden väriainemolekyylien avulla. Työssä esitellään väriainekennon toimintaperiaate ja tarkastellaan sen taustalla olevia fysikaalisia ja kemiallisia prosesseja, sekä tehdään järjestelmällinen kirjallisuuskatsaus perusväriainekennon materiaaleihin ja tärkeimpiin valmistusmenetelmiin.

Väriainekennon suorituskykyä tarkastellaan energian konversion hyötysuhteen ja pitkäaikaisstabiilisuuden osalta. Tärkeitä kehityssuuntia ovat siirtyminen lasisubstraateista muovikalvoihin ja vaiheittaisesta valmistusprosessista jatkuvaan prosessiin sekä kiinteiden elektrolyyttien käyttö. Lasisubstraattiin perustuva väriainekennoteknologia on kaupallistumisen kynnyksellä ja sen valmistuskustannusarviot ovat lähellä muiden aurinkosähköteknologioiden kustannusennusteita.

Puhtaasti orgaanisia aurinkosähkökennoja tarkastellaan erikseen alkaen orgaanisten aurinkosähkömateriaalien fysikaalisista perusteista. Tämän jälkeen esitellään erilaiset orgaaniset aurinkosähkömateriaalit, joihin kuuluu puolijohtavia polymeerejä, väriaineita, pigmenttejä ja nestekiteisiä materiaaleja, sekä tehdään katsaus orgaanisten kennojen tuloksiin luokitellen kennot niiden rakenteen mukaan. Orgaanisten aurinkosähkömateriaalien kehitys on vielä alkuvaiheessa eikä selkeästi suorituskyvyltään muita parempia materiaaleja ja kennorakenteita ole vielä ilmennyt.

Lopuksi esitetään kokeelliset tulokset väriaineherkistyksen havainnollistamisesta luonnon väriaineella sekä ruteeni-väriaineeseen perustuvien väriainekennojen valmistuksesta ja testauksesta. Ulkomittauksissa 600 W/m^2 auringonvalossa saavutettiin väriainekennojen hyötysuhteeksi 0.6%.

Sivumäärä: 115

Avainsanat: Aurinkokenno, väriaineherkistetty aurinkokenno, orgaaniset aurinkosähkömateriaalit

Osasto täyttää:

Hyväksytty: **Kirjastotunnus:**

Table of contents

Abbreviations, symbols and synonyms

Abbreviations

A	acceptor
AM1.5	air mass 1.5
a-Si	amorphous silicon
CB	conduction band
CIGS	copper indium gallium diselenide
D	donor
DSSC	dye-sensitized solar cell
EQE	external quantum efficiency
FF	fill factor
HOMO	highest occupied molecular orbital
IPCE	incident photon to current efficiency
IR	infrared
ITO	indium tin oxide
IV	current-voltage
LUMO	lowest unoccupied molecular orbital
mc-Si	multicrystalline silicon
MIM	metal-insulator-metal
MLCT	metal to ligand charge transfer
MPP	maximum power point
PET	poly(ethylene terephalate)
PV	photovoltaic
sc-Si	single-crystal silicon
TBP	4-*tert*-butylpyridine
TCO	transparent conductive oxide
UV	ultraviolet
VB	valence band

Symbols

e^-	electron
E_f	Fermi energy
η	efficiency
hv	light quantum
I_{MPP}	current at the maximum power point
I_{SC}	short-circuit current
P_{light}	power of the incident light
P_{MAX}	power at the maximum power point
S	sensitizer
S^*	excited energy state of the sensitizer
S^+	oxidized state of the sensitizer

S^0	ground energy state of the sensitizer
V_{MPP}	voltage at the maximum power point
V_{OC}	open-circuit voltage
W_p	peak watt, the nominal power output of a solar cell (determined at the standard conditions of 1000 W/m^2 AM1.5 solar illumination at 25°C temperature)

Synonyms

counter-electrode	cathode, positive electrode
dye-sensitized solar cell	dye-sensitized nanostructured solar cell,
efficiency	energy conversion efficiency, light-to-energy conversion efficiency
	Grätzel cell, dye cell
EQE	IPCE
irradiance	light intensity (W/m^2)
multicrystalline silicon	polycrystalline silicon
nanostructured electrode	porous nanocrystalline electrode
n-type material	electron transport material
photocurrent	light-induced current
photovoltage	light-induced voltage
photovoltaic cell	solar cell
p-type material	hole transport material
spectral response	IPCE, incident photon to current efficiency

Foreword

This thesis was carried out in the Laboratory of Advanced Energy Systems, Department of Engineering Physics and Mathematics at Helsinki University of Technology. The thesis was financed by the National Technology Agency (TEKES) as a part of the project "Large surface area and 3rd generation solar cells".

I would like to thank Professor Peter Lund for giving me an interesting research topic and for supervising the thesis as well as for his guidance in selecting the guidelines for the work. I would also like to thank the Laboratory of Advanced Energy Systems for providing the facilities for carrying out this work, and especially the fantastic people in the laboratory for the pleasant working environment and their helping hand in practical problems.

Especially I would like to thank my parents for their support during my studies. The dearest and greatest thanks however belong to Noora Alakulppi for her invaluable understanding, support and encouragement during the work.

Espoo, February 2002 Janne Halme

1 Introduction

Background of the study

Solar electricity is a steadily growing energy technology today and solar cells have found markets in variety of applications ranging from consumer electronics and small scale distributed power systems to centralized megawatt scale power plants.

Direct utilization of solar radiation to produce electricity is close to an ideal way to utilize the nature's renewable energy flow. With photovoltaic cells power can be produced near the end user of the electricity, thus avoiding transmission losses and costs, and the solar panels themselves operate without noise, toxic and greenhouse gas emissions, and require very little maintenance. Furthermore, the huge theoretical potential and the very high practical potential of the solar electricity make it attractive for large-scale utilization.

Despite the significant development over the past decades the high cost of solar cells has remained a limiting factor for the implementation of the solar electricity in a large scale. The standard silicon solar cell technology has matured to a stage where costs reductions are mostly foreseen only by the economies of scale. Costs calculations of the thin film photovoltaic technologies on the other hand place them more or less in the same line with the standard silicon technology (see e.g. Frantzis et al. 2000). There is therefore a prevailing need for the development of new materials and concepts for the photovoltaic conversion, to lower the price of the solar cells.

Nanotechnology is currently a booming trend in the science and technology. It is included in the proposal for the 6th framework program 2002-2006 of the European Community for research, technological development and demonstration activities, and received 500 million dollars of public funding in 2001 in the United States[1].

The general trend of nanotechnology has recently emerged also in the field of photovoltaic energy conversion. Development of material engineering in the nanometer scale has generated new photovoltaic materials and systems that could potentially lead to realization of low-cost solar cells in the future. These materials include for example different types of synthetic organic materials and inorganic

[1] http://europa.eu.int/eur-lex/en/com/dat/2001/en_501PC0094_01.html

nanoparticles and nanoparticle systems. The solar cells based on these materials are called for example organic solar cells or molecular solar cells. In the process chemistry has emerged as a new key science alongside with physics in the development of new photovoltaic materials.

The most well known and studied unconventional photovoltaic system is the dye-sensitized nanostructured solar cell developed by Professor Grätzel in 1991. At the moment this unique photoelectrochemical solar cell based on a TiO_2 nanoparticle photoelectrode sensitized with a light-harvesting metallo-organic dye, is on the verge of commercialization offering an interesting alternative for the existing silicon based solar cells as well as for the thin film solar cells. At the same time the research activity as well as the industrial interest around the technology is growing fast.

Another group of new type of solar cells grabbing increasing industrial and research attention is the purely organic solar cells based on for example organic semiconducting polymers, macromolecules, dyes, pigments or liquid crystalline materials.

In Finland the research of molecular level photovoltaic materials has been quite inactive so far. Research directly related to the subject of this study has been carried out only in the Professor Jouko Korppi-Tommola's research group in University of Jyväskylä partly in collaboration with Åbo Akademi and University of Joensuu. Their research with the dye-sensitized solar cell has been concentrated in the electron transfer reactions of charge sensitizer dyes in the nanostructured TiO_2 electrodes (e.g. Kallioinen et al. 2001). Areas of research with some indirect point of contact to the subject of this study such as metallo-organic chemistry, nanoparticle preparation and semiconducting polymers has however been active in several individual laboratories in Finland.

Objectives of the study

The objectives of this study in the order of importance was to

1. make a comprehensive literature review on the new molecular solar cells including the dye-sensitized nanostructured and organic solar cells, their operating principles, materials, and manufacturing methods, as well as their technological status of development, and to
2. gather experimental experience on the preparation of the dye-sensitized nanostructured solar cells to evaluate the feasibility of manufacturing these solar cells in basic laboratory conditions.

The literature review was partly aimed to serve directly the experimental part of the work by generating information of the materials and preparation methods of the solar cells.

Reviews of the subject of the thesis have been published previously for example by Hagfeldt & Grätzel (1995, 2000) and Kalyanasundaram & Grätzel (1998) about the dye-sensitized nanostructured solar cells and by Wallace et al. (2000), Brabec & Sariciftci (2001c) and Brabec et al. (2001b) about the organic solar cells. The purpose of the literature review in this thesis is to be a more comprehensive and systematic survey on the subject with an emphasis on the technical issues.

Exclusions

It was decided to give an emphasis to the dye-sensitized solar cell technology in the first place. This was appropriate because on one hand the dye-sensitized solar cell was known as the most actively studied molecular solar cell technology and the one closest to commercialization and on the other hand it was chosen for the subject of the experimental part of the work. The purely organic solar cells were to be treated therefore in a less detail.

A lot of technical information can generally be found in patent documents. However, because the research field covered in this study is very large as a whole, a compilation of a patent survey was excluded from the work. Information presented in the thesis is thus based solely on scientific journals and textbooks or on the author's experience from the experimental part of the work. It must be therefore emphasized that when considering further studies on a specific subject within the research area at issue, a comprehensive patent survey is recommended.

Since the thesis is aimed to be a technical review on the subject, a rigorous theoretical treatment of the subjects was omitted. Instead an overall picture was pursued concentrating to the materials, preparation methods and technological status of the different types of solar cells discussed. This was appropriate also because the theoretical picture of the behavior of the discussed molecular solar cells is still partly incomplete.

Outline of the thesis

The thesis is arranged into ten Chapters, the first one giving an introduction to the thesis by describing the background and purpose of the study as well as the outline of the thesis.

Chapter 2 is aimed to introduce the backgrounds of the photovoltaic energy conversion to help the reader to place the primary subjects of this study into the right context. First, the present status of photovoltaics is discussed including a discussion of the possibilities for cost reductions of the solar cells. This is followed by a short introduction to the different existing photovoltaic technologies and to the principles of photovoltaic energy conversion and availability of solar electricity.

Chapter 3 introduces the dye-sensitized nanostructured solar cell beginning with a short description of the operating principle of the cell in the first part. The second part concentrates to the discussion of the fundamental physical and chemical processes of the cell operation. A qualitative discussion about the fundamental steps of photovoltaic conversion is given to help the reader to form an intuitive physical picture of the operation of the cell and issues related to it.

Chapter 4 describes the materials of the dye-sensitized nanostructured solar cell. The components of the cell are treated one by one at each time making a cut-through to the literature by examining the used materials, their key properties and the related preparation methods. This Chapter also gives the background for the experimental part of this work.

The status of the dye-sensitized solar cell technology is reviewed in Chapter 5. In the first part the performance of the cells is reviewed in terms of energy conversion efficiency and long-term stability. The second part describes progress towards applications by a discussion of the different cell and module architectures and the use of plastic substrates and solid state electrolytes in the cell, followed by a discussion of the industrial and commercial activities and the cost estimates of the dye-sensitized solar cells.

Chapter 6 concerns the purely organic solar cells. The fundamentals of organic photovoltaics are firstly discussed followed by introduction of different types of organic photovoltaic materials and their processing to solar cells. A review is made on the performance results of organic solar cells categorizing the cells by their device architecture.

The results from the experimental part of the work are presented in Chapter 7. In the first part the dye-sensitization effect is shortly demonstrated with a cell based on a natural dye and the second part describes the results from the preparation of ruthenium dye based dye-sensitized solar cells.

Conclusions from the literature study of the dye-sensitized solar cells and the organic solar cells as well as from the experimental part are given separately in Chapter 5.3, Chapter 6.6 and Chapter 7.3 respectively.

The thesis is summarized in Chapter 8, suggestions for further research are given in Chapter 9 and a comprehensive bibliography is given in Chapter 10.

The thesis includes 115 pages, 28 figures and 9 tables and 161 references.

2 Photovoltaics - general

2.1 Current status of photovoltaics

2.1.1 The photovoltaic market

After the development of the first silicon solar cell in 1954, the solar cells were used primarily in space applications until about the mid-70s (Kazmerski 1997). Since then the solar cells have found applications in customer electronics, small scale remote residential power systems, as well as in communication and signaling. However, it is only in the second half of last decade that grid connected photovoltaic (PV) systems entered the market with significant contribution as a result of the intensive roof programs in Japan, Germany and US.

Today's photovoltaic market has exceeded 200 MW per year and the market growth has been between 15% and 20% in the last decade (Figure 1). In 2000 the production of PV panels exceeded 280 MW, and has been forecasted to surpass 350 MW in 2001 (SolarAccess 2001c)[2]. According to market forecasts predicting an average growth of about 25% world PV market could reach 550 MW in 2005 and 1700 MW in 2010 (Maycock 2000).

2.1.2 Viability of photovoltaics

In order to be a fully sustainable energy technology, photovoltaics has to qualify in certain indicators of viability such as: the energy pay-back time, the CO_2 emissions and the end-of-life management and recycling.

The energy payback time of the photovoltaic systems depends not only on the energy content of the entire photovoltaic system, but also on the local irradiation conditions. An energy pay-back time of 2.5-3 years has been estimated for present-day grid connected roof-top installations in Southern Europe conditions (Alsema & Nieuwlaar 2000). This should be compared to the expected life times of over 30 years of the present PV systems (Oliver & Jackson 2000).

[2] As a reference: a typical net electric power of a nuclear power plant is about 500 MW

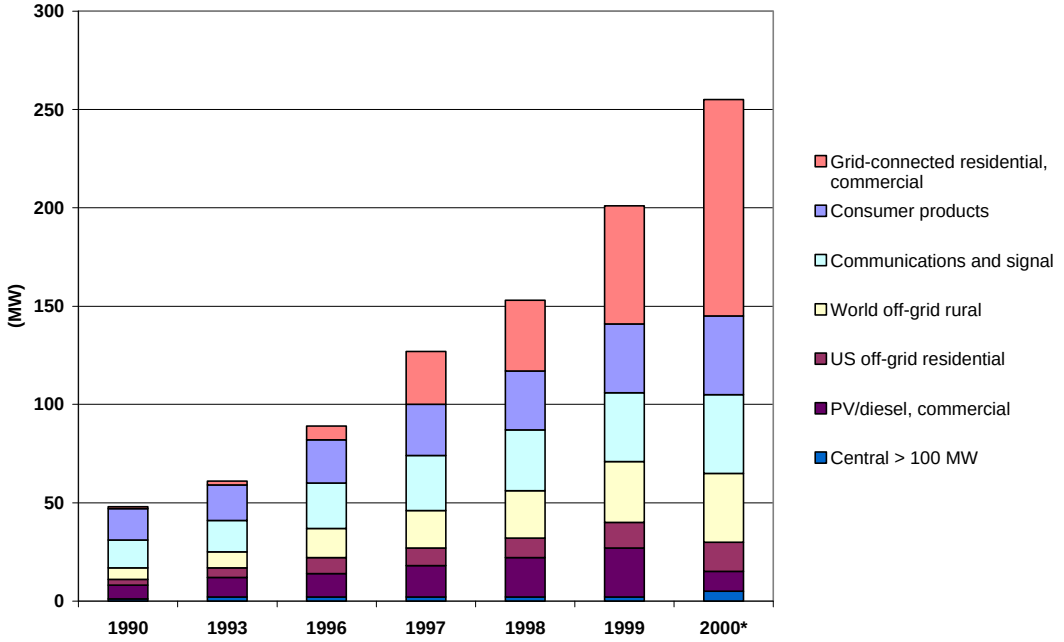

Figure 1. Photovoltaic world market (shipments in MW per year). The figures for the year 2000 are past forecasts. The shown data are from Maycock (2000).

Quite opposite to the fossil energy sources, the CO_2 emissions associated with photovoltaic energy conversion occur almost entirely during system manufacturing instead of system operation. Therefore the CO_2 emissions depend on the CO_2 emission factor of the local energy utility system, which provides the energy for the manufacture of the PV system. The CO_2 emissions (g/kWh) of the present grid connected roof-top systems have been estimated to be significantly lower than those of fossil fuel power plants, but somewhat higher than those of biomass, wind energy and nuclear energy (Alsema and Nieuwlaar 2000).

The requirement of sustainability of photovoltaic energy conversion extends beyond the operating lifetime of a PV system. Depending on the PV technology the cells contain small amounts of different hazardous and regulated materials, such as Cd, Pb and Se, which raises concerns about their disposal into municipal landfills. However, the technology for recycling the solar cells already exists and it can be considered also economically feasible (Fthenakis 2000).

2.1.3 Cost of solar electricity

Photovoltaics is already a valuable technology in those areas of world where there is no immediate access to central power stations or where energy prices are high for some other reasons. Another important market where photovoltaics succeed is small-

scale applications for leisure time activities like boating, caravanning, and camping. However, power generation by grid connected PV systems is perhaps the main application today pursued to be realized in the future in a large scale. To reach this goal, the cost of the PV systems and thus the cost of solar electricity need to be reduced significantly.

The cost of solar electricity is affected not only by the cost of the whole PV systems measured in €/W_p[3], but also on the irradiation level on the site of the PV installation. Also the type of the system affects the system cost, the stand-alone systems with batteries and possibly auxiliary power generators being generally more expensive than the gird-connected systems.

In the past the average selling price of photovoltaic modules has followed quite closely an 80% learning curve, i.e. each doubling of the accumulated shipments has decreased the price to 80% of their original price (Green 2000a). The profitable PV module costs are about US \$3.50/W_p at present, and are expected to decrease to US \$2.00 in 2005 and US \$1.50 in 2010. As a rule of thumb the cost of installed grid-connected PV systems is at least about twice the cost of the PV modules alone, i.e. today about US \$7.00-12.00/W_p. As such, without any governmental subsidies for PV installations, the grid-connected PV electricity is about 3-7 times more expensive in the US, and about 2 and 3 times in Japan and Germany respectively, than electricity produced by other means (the grid electricity). (Maycock 2000).

At present the application driving the market growth is the grid-connected roof-top systems in urban area (Figure 1). The grid-connected systems are expected to dominate the growth of the PV market in the future, and are forecasted to contribute to almost 50% of the PV market in 2010 (Maycock 2000). In this progress supporting governmental action has been playing a crucial role, and will do so also in the future until the costs of PV drops closer to the grid electricity price. Although governmental subsidies are essential to help the photovoltaics to enter the market, the way for a significant market penetration will become much easier as soon as the PV electricity turns to truly economic without any major subsidies.

2.1.4 Possibilities for cost reduction of solar cells

The driving force for the development of new photovoltaic materials is the reduction of the manufacturing costs of the photovoltaic cells and modules. A general

[3] The electric power output of a solar cell in the standard conditions of 1000 W/m^2 solar irradiance and at 25°C temperature, i.e. the nominal power rating of the solar cell, is reported in the unit W_p (watt peak).

discussion of the possibilities for cost reductions and alternative strategies for its pursuit is therefore worthwhile in this connection.

First of all, the cost of the photovoltaic module itself is only less than half of the total systems costs today (Maycock 2000). In other words: today the cost of solar electricity would be high even if the photovoltaic modules were totally free of charge. This highlights the fact that costs reduction of other factors such as inverters and installation (structures and labor), are at least equally as important as cutting down the price of the PV modules itself. However, in the view of the present study discussing new photovoltaic materials, only the cost of PV modules is a relevant point of examination, while the development and the future cost reduction of the other components will be equally available for all photovoltaic cell technologies.

There is essentially two ways of reducing PV module prices ($/$W_p$): improvement of performance (output W_p/m^2, or in other words efficiency) and reduction of direct manufacturing costs ($/$m^2$)[4]. With this respect, two different strategies may be separated: *the high efficiency strategy* and *the low manufacturing cost strategy*.

Needless to say of course, the absolute winner would be a dirt-cheap solar cell with extremely high efficiency, but no serious candidate technology has yet emerged with demonstrated potential for both of these goals.

The high efficiency strategy

The fact that the manufacturing costs in $/$m^2$ are quite high for the existing PV modules emphasizes the need for high cell efficiencies. The efficiency of the solar cells can be increased to a certain point by developing the manufacturing methods, materials and device engineering of a certain emerged PV technology, like the silicon solar cells. As the technology matures, it will eventually become more and more expensive to increase the efficiency further, and at a certain point the corresponding power increase of the cell may not pay its price. This is more or less the case with silicon solar cells today, where the only practical cost reduction can be seen via economies of scale.

In the future, alternative or completely new technologies may open up the way to significantly higher efficiencies. Well-known strategies to increase the efficiencies include tandem or multi-junction cells and concentrating systems. New high efficiency photovoltaic conversion principles on the other hand include e.g. multiple electron-hole pair cells, hot carrier cells, multi-band and impurity cells (Green 2001).

[4] Module price ($/$W_p$) = manufacturing cost ($/m^2) / module performance (W_p/m^2)

These kind of complicated semiconductor devices will however most likely be very expensive to manufacture in reality, and on the other hand remain still mostly at a theoretical level.

The low manufacturing cost strategy.

In principle it can be argued that high efficiencies are not necessary if sufficiently low costs for the PV modules can be achieved. This kind of reasoning has been often associated with the organic photovoltaic materials with a picture of large area plastic photovoltaic cells cut from rolls and assembled onto roofs in mind. There are however certain issues that limit the feasibility of this strategy.

Firstly, the lower the efficiency, the larger the total area needed for producing desired power output from the solar cells. Considering the most practical application of large area photovoltaics, the roof-integrated grid-connected systems, simply the limited amount of roof area may decrease the practical usefulness of low efficiency - low cost photovoltaic cells, and make high efficiency - high cost cells more attractive. This question is however relevant only when a significant part of the user's electricity demand is to be met with the roof-top PV system[5].

Secondly, the realization of very low area related manufacturing costs (in $\$/m^2$), may be difficult in practice unless totally new manufacturing approaches are developed. Examination of the manufacturing cost breakdown of the current PV modules can elucidate this point. For example the costs of active materials, i.e. mostly the semiconductors and electrical contacts of the cells, amounts to only about 6% of the total manufacturing costs of the CdTe modules (Zweibel 2000) or respectively 41% of that of the multicrystalline silicon modules (Little & Nowlan 1997, see Chapter 5.2.5). Thus, simply replacing the active materials in current PV modules by cheaper ones can even in the best case bring about only moderate cost reductions.

What are truly needed then are totally new *module* technologies, by which the costly encapsulations and modularization parts and all possible support structures could be avoided and the other costs reduced by volume production. Ideally, the solar cells would be manufactured in a continuous roll-to-roll process onto large area flexible metal or plastic foils. Thin, flexible and lightweight modules could be for example directly integrated onto building structures such as roof sheets. Progress in this

[5] See in Chapter 2.3.1 for the discussion of the relative availability of rooftop solar electricity.

direction has indeed already been made with amorphous silicon cells for example by United Solar Systems Corp. and Iowa Thin Film Technologies, Inc.[6].

2.2 Photovoltaic technologies

2.2.1 Single-crystal and polycrystalline silicon solar cells

The first silicon solar cell was developed by Chapin, Fuller and Pearson at the Bell Telephone Laboratories in the mid 1950's, and it had already about 6% efficiency (Kazmerski 1997). Today the silicon solar cells dominate the photovoltaic market by 82% (Figure 2) and the record efficiency for a laboratory cell is 24.7% (Green 2001), while the efficiency of the commercial crystalline silicon solar panels is in the best case about 15% (Shah et al. 1999).

The main reason why Si has dominated the PV market is that high quality Si has been already produced at large quantities by the semiconductor industry. The processing of crystalline silicon wafers is high-level semiconductor technology, and as such expensive and very capital intensive. This also adds directly to the cost of the photovoltaic modules, so that the cost of processed silicon wafers contribute to fifty per cent of the total manufacturing cost of the module (Goetzberger & Hebling 2000).

A big question for the Si photovoltaic technology is the availability of highly purified Si. The PV industry has been using mainly low cost reject material from the semiconductor industry. This has created a problematic dependence on the volatile semiconductor market causing fluctuations also in the cost of Si material for the solar cells. In fact, it is generally seen that the dominance of the standard Si PV technology in the growing PV market can be realized only by production of a special solar cell grade silicon. Yet the first efforts to produce such material has been unsuccessful because of the high purity requirements and the small market for the special silicon at the moment. (Goetzberger & Hebling 2000)

While the crystalline silicon technology is relatively mature is has still a large cost reduction potential. It seems to be generally understood however, that the cost reduction can be achieved only by increasing manufacturing volume. From the manufacturers' point of view this is coupled to the need for the special solar cell grade silicon supply and from the market's point of view not very easy to achieve at

[6] See http://ovonic.com/unitedsolar/unisolar.html, http://www.iowathinfilm.com/, http://www.rolltronics.com/ and Guha et al. (2000)

present PV system costs without governmental subsidies for customers to create artificial markets for the solar electricity.

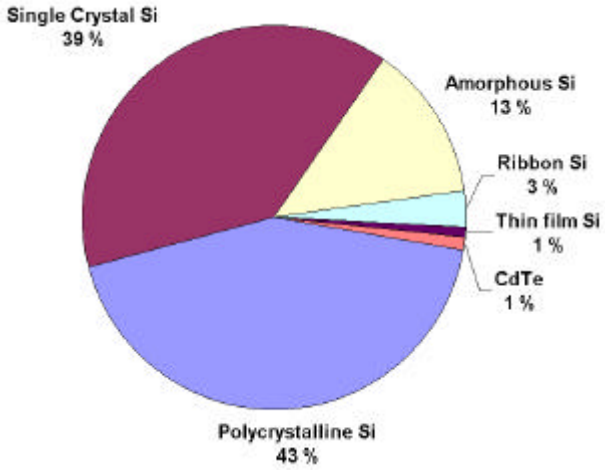

Figure 2. World photovoltaic market in 1998 by technologies. The shown data are from Goetzberger & Hebling (2001).

2.2.2 Thin film solar cells

The crystalline silicon is often referred to as the first generation photovoltaic technology, while the second generation photovoltaics consists of thin film solar cell materials such as amorphous silicon (a-Si), cadmium telluride (CdTe), copper indium gallium diselenide (CIGS), and thin film crystalline silicon. The driving force for the development of thin film solar cells has been their potential for the reduction of manufacturing costs. While silicon solar panels are assembled from individual cells processed from about 100 cm^2 silicon wafers, thin film semiconductor materials can be deposited onto large surfaces, which is beneficial for volume production.

Also as direct band gap semiconductors the thin film semiconductor materials have much higher absorption coefficient than silicon, and therefore typically less than 1 μm thick semiconductor layer is required, which is 100-1000 times less than for Si. The amount of expensive semiconductor material is thus reduced, or on the other hand, more expensive semiconductors can be used in the thin films.

CdTe

Cadmium telluride has a nearly optimal band gap and is easily deposited with thin film techniques. Over 16% efficiencies have been demonstrated in the laboratory (Green 2001). An often discussed issue of the CdTe technology is the cadmium content of the cells. While this question can be most certainly solved by recycling the

Cd if necessary, the public acceptance of the technology may be somewhat trickier question. Solar electricity, usually marketed as an environmentally benign energy form, may not be tolerated to imply environmental concerns about hazardous metals used for the manufacture of the solar cells. However, production plants for commercial presentation of the CdTe cells are being built, and the expected module efficiencies are in the range of 8 to 9% (Shah et al. 1999).

CIGS

Copper indium diselenide (CIS) or CIGS, when gallium is added, is perhaps the most promising thin film material at the moment. It holds the record laboratory efficiency of 18.8% among thin film materials (Green 2001) and shows excellent stability. Actually the efficiency of the CIS cells tend to rise during the first 10-30 minutes of light exposure (Kazmerski 1997). First pilot line products are now being marketed by Siemens with efficiencies above 10% (Goetzberger & Hebling 2000). Small amount of cadmium and selenium is present also in the CIGS solar cell, so the concerns associated usually with the CdTe apply strictly speaking also to the CIGS technology to some extent.

a-Si

The amorphous silicon (a-Si)[7] solar cells have been commercially available since many years and hold 13% of the worlds PV market. The special market for a-Si cells has been low-power sources for consumer electronics, where processability weights more than the absolute solar conversion efficiency.

The problem with a-Si has been the degradation of efficiency by the Stäbler-Wronski effect and stabilized efficiencies only in the 4-5% range have been obtained for single junction cells (Green 2000b). However, decreasing the thickness of the active a-Si layer can enhance the stability of the a-Si cells. The best commercial a-Si cells utilizes a stacked three-layer structure with stabilized efficiencies of 6.4% (Green 2000b). The three-junction concept also enables tuning the band gap of individual layers to achieve higher efficiencies. A three-junction a-Si tandem-cell technology utilizing a-SiGe alloys in the two lower junctions holds the record confirmed module efficiency of 10.4% (Green 2001).

Thin film Si

One way to reduce the amount of Si in the solar cell is to use optical confinement (light trapping). This idea is utilized in the thin film crystalline silicon technology.

[7] *Amorphous silicon as used in solar cells is actually a silicon-hydrogen alloy containing 20-30% hydrogen*

When crystalline Si layer with flat surface is deposited on a Lambertian reflector surface the thickness of the Si layer can be reduced, typically to 5-50 μm. Such a thin Si layer needs a supporting substrate, which can be either low-grade silicon or foreign materials like graphite or glass.

Presently the crystalline thin film Si technology is actively developed in the laboratories and the first crystalline silicon thin film product with 12.2% efficiency is about to be brought commercially available by Astropower (Goetzberger & Hebling 2000).

2.2.3 III-V Semiconductors

Semiconductors such as GaAs, GaAlAs, GaInAsP, InAs, InSb, and InP are interesting solar cell materials because they have near-optimal band gaps. These materials are extremely expensive, and have found applications only in the space solar cells, where performance is more important criteria than cost, and in some extent in concentrating systems where the active surface area of the cells can be reduced significantly and therefore expensive materials be used.

2.2.4 Photoelectrochemical solar cells

The oldest type of photovoltaic cell is the photoelectrochemical solar cell, used already by Becquerel for the discovery of the photovoltaic effect in 1839. In the photoelectrochemical solar cell a semiconductor-electrolyte junction is used as a photoactive layer. While energy conversion efficiencies exceeding 16% have been achieved with the photoelectrochemical solar cells utilizing semiconductor photoelectrodes (Meissner 1999), instability of these solar cells by photocorrosion has left them without practical importance. Furthermore, the photoelectrochemical solar cells using same semiconductor materials as in the commercial solar cells, such as Si, $CuInSe_2$ or GaAs does not offer any real advantages over the established solid state solar cells.

2.3 Basics of photovoltaic energy conversion

2.3.1 Solar irradiation and availability of solar electricity

The intensity of solar radiation in the earth's distance from the sun is approximately 1353 kW/m^2, a number also called *the solar constant*. The solar radiation is emitted from the sun's photosphere at 6000 K temperature, which gives it a spectral

distribution resembling closely that of a black body at the corresponding temperature. Passing through the earth's atmosphere the solar radiation is attenuated by scattering from the air molecules, aerosols and dust particles, as well as by absorption by the air molecules, in particular oxygen, ozone, water vapor, and carbon dioxide. This gives a characteristic fingerprint to the solar radiation spectrum on the earth's surface (Figure 3).

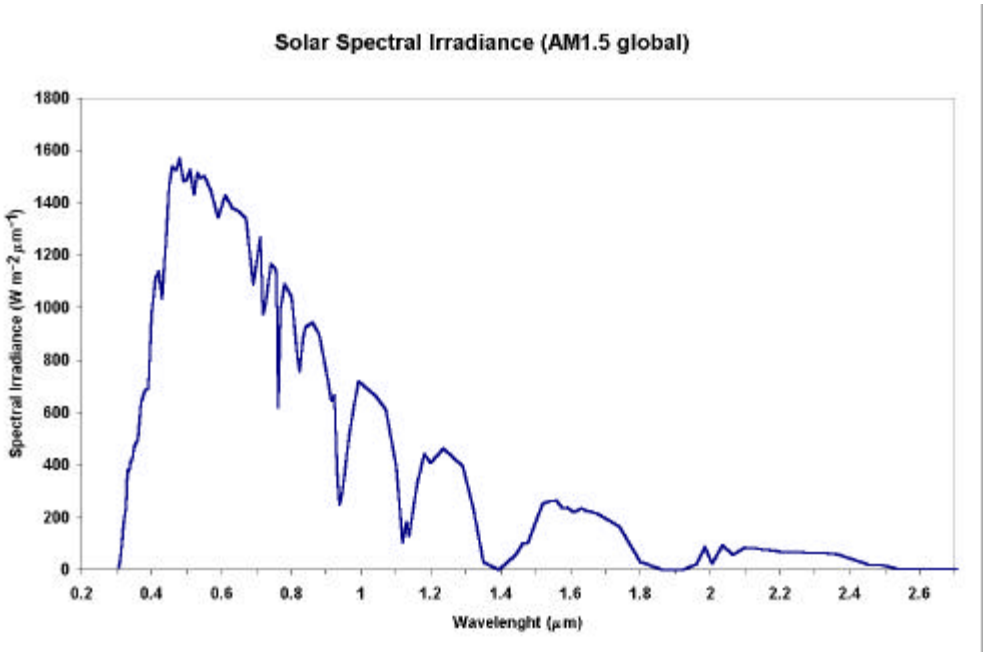

Figure 3. The standard AM1.5 global solar spectrum. Shown data are from http://www.pv.unsw.edu.au/am1.5.html.

The available solar irradiation in a certain place depends on the latitude, the altitude and the climatic type in a yearly basis, and on the season, the time of day and the weather conditions in a specific time. The total yearly solar irradiation on horizontal surface is 700-1000 kWh/m^2 in North Europe, 900-1300 kWh/m^2 in Middle Europe, 1300-1800 kWh/m^2 in South Europe, 1800-2300 kWh/m^2 in the equator, and 2000-2500 kWh/m^2 in the so called "solar belt" i.e. between 20° and 30° latitude (Peippo 1992).

An order of magnitude estimate of the usefulness of these yearly solar energy densities, converted to electricity with a grid-connected PV system, can be made by comparing these to an area related yearly electricity consumption of a typical detached house. In Finland, a typical electricity consumption for a 4 person family living in a detached house with floor area of 120 m^2 and using electric heating is 18500 kWh/year (Motiva 2001). The yearly solar irradiation falling to the same horizontal area in North Europe conditions (about 1000 kWh/m^2/year), converted to

solar electricity with total PV system efficiency of 10% amounts to about 12000 kWh/m^2, i.e. about 65% of the yearly electricity consumption of the examined typical Finnish family.

In a large scale, the determination of the actual practical grid-connected PV potential is of course a far more complicated task, since factors such as type of the buildings, roof shapes, tilt angles, shading questions, ages of the buildings, and other technical questions has to be concerned. By an analysis of the building stock Gutschner and Nowak (2000) estimated that 16% of the electricity consumption of a urban area (City of Zürich) and almost half of the consumption of a rural area (Canton of Fribourg) could be met by solar electricity generated by building-integrated photovoltaics covering the available roof-top area having a good solar yield (more than 80% of the maximum annual solar irradiation).

2.3.2 Photovoltaic cell performance

A photovoltaic cell is a device, which converts incident light to electrical energy. Generation of electrical power under illumination is achieved by the capability of the photovoltaic device to produce voltage over an external load and current through the load at the same time. This is characterized by the current-voltage (IV) curve of the cell at certain illumination and temperature (Figure 4).

When the cell is short circuited under illumination, the maximum current, the short circuit current (I_{SC}), is generated, while under open circuit conditions no current can flow and the voltage is at its maximum, called the open circuit voltage (V_{OC}). The point in the IV-curve yielding maximum product of current and voltage, i.e. power, is called the maximum power point (MPP). Another important characteristic of the solar cell performance is the fill factor (FF), defined as

$$FF = \frac{V_{MPP} \cdot I_{MPP}}{V_{OC} \cdot I_{SC}} \quad . \tag{1}$$

Using the fill factor, the maximum power output of the solar cell can be written as

$$P_{MAX} = V_{OC} \cdot I_{SC} \cdot FF \quad . \tag{2}$$

While the physical principles behind the operation of different types of photovoltaic cells are generally different, the current-voltage curve of well performing cells are similar, and can be characterized and compared with each other in terms of FF, V_{OC}, and I_{SC}.

Finally, the energy conversion efficiency of the solar cell is defined as the power produced by the cell (P_{MAX}) divided by the power incident on the representative area of the cell (P_{light}):

$$h = \frac{P_{MAX}}{P_{light}} \quad . \tag{3}$$

The efficiency of the solar cell depends on the temperature of the cell, and which is even more important, on the quality of the illumination, i.e. the total light intensity and the spectral distribution of the intensity. For this reason, a standard measurement condition has been developed to facilitate comparable testing of the solar cells between different laboratories. In the standard condition used for testing of terrestrial solar cells the light intensity is 1000 W/m^2, the spectral distribution of the light source is that of AM1.5 global standard solar spectrum (Figure 3), and temperature of the cell is 25°C. The power output of the solar cell at these conditions is the nominal power of the cell, or module, and is reported in *peak* watts, W_p. In practice, special solar simulator light sources are used for the standard measurements.

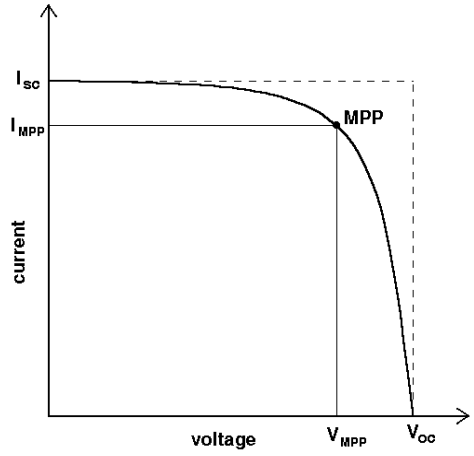

Figure 4. Typical shape of the current-voltage curve of a photovoltaic cell showing the open-circuit voltage V_{OC}, short circuit current I_{SC}, and the maximum power point MPP, and the current and voltage at the MPP: I_{MPP}, $V_{MPP.}$

2.3.3 Operating principle of the standard silicon solar cell

The standard silicon solar cell is based on a semiconductor pn-junction. The cell consists of n-doped and p-doped semiconductor layers forming the pn-junction, an antireflection coating, current collectors and a metal substrate for the collection of photogenerated charge carriers from n-type (electrons) and p-type (holes) layers respectively.

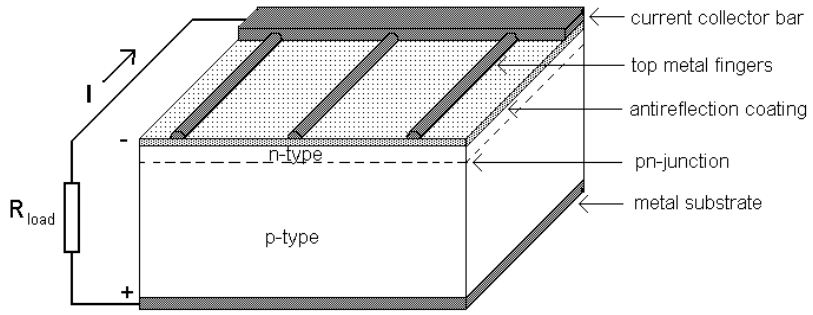

Figure 5. The standard pn-junction solar cell configuration from the 1960s.

N-type semiconductors are obtained by doping with impurity atoms (from group V in the case of silicon) having an excess valence electron with respect to the surrounding host atoms. P-type semiconductors on the other hand are obtained by doping with impurity atoms (from group III in the case of silicon) with one valence electron less than the surrounding atoms. The n-type doping results in localized energy states just below the conduction band edge of the host semiconductor lattice and occupied by the excess electrons from the impurity atoms, while p-type doping results in (Figure 6a) localized empty states with energy slightly above the valence band edge of the semiconductor.

The donor atoms in the n-type material are easily ionized by thermal excitation, due to the closeness of the donor states and the conduction band edge. The ionization of the donor atoms generates free electrons to the conduction band and leaves immobile empty donor states behind. For the same reason in the p-type material the originally empty acceptor states are partly filled by electrons from the valence band leaving mobile holes to the valence band.

Bringing an n-type and p-type semiconductor in contact leads to a transport of electrons and holes across the junction until equilibrium is reached. This can be described as equalization of the Fermi-level[8] in the both materials in thermal equilibrium with each other, and this process sets up a depletions zone near the junction where there are practically no free charges, but an electric field (potential

[8] In a system in a thermodynamic equilibrium there exists an unambiguous energy level called Fermi energy E_f that describes the electron energy distribution. In the solar cells the Fermi energy can be interpreted as electrical potential energy, since the associated electric potential difference, the electrochemical potential difference, of the opposite electrodes (contacts), is the output voltage measure from the solar cell. The junction voltage is however a contact potential or "inner" electrical potential (also called Galvani potential) difference and cannot be measured directly by a voltmeter connected to the cell. See e.g. (Levine 1978, p. 359-361).

difference) across the region. The formation of the pn-junction is pictured schematically in Figure 6.

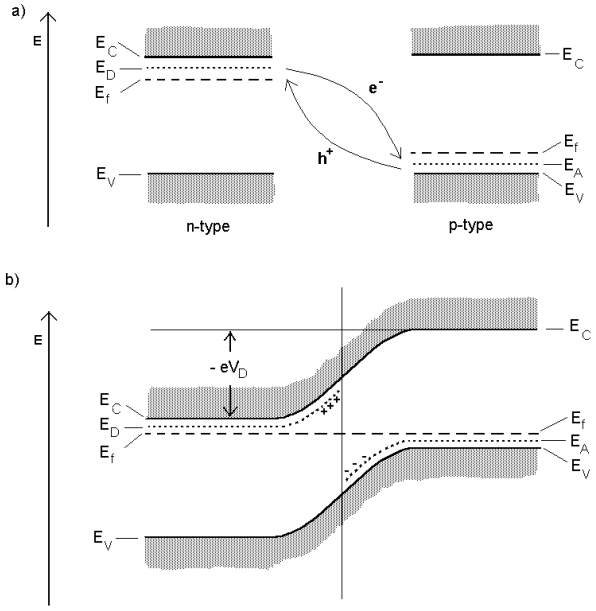

Figure 6. Formation of the abrupt semiconductor pn-junction. a) Schematic band structure of an n-type and a p-type semiconductor showing conduction and valence band edges E_C and E_V, donor level E_D in n-type material and acceptor level E_A in the p-type material and the Fermi level E_f. b) pn-junction in thermal equilibrium shoving the potential difference V_D across the junction.

Upon illumination of the pn-junction photons are absorbed by excitation of electrons from the valence band to the conduction band leaving holes to the valence band. Due to the high crystallinity of the semiconductor, which is essential for good operation, the electrons and holes are more or less free to move in the material by drift due to potential (or Fermi energy) gradients and by diffusion due to concentration gradients.

The existence of the built-in electric field in the pn-junction region is the source of photovoltaic activity in the cell. Under illumination, a large number of electrons and holes are generated in the semiconductor material. Minority charge carriers (holes in the n-type and electrons in the p-type layers) generated in the depletion region of the pn-junction, or within their diffusion length from it, are swept to the opposite side of the junction by the built-in electric field of the junction. Under illumination, electrons are therefore accumulated in the n-type material and holes in the p-type material, generating voltage[9] between the opposite sides of the pn-junction and

[9] Difference in electrochemical potential, or Fermi level between the opposite electrical contacts.

electrical contacts attached to them, as well as current through an external load attached between the contacts.

The basic steps of photovoltaic energy conversion

The operation of a photovoltaic cell can be generally divided into three basic steps:

1. Light absorption,
2. Charge separation,
3. Charge collection.

The physical or chemical processes behind these principal steps vary between different types of solar cells and photovoltaic materials. The efficiency of a solar cell depends on the efficiency of each of these steps and is maximized by the materials selection and the cell design.

To sum up: In the standard pn-junction solar cell, light absorption occurs via band gap excitation of electrons in the bulk of the semiconductor, charge separation in the internal electric field of the pn-junction and charge collection by transport of electrons and holes (electric current) through the bulk of the semiconductor to the electrical contacts.

3 Dye-sensitized nanostructured solar cells

Historically the dye-sensitization dates back to the 19th century, when photography was invented. The work of Vogel in Berlin after 1873 can be considered the first significant study of dye-sensitization of semiconductors, where silver halide emulsions were sensitized by dyes to produce black and white photographic films (referred in McEvoy & Grätzel 1994).

The use of dye-sensitization in photovoltaics remained however rather unsuccessful until a breakthrough at the early 1990's in the Laboratory of Photonics and Interfaces in the EPFL Switzerland. By the successful combination of nanostructured electrodes and efficient charge injection dyes professor Grätzel and his co-workers developed a solar cell with energy conversion efficiency exceeding 7% in 1991 (O'Regan & Grätzel) and 10% in 1993 (Nazeeruddin et al.). This solar cell is called *the dye-sensitized nanostructured solar cell* or *the Grätzel cell* after its inventor.

In contrast to the all-solid conventional semiconductor solar cells, the dye-sensitized solar cell is a photoelectrochemical solar cell i.e. it uses a liquid electrolyte or other ion-conducting phase as a charge transport medium. Due to the high efficiencies and good long-term stability reported for the dye-sensitized solar cells, the research interest in this technology grew rapidly during the 1990's. While the patent holders and the licensees developed the original patented concepts towards practical products, numerous research groups explored the replacement of the original materials with new ones.

In this chapter the technology of the dye-sensitized solar cells is introduced starting with a short description of the operating principles of the cell. After this, a more detailed look is taken to the cell operation in light of the key steps of photovoltaic conversion, as well as the other important fundamental operational aspects of the cell physics and chemistry.

3.1 Operating principle of the dye-sensitized solar cell

At its simplest configuration (Figure 7), the dye-sensitized solar cell (abbreviated hereafter as the DSSC or the dye cell) is comprised of a transparent conducting glass electrode coated with porous nanocrystalline TiO_2 (nc-TiO_2), dye molecules attached to the surface of the nc-TiO_2, an electrolyte containing a reduction-oxidation couple

such as I^-/I_3^- and a catalyst coated counter-electrode. At the illumination the cell produces voltage over and current through an external load connected to the electrodes.

The absorption of light in the DSSC occurs by dye molecules and the charge separation by electron injection from the dye to the TiO_2 at the semiconductor electrolyte interface. A single layer of dye molecules however, can absorb only less than one percent of the incoming light (O'Regan & Grätzel 1991). While stacking dye molecules simply on top of each other to obtain a thick dye layer increases the optical thickness of the layer, only the dye molecules in direct contact to the semiconductor electrode surface can separate charges and contribute to the current generation. A solution to this problem, developed by the Grätzel group, was to use a porous nanocrystalline TiO_2 electrode structure in order to increase the internal surface area of the electrode to allow large enough amount of dye to be contacted at the same time by the TiO_2 electrode and the electrolyte (Figure 7).

Having this construction, a TiO_2 electrode typically 10 µm thick, with an average particle (as well as pore) size typically in the order of 20 nm, has an internal surface area thousands of times greater than the geometrical (flat plate) area of the electrode, (O'Regan & Grätzel 1991). Essential to the optical operation of this porous electrode structure is the fact that TiO_2, as a large band gap semiconductor, absorbs only below

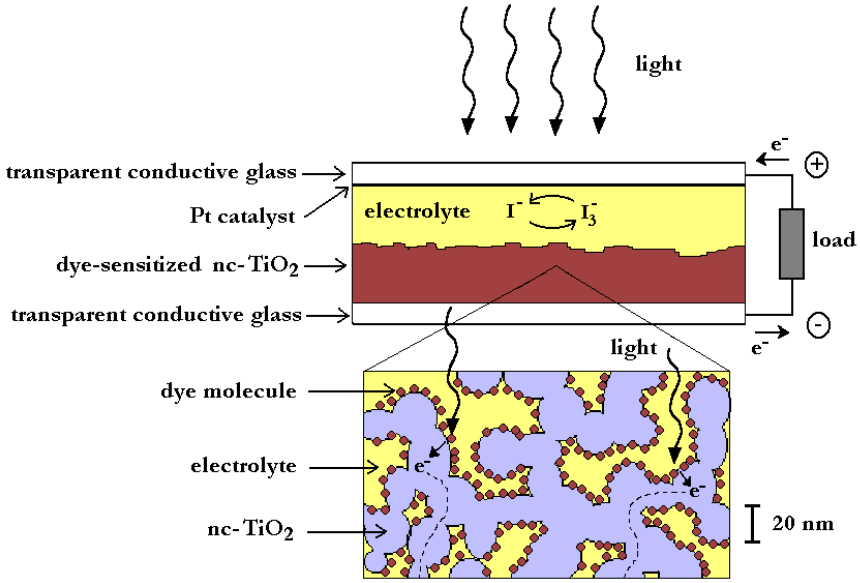

Figure 7. A schematic representation of the structure and components of the dye-sensitized solar cell

about 400 nm (See Chapter 4.2), letting the major part of the solar spectrum available for the dye molecules.

The regenerative working cycle of the dye-sensitized solar cell is depicted in Figure 8, showing schematically the relative energy levels of a working DSSC. The incoming photon is absorbed by the dye molecule adsorbed on the surface on the nanocrystalline TiO_2 particle and an electron from a molecular ground state S^0 is exited to a higher lying excited state S^* (1). The exited electron is injected to the conduction band of the TiO_2 particle leaving the dye molecule to an oxidized state S^+ (2). The injected electron percolates through the porous nanocrystalline structure to the transparent conducting oxide layer of the glass substrate (negative electrode, anode) and finally through an external load to the counter-electrode (positive electrode, cathode) (3). At the counter-electrode the electron is transferred to triiodide in the electrolyte to yield iodine (4), and the cycle is closed by reduction of the oxidized dye by the iodine in the electrolyte (5).

The operating cycle can be summarized in chemical reaction terminology as (Matthews et al. 1996):

Anode:	$S + h\nu \rightarrow S^*$	*Absorption*	(4)
	$S^* \rightarrow S^+ + e^-(TiO_2)$	*Electron injection*	(5)
	$2S^+ + 3I^- \rightarrow 2S + I_3^-$	*Regeneration*[10]	(6)
Cathode:	$I_3^- + 2e^-(Pt) \rightarrow 3I^-$		(7)
Cell:	$e^-(Pt) + h\nu \rightarrow e^-(TiO_2)$		(8)

Due to the energy level positioning in the system (Figure 8), the cell is capable of producing voltage between its electrodes and across the external load. The maximum theoretical value for the photovoltage at open circuit condition is determined by the potential difference between the conduction band edge of the TiO_2 and the redox potential of the I^-/I_3^- pair in the electrolyte (Cahen et al. 2000). The operation of the cell is regenerative in nature, since no chemical substances are neither consumed nor produced during the working cycle, as visualized in the cell reaction (8).

[10] The regeneration and cathode reactions involving two electrons are actually composed of sequences of partial reactions (see e.g. Fisher et al. (2000) for the regeneration partial reactions).

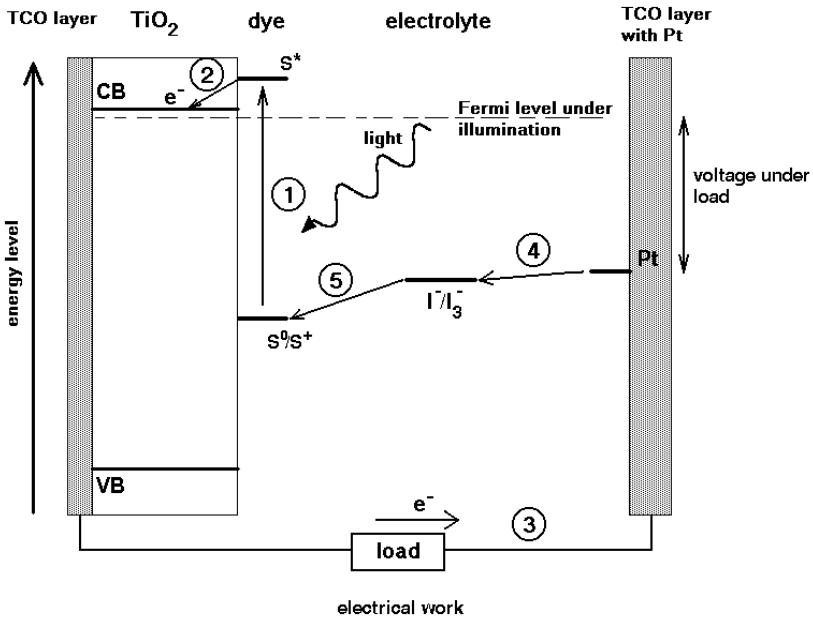

Figure 8. The working principle of the dye-sensitized nanostructured solar cell. See text for the explanation of the basic processes in the cell.

3.2 Theoretical issues of the dye cell operation

Since the invention of the nanostructured DSSC, a lot of theoretical and experimental work has been carried out to explain the surprisingly efficient operation of these solar cells. The need for unique theoretical considerations of the photovoltaic effect in the DSSCs arises from the fundamental differences in the operation between the DSSCs and the traditional semiconductor pn-junction solar cells:

1. In contrast to the semiconductor pn-junction solar cells, where light absorption and charge transport occurs in the same material, the DSSC separate these functions: photons are absorbed by the dye molecules and transport of charges is carried out in the TiO2 electrode and electrolyte.
2. While the charge separation in the semiconductor pn-junction cells is induced by the electric field across the junction, no such long-range electric fields exist in the DSSC. The charge separation occurs via other kinds of kinetic and energetic reasons at the dye-covered semiconductor-electrolyte interface (see Chapter 3.2.2).
3. In the semiconductor pn-junction cells the generated opposite charges travel in the same material, while in the DSSC, electrons travel in the nanoporous TiO2

network and holes in the electrolyte11. This means that the requirement for a pure and defect free semiconductor material in the case of semiconductor pn-junction solar cell is relaxed for the DSSC, where the recombination can occur only at the semiconductor electrolyte interface.

3.2.1 Light absorption

While the high efficiency of the dye sensitized solar cell arises from a collective effect of numerous well-tuned physical-chemical nanoscale properties as will become apparent later, the key issue is the principle of dye-sensitization of large band-cap semiconductor electrodes. As already mentioned, in the DSSC this is accomplished by coating the internal surfaces of the porous TiO_2 electrode with special dye molecules tuned to absorb the incoming photons. Figure 9 represents the molecular structures of three efficient photosensitizers for DSSCs including the so-called N3 dye and the black dye (See Chapter 4.3).

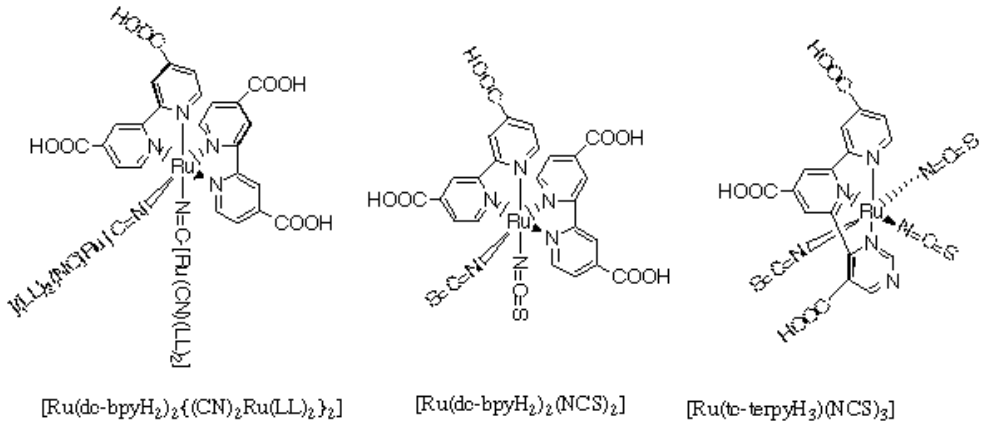

Figure 9. Molecular structures of three efficient photosensitizer for DSSCs. From left: a trinuclear Ru dye, the N3 dye, and the black dye. Picture from (http://dcwww.epfl.ch/icp/ICP-2/solarcellE.html).

Adsorption of the dye molecule

The adsorption of the dye to the semiconductor surface usually takes place via special anchoring groups attached to the dye molecule. In the N3 dye these are the four carboxylic groups (COOH) at the end of the pyridyl rings (Figure 6a). The COOH groups form a bond with the TiO_2 surface by donating a proton to the TiO_2

[11] In the words of the semiconductor terminology, DSSC is not a minority carrier device in contrast to the semiconductor pn-junction solar cells.

lattice (Hagfeldt & Grätzel 2000). The area occupied by one N3 molecule at the TiO_2 surface at full monolayer coverage is 1.65 nm^2 (Hagfeldt & Grätzel 2000).

Light absorption via MLCT excitation

The absorption of a photon by the dye molecule happens via an excitation between the electronic states of the molecule. For example the N3 dye has two absorption maxima in the visible region at 518 nm and at 380 nm (Hagfeldt & Grätzel 2000).

The excitation of the Ru complexes via photon absorption is of metal to ligand charge transfer (MLCT) type (Figure 10). This means that the highest occupied molecular orbital (HOMO) of the dye is localized near the metal atom, Ru in this case, whereas the lowest unoccupied molecular orbital (LUMO) is localized at the ligand species, in this case at the bipyridyl rings. At the excitation, an electron is lifted from the HOMO level to the LUMO level[12]. Furthermore, the LUMO level, extending even to the COOH anchoring groups (Hagfeldt & Grätzel 2000), is spatially close to the TiO_2 surface, which means that there is significant overlap between the electron wavefunctions of the LUMO level of the dye and the conduction band of TiO_2. This directionality of the excitation is one of the reasons for the fast electron transfer process at the dye-TiO_2 interface.

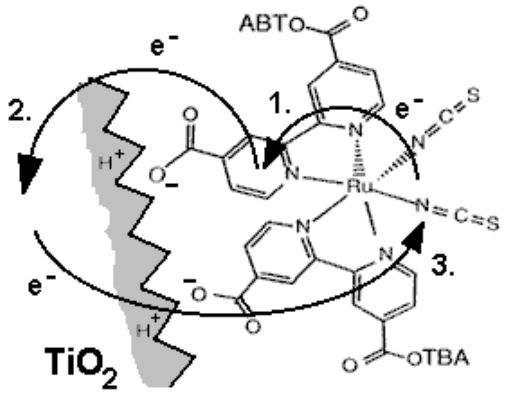

Figure 10. Charge transfer processes between dye and the TiO_2 lattice: 1. MLCT excitation, 2. Electron injection and 3. Charge recombination.

[12] Strictly speaking, as large molecules the sensitizer dyes have actually a complex structure of excited electron energy states and naturally also the fine structure of vibrational energy states. While the exact positioning of the electronic states is evidently important for the properties of the sensitizer dye, the separation into the HOMO and LUMO levels or bands is suitable for the general discussion.

The sensitization effect

The efficient spectral sensitization in the DSSC is made evident in Figure 11, where the spectral response curves, i.e. the photon to current efficiency curves, for cells sensitized with different dyes is compared with a naked TiO_2 electrode. The actual sensitization effect can be seen in Figure 8 as a shift of the IPCE curve of the naked TiO_2 to the higher wavelenghts when coated with the dye. The current efficiency of the cell is related to the 'height' of the IPCE curve, which depends on the charge separation and charge collection efficiencies. The IPCE curves in Figure 11 are not corrected for the optical losses in the glass substrate, which only makes the obtained peak IPCE values more significant.

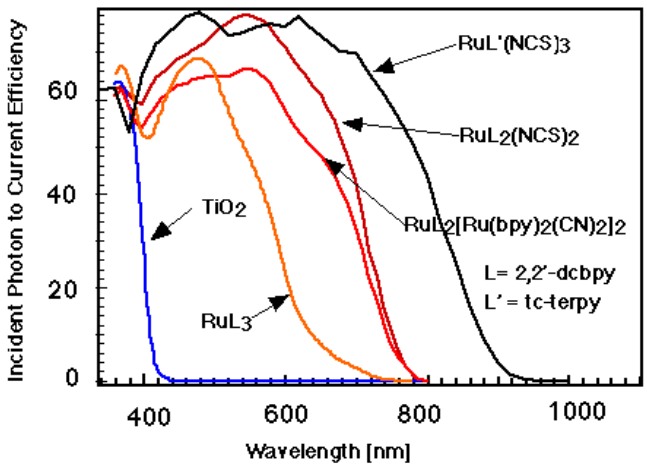

Figure 11. Spectral response (IPCE) of dye-sensitized solar cell for different dyes compared with the spectral response of bare TiO_2 electrode and the ideal IPCE curve for a single band-gap device. Picture from http://dcwww.epfl.ch/icp/ICP-2/solarcellE.html.

3.2.2 Charge separation

The charge separation in DSSCs is based on an electron transfer process from the dye molecule to TiO_2 and a hole transport process from the thereby oxidized dye to the electrolyte.

The electron transfer mechanism is strongly dependent on the electronic structure of the adsorbed dye molecule and the energy level matching between the excited state of the dye and the conduction band of the TiO_2.

While charge separation in the semiconductor pn-junction arises from the electric field in the space-charge layer in the junction area, the situation in a nanoparticle electrode - electrolyte interface is quite different. The individual particle size in the

nanostructured electrode, typically a few tens of nanometers, is too small for the formation of a space charge layer inside the particles (Hagfeldt & Grätzel 1995).

Furthermore, no significant macroscopic electric fields are present between the individual nanoparticles in the bulk of the electrode. In this case, the absence of band bending is a result of the individuality of each nanocrystalline particle: A sufficiently thick nanoparticle film could have a collective space charge, if the film behaved as an ensemble. However, the electrolyte surrounding all the particles effectively decouples the particles and screens any existing electric fields within about a nanometer (Pichot & Gregg 2000b).

While the band bending inside the particles is inhibited, there exists however an electric field at the semiconductor - electrolyte interface due to the adsorbed dye molecules (Figure 2). The dye molecules have usually acid groups (COOH) as attachment units and upon binding a proton (H^+) is released to the oxide surface leaving the dye molecule negatively charged (Figure 10b). The potential difference across the consequently formed Helmholtz's layer is estimated to be approximately 0.3 eV, and it will help to separate the charges and to reduce recombination (Cahen et al. 2000).

The major mechanism for the charge separation is however the energy level positioning (Figure 8) between the dye molecule and the nanoparticle. The exited state of the dye (the LUMO level) is above the conduction band edge of the TIO_2 and the dye's HOMO level is below the chemical potential of the redox pair iodide/triiodide in the electrolyte, both presenting an energetic driving force for the electron and hole separation.

In addition to the favorable energetics for the charge separation, also entropic factors arise. The large density of delocalized states in the nanoparticle compared to small number of dye molecules on the particle surface means that the electron injection to the TiO_2 conduction band is associated with an entropy increase presenting a driving force of approximately 0.1 eV for the charge separation (Cahen et al. 2000, Hagfeldt & Grätzel 1995).

3.2.3 Charge transport

In the DSSCs charge transport happens by electron transport in the nanostructured TiO_2 electrode and hole transport in the electrolyte as I_3^-. Although the electron transport process has attracted an intensive study due to several interesting fundamental questions concerning it, both charge transport mechanisms are equally important for the operation of the solar cell.

Electron transport in the nanostructured semiconductor electrode

The semiconductor nanoparticle network works not only as a large surface area substrate for the dye molecules but also as a transport media for the electrons injected from the dye molecules. The nature of the highly efficient electron transport in the dye-sensitized electrode is particularly intriguing and has puzzled researchers since the invention of the dye cell. Is the electron transport driven by built-in electric fields or by diffusion? How can the inherently poor conductor TiO_2 perform high photocurrents in the dye cell? Are the electrons travelling in the bulk or on the surface of the particles?

Because of the porous structure of the electrode and the screening effect of the electrolyte, the electrode can be viewed as a network of individual particles through which electrons percolate by hopping from one particle to the next (Hagfeldt & Grätzel 2000). As mentioned above, the small size of the particles prevents the formation of a space charge layer and a built-in electric field inside the particles, and therefore the transport of electrons cannot be drift in an electric field. Recombination processes being efficiently blocked at the semiconductor electrolyte interface the generation of electrons to the conduction band of the TiO_2 particles under illumination results in an electron concentration gradient in the electrode and the electrons are transferred to the TCO back contact layer by diffusion.

Measurements have shown that the diffusion of electrons is characterized by a distribution of diffusion coefficients, which have been related to hopping of electrons via surface traps of different depths (Hagfeldt & Grätzel 2000). These electron traps are localized energy states just below the conduction band edge of the TiO_2 and they play a significant role in the electron transport. Because of the majority carrier nature of the TiO_2 electrode, trapping of electrons in the bulk states does not lead to recombination losses. Instead trapping of electrons at the TiO_2 surface may be a pathway for recombination, resulting in photocurrent losses and also photovoltage losses for kinetic reasons (Hagfeldt & Grätzel 1995). In addition, the trap states will lead to a lower quasi-Fermi level[13] for the electrons under illumination and thus to a reduced photovoltage (Hagfeldt & Grätzel 1995).

The diffusion coefficient of electrons depends on the electron quasi-Fermi level under illumination. At low light conditions only deep traps participate in the electron transport causing a low diffusion coefficient. Increasing the light intensity raises the

[13] The distribution of electrons and holes cannot be described with single Fermi level in a thermodynamic disequilibrium (under illumination of the solar cell), but with the so-called Quasi-Fermi levels individually assigned for both the electrons and holes in the system.

electron quasi-Fermi level and deep traps are filled at steady state condition, while shallow traps contribute to the electron motion, resulting in a larger diffusion coefficient (Hagfedlt & Grätzel 2000). Increasing the illumination level thus increases the conductivity of the TiO_2 electrode by filling the trap states.

It has also been suggested that the motion of the electrons in the semiconductor particles is coupled to the species in the electrolyte at the semiconductor-electrolyte interface (Hagfedlt & Grätzel 2000). Cahen et al. (2000) calculated that the screening by the electrolyte keeps the electrons near the particle surface, consistently with the picture of electron transport via surface electron traps. The electron together with its screening charge in the electrolyte side of the particle surface can be viewed as a polaron moving by the electron diffusion towards the back contact where the electron is subsequently separated.

All in all, the picture of the electron transport in the nanostructured electrode of the dye cell is presently incomplete and a lot of basic research has to be done. Understanding the mechanisms of charge transport in the nanostructured electrode-electrolyte systems is important for the further development of the dye-sensitized nanostructured solar cell concept and especially for designing cells with solid polymer or gel electrolytes (see Chapter 5.2.3).

Ion transport in the redox electrolyte

The electrolyte in the DSSCs is usually an organic solvent containing the redox pair I^-/I_3^-, which in this case works as a hole-conducting medium. At the TiO_2 electrode the oxidized dye, left behind by the electron injected to the TiO_2, is regenerated by I^- in the electrolyte in the reaction (Equation 6)

$$2S^+ + 3I^- \rightarrow 2S + I_3^- \,, \tag{9}$$

while at the counter-electrode I_3^- is reduced to I^- in the reaction (Equation 7)

$$I_3^- + 2e^-(Pt) \rightarrow 3I^- \,. \tag{10}$$

In other words, I_3^- is produced at the TiO_2 electrode and consumed at the counter-electrode and thus diffused across the electrolyte correspondingly. This is why I_3^- is often labeled as the hole carrier to draw similarities with the conventional pn-junction solar cells. Similarly, I^- is produced at the counter-electrode and diffused to the opposite direction in the electrolyte.

The most simple way of dealing with the electrolyte might be to think it as an essentially neutral sink of I^- and I_3^- feeding the reactions (9) and (10) at the electrodes

and maintaining the redox potential in the bulk of the electrolyte via the fast redox reaction of the I^-/I_3^- pair. This redox reaction in the electrolyte is a two-electron reaction (Ferber et al. 1998)

$$3I^- \Leftrightarrow I_3^- + 2e^-, \tag{11}$$

which is composed of series of successive reactions

$$\left(I^- \Leftrightarrow I + e^-\right)\times 2 \qquad \textit{charge transfer reaction,} \tag{12}$$

$$2I \Leftrightarrow I_2 \qquad \textit{fast chemical reaction,} \tag{13}$$

$$I_2 + I^- \Leftrightarrow I_3^- \qquad \textit{fast chemical reaction.} \tag{14}$$

The redox electrolyte chemistry appears to be a more or less standard and established area of chemistry, or at least it is only rarely discussed in much more detail than this in conjunction with DSSC research reports in the literature.

3.2.4 Recombination

Recombination of the generated electrons with holes in the dye-sensitized nanostructured TiO_2 electrode can in principle occur both after the electron injection or during its migration in the TiO_2 electrode on its way to the electrical back contact.

Illumination of the dye-sensitized electrode initially in equilibrium (in the dark) generates a transient electric field between the injected electrons in the TiO_2 and the oxidized species in the electrolyte. This electric field could in principle oppose further charge separation and promote recombination. However, in the dye cell the mobile ions in the electrolyte can easily rearrange and effectively screen the light induced opposing fields in steady state conditions through out the electrode film, and thus enable an efficient charge separation (Zaban et al. 1997).

In the silicon solar cells the recombination of charge carriers in trap states in surfaces, grain boundaries, and in the bulk degrades the cell performance easily, and thus semiconductor material of high crystal purity is required. In the dye-sensitized TiO_2 electrode, there is on the contrary vast amount of particle boundaries and a huge surface to volume ratio. Yet the dye solar cell does not seem to suffer from the recombination losses at the grain boundaries at all. The reason for this is that only electrons are transported through the semiconductor particles, while holes (oxidized ions) are carried by the electrolyte. In other words, the dye cell works as a majority

carrier device, similar to a metal-semiconductor junction or a Schottky diode (Green 1982, p. 175).

In the absence of holes in the semiconductor particles, the recombination occurs mostly by loss of electron to an oxidized dye molecule or to a hole in the electrolyte, i.e. the oxidized triiodide. The former process is negligible, as assumed in most electrical models of the cell, but may be important in near open circuit conditions, i.e. in the case of the accumulation of electrons into the TiO_2 particles (Hague et al. 1998). The latter recombination pathway on the other hand, is made inefficient by reaction kinetic reasons. According to Huang et al. (1997) the net recombination reaction at the TiO_2 - electrolyte interface is a two electron reaction

$$I_3^- + 2e^- \Rightarrow 3I^- \quad , \tag{15}$$

composed of sub-reactions

$$I_3^- \Leftrightarrow I_2 + I^- , \tag{16}$$

$$I_2 + e^- \Rightarrow I_2^- , \tag{17}$$

$$2I_2^- \overset{slow}{\Rightarrow} I_3^- + I^- , \tag{18}$$

the last of which is a slow dismutation reaction and rate limiting in the net recombination reaction. The reaction equation (17) also tells, that the actual electron acceptor in the recombination reaction is I_2.

Because of the porous structure of the electrode the conducting glass substrate may be partly exposed to the electrolyte setting up a potential recombination pathway between electrons in the conducting substrate and hole carriers in the electrolyte. However, there is experimental evidence that this effect is insignificant, most likely due to low electrocatalytic activity of Pt-free SnO_2:F (as well as ITO) surface for the iodine/triiodide redox system (Cahen et al. 2000).

3.2.5 Interfacial kinetics

The dye-sensitized solar cell is based on photoelectrochemical reactions at the semiconductor-electrolyte interface, as already discussed, and the operation of the cell is therefore an outcome of competing opposite chemical reactions having different rate constants. A desired direction of the electrochemical reactions is achieved with fast wanted reactions (high rate constants) and slow unwanted

reactions (low rate constants). The greater the difference between the rate constants, the higher the efficiency of the system.

The kinetics of the DSSC is summarized in a highly simplified manner in Figure 12. The desired reaction, the electron injection from the exited state of the dye to the conduction band of TiO_2, exceeds any unwanted reaction in an order of magnitude or more. In fact, occurring in the femtosecond time scale, the electron injection process between the N3 dye and TiO_2 in the DSSC is one of the fastest chemical processes known (Hagfeldt & Grätzel 2000). The another desirable reaction, the regeneration of the dye by I^- is also a very fast reaction occurring in 10 ns in the normal conditions in the DSSC. This is important for obtaining high cycle life for the dye, since lack of adequate conditions for the regeneration leads to dye degradation (Hagfeldt & Grätzel 2000). The electron percolation through the nanostructured TiO_2 has been estimated to occur in the millisecond to second range (Hagfeldt & Grätzel 1995).

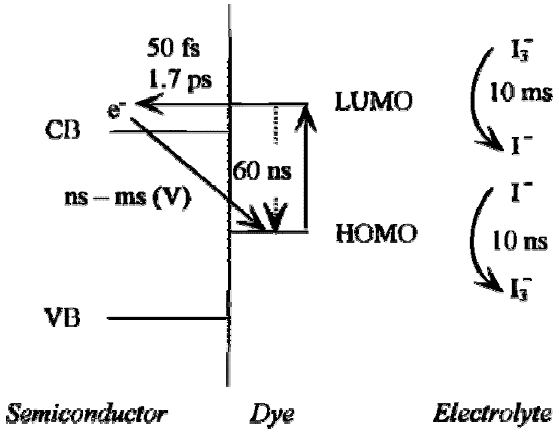

Figure 12. Kinetics in the DSSC, showing by arrows excitation of the dye from the HOMO to the LUMO level, relaxation of the exited state (60 ns), electron injection from the dye LUMO level to the TiO_2 conduction band (50 fs - 1.7 ps), recombination of the injected electron with the hole in the dye HOMO level (ns - ms), recombination of the electron in the TiO_2 conduction band with a hole (I_3^-) in the electrolyte (10 ms), and the regeneration of the oxidized dye by I^- (10 ns). Picture from (Hagfeldt & Grätzel 2000).

4 Materials of the dye-sensitized solar cell

In this Chapter an engineering point of view is taken to the preparation of the standard DSSCs. Materials used in the literature in the different cell components are reviewed and the key material properties required for the cell components as well as some essential preparation methods are discussed.

Going through the literature, it becomes evident, that the components of the state-of-the-art dye-sensitized solar cell have changed relatively little since its inventing over ten years ago. The development has concentrated on the one hand to the tuning of the properties of the original components, such as the morphology and surface properties of the TiO_2 electrode and the chemical composition of the electrolyte. On the other hand new alternative materials and methods such as solid electrolytes and plastic substrates have been explored. These promising new research directions are discussed in the Chapter 5, while this Chapter introduces the materials of the standard DSSCs technology based on a liquid electrolyte and glass substrates.

4.1 Substrates

The electrodes of the standard DSSC are prepared onto transparent conducting oxide (TCO) coated glass substrates, between which the cell is assembled. The conducting coating of the substrate works as a current collector and the substrate material itself both as a support structure to the cell and as a sealing layer between the cell and the ambient air.

Fluorine-doped tin oxide (SnO_2:F) and indium tin oxide (In_2O_3:Sn or ITO) are the most frequently used TCOs in thin film photovoltaic cells. The standard preparation procedure of the nanostructured TiO_2 electrode includes sintering of the deposited TiO_2 film at 450-500 °C. As the only TCO coating stable at these temperatures (Gordon 2000), the SnO_2:F has been the material of choice for DSSCs.

The choice of sheet resistance of the SnO_2 -coated glass plates is a compromise between conflicting beneficial properties of the TCO-coated glass: the higher the conductance the lower the transmittance and vice versa. For example Sustainable Technologies International has optimized the performance of their cells by using Libbey Owens Ford (LOF) TEC 15 (15 Ω/sq) in the working electrode (TiO_2) for

high transmittance and TEC 8 (8 Ω/sq) in the counter-electrode for high conductance[14].

The SnO_2:F -coated glass plates can be purchased from several commercial manufactures such as Libbey Owens Ford (e.g. Chmiel et al. 1998), Asahi (e.g. Deb et al. 1998), Pilkington (e.g. Hagfeldt et al. 1994) and Nippon Sheet Glass (e.g. Barbé et al. 1997) to only mention a few. Since the technology is well established, the details of the production methods of the TCO-coatings are usually not of interest to a cell designer and will therefore not be discussed in this study.

An alternative to the glass substrates is TCO coated plastic foils, which has been introduced and studied especially the commercialization of the dye solar cell in mind. The plastic substrates are discussed in Chapter 5.2.2.

4.2 Nanoparticle electrodes

4.2.1 Oxide semiconductors

Oxide semiconductors are preferential in photoelectrochemistry because of their exceptional stability against photo-corrosion on optical excitation in the band gap (Kalyanasundaram & Grätzel 1998). Furthermore, the large band gap (>3 eV) of the oxide semiconductors is needed in DSSCs for the transparency of the semiconductor electrode for the large part of the solar spectrum.

In addition to TiO_2, semiconductors used in porous nanocrystalline electrodes in dye-sensitized solar cells include for example ZnO, CdSe, CdS, WO_3, Fe_2O_3, SnO_2, Nb_2O_5, and Ta_2O_5 (references in Hagfeldt & Grätzel 1995). However, titanium dioxide has been, and still is, the cornerstone semiconductor for dye-sensitized nanostructured electrodes for DSSCs.

TiO_2

Two crystalline forms of TiO_2 are important, anatase and rutile. Anatase appears as pyramid-like crystals and is stable at low temperatures, whereas needle-like rutile crystals are dominantly formed at high temperature processes. Single crystals of TiO_2 also have rutile structure. The densities are 3.89 g/cm^3 and 4.26 g/cm^2 for anatase and rutile respectively. Rutile absorbs ca. 4% of the incoming light in the near-UV region, and band gap excitation generates holes that act as strong oxidants reducing

[14] See http://www.sta.com.au/sol_cell.htm

the long-term stability of the dye-sensitized solar cells. The third crystalline form of TiO_2, brookite, is difficult to produce and is therefore not of practical interest for the dye solar cells. The band-gaps of the crystalline forms are 3.2 eV (the absorption edge at 388 nm) for anatase and 3.0 eV (the absorption edge at 413 nm) for rutile (Kalyanasundaram & Grätzel 1998).

Anatase has been the main subject of study in DSSCs since it is the primary crystal formed in the usual colloidal preparation method of the nanostructured TiO_2 electrodes (Barbé et al. 1997). However recent study revealed that dye-sensitized nanostructured TiO_2 electrodes with pure rutile structure exhibited only 30% smaller short circuit photocurrents than pure anatase films and practically equal open circuit photovoltages (Park et al. 2000).

4.2.2 Preparation of nanostructured TiO_2 electrodes

In the standard preparation method, the nanostructured TiO_2 electrodes are deposited from a solution or a paste containing TiO_2 nanoparticles of desired size. Mastering the properties of the nanoparticle solutions and the nanoparticle films obtained from these solutions belongs to the fields of colloid and sol-gel chemistry, which have been the essential enabling technologies for the development of high efficiency DSSCs.

Some important topics of preparing nanostructured TiO_2 electrodes for the DSSCs will be highlighted next. Details of the preparation steps can be found for example in the references (O'Regan & Grätzel 1991, Nazeeruddin et al. 1993, Smestad et al. 1994, Deb et al. 1998, Barbé et al. 1997 and Kalyanasundaram & Grätzel 1998).

Synthesis of colloidal TiO_2 solutions

The final properties of the nanostructured TiO_2 electrode are highly dependent on the properties of the colloidal[15] solution used for the film deposition. Kalyanasundaram and Grätzel (1998) have summarized the preparation procedure of the TiO_2 colloid solution developed at the EPFL as follows[16]:

1. Precipitation (hydrolysis of Ti-alkoxides, using 0.1 M HNO_3),
2. Peptization (heating at 800°C for 8 h) followed by filtering,
3. Hydrothermal growth/autoclaving (12 h, 200-250 °C),

[15] Colloids are small particles with radius below 1000 Å and they give clear solutions (Hagfedlt & Grätzel 1995).
[16] A detailed description of these steps can be found in the references of (Kalyanasundaram & Grätzel 1998).

4. Sonication (ultrasonic bath, 400W, 15 × 2 s)
5. Concentration (45°C, 30 mbar), and
6. Binder addition (Carbowax/PEG, M_w 20 000).

By carefully controlling each of these steps monodispersed particles of desired size, crystal structure and other properties are obtained. For example the optical properties of the electrodes depends on the autoclaving temperature of the colloid used: electrodes made from colloids autoclaved at or below 230°C are transparent whereas with higher autoclaving temperatures translucent or opaque electrodes are obtained. Transparent electrodes are used in electrochromic display applications and opaque electrodes in the solar cells. (Kalyanasundaram & Grätzel 1998).

The influence of the processing parameters of the TiO_2 paste preparation to the obtained TiO_2 film porosity, pore-size distribution, light scattering, and electron percolation in the film and thus to the solar cell efficiency has been investigated in more detail by Barbé et al. (1997).

Using commercial TiO_2 powders

Preparing the colloidal TiO_2 solution via a lengthy and delicate synthesis described above is fortunately not prerequisite for reasonably high energy conversion efficiencies in the dye cell. In fact, as recognized already by Nazeeruddin et al. (1993) and verified by Hagfeldt et al. (1994) well performing TiO_2 electrodes can be made by using pastes prepared from commercial TiO_2 powders. Powders used or tested in literature include for example P25 and F387 from Degussa AG (Kalyanasundaram & Grätzel 1998), H37 from Transcommerce International AG, AK1 and PK5585 from Bayer AG (Wienke et al. 1997) and SDS729 from SCM Chemicals Ltd. (Stanley et al. 1998). From these the P25 is the most frequently used. The crystal structure of P25 is about 70% anatase and 30% rutile and it is produced by flame hydrolysis of $TiCl_4$ (Nazeeruddin et al. 1993).

In the paste preparation the aggregated TiO_2 particles in the commercial TiO_2 powder are dispersed by grinding in a mortar with particle stabilizers (such as acetylacetone or HNO_3 in water) to prevent reaggregation of the particles. Detergents (such as Triton ™X-100) are added to lower the surface tension of the colloid in order to facilitate easier spreading onto the conducting glass plate. (Kalyanasundaram & Grätzel 1998).

Wienke et al. (1997) investigated the dependence of the cell efficiency on the microstructure of the nanostructured electrodes prepared from different commercial TiO_2 powders and on the composition of the TiO_2 paste. While the microstructure of

the electrodes prepared from different powders differed significantly, it caused only small differences in the cell efficiencies. Instead, the paste composition was found to be more important factor for the cell performance.

Depositing the TiO_2 layer on the glass plate

The colloid is deposited on conducting glass either by tape casting technique[17], screen printing (Kalyanasundaram & Grätzel 1998), or spray painting (Hagfeldt et al. 1994), and sintered in 450°C for 30 minutes. The sintering is needed to burn out organic binders and surfactants and to establish a good electrical contact between adjacent TiO_2 particles in the porous layer as well as between the TiO_2 electrode and the conducting SnO_2:F layer. A heating rate of 20°-50°C/min has been mentioned (Barbé et al. 1997). Increasing the sintering temperature increases the average pore size in the TiO_2 layer. A roughness factor[18] of about 1000 has been estimated for a 10 μm thick TiO_2 film (Kalyanasundaram & Grätzel 1998).

Finishing the TiO_2 electrode by an additional TiO_2 layer of high purity

Deposition of an additional TiO_2 layer to the porous TiO_2 layer improves significantly the cell performance (Kalyanasundaram & Grätzel 1998). This can be done by immersing the TiO_2 electrode into solution of TiCl4 in ice water (e.g. 0.2 M solution) for a period from one hour (Smestad et al. 1994) to two days (Deb et al. 1998) followed by firing at 450°C for 30 min. Instead of $TiCl_4$, also titanium butoxide can be used (Smestad et al. 1994). Alternatively, the TiO_2 top layer can be deposited electrochemically by anodic oxidative hydrolysis of $TiCl_3$ (Kavan et al. 1993). This treatment causes nucleation of nanometer sized TiO_2 particles of high purity onto the TiO_2 particles (Nazeeruddin et al. 1993).

Barbé et al. (1997) presumed that one probable reason for the increased performance of the cell after the $TiCl_4$ treatment is the enhanced necking of the TiO_2 nanocrystalline particles: Titanium complexes from the $TiCl_4$ solution condense at the interparticle necks and lower the recombination probability of the electrons leading thereby to a global increase of the current. Park et al. (1999) reported that the $TiCl_4$ treatment resulted in a rutile top layer on the anatase TiO_2 particles, increased film thickness and enhanced light scattering properties of the film, which were presumed to explain in part the observed improved cell performance.

---

[17] The method is also called doctor blading or squegee printing and is described in Chapter 7.

[18] Roughness factor is the ration of actual (internal) surface area to the geometrical (flat plate) area of the electrode.

Reducing recombination by surface treatment

Dark current arises in the dye cell from the recombination of charge carriers by reduction of I_3^- at the dye-free sites at the TiO_2 particle surfaces and, at least in principle, at the TCO-coated electrode exposed to the electrolyte through the pores of the nanoporous electrode (see Chapter 3.2.4). The dark current reduces the maximum cell voltage obtainable, and of course the photocurrent, and it should be minimized by the design of the potential recombination interfaces.

In order to reduce the possible dark current at the TCO - electrolyte interface, a TiO_2 underlayer can be deposited to the conducting glass substrate before the deposition of the porous TiO_2 layer (Kavan et al. 1993). However, only small (Kavan et al. 1993) or non-noticeable (Lee et al. 2001) improvement in cell performance have been reported for this treatment.

Alternatively, soaking the dye-coated electrode in 4-*tert*-butylpyridine (TBP) (for 15 min, Deb et al. 1998) has been found to improve significantly the fill factor and open circuit voltage of the cell (Kalyanasundaram & Grätzel 1998, Huang et al. 1997) via passivation of the dye-free recombination sites on the TiO_2 particles. Also results showing only minor improvements from TBP treatment have been presented (Stanley et al. 1998). The effectiveness of the TiO_2 surface treatment only supports the findings that the recombination occurs mainly by loss of electrons from the TiO_2 and not from the TCO coating of the glass substrate (see Chapter 3.2.4).

Interesting practical results can be found from the long-term stability tests conducted at the Energy Research Centre of the Netherlands ECN (Rijnberg et al. 1998). Cells with electrodes treated with TBP showed decrease in the cell performance, whereas untreated cells showed increase in their initially lower performance, compared to TBP-treated cells. After 200 hours the performance of both cells were similar. Furthermore, TBP was found to protect the cells from the usually destructive effect due to presence of water and ethanol in the cell (Rijnberg et al. 1998).

Treatment of the dye-coated electrode by other pyridines (Huang et al. 1997) and ammonia (Deb et al. 1998, Schlichthörl et al. 1997) has also shown improvement of the cell performance.

Properties of the nanostructured TiO_2 electrodes

The efficiency of the DSSC depends significantly on the properties of the nanostructured TiO_2 electrodes, and it may not be exaggerated to say that the art of preparing high efficiency DSSCs is the art of controlling the morphology and interfacial properties of the TiO_2 electrode. The interdependence of the properties of

the TiO_2 film and the performance of the cell are diverse. For example, the internal surface area of the film determines the dye uptake, the pore size distribution affects the ion diffusion, the particle size distribution determines the optical properties, and the electron percolation depends on the interconnection of the TiO_2 particles. When the nanoparticles are stacked in a continuous network in the electrode, these effects become related and optimization of the properties with respect to cell performance arises as a key issue (e.g. Barbé et al. 1997).

Other preparation methods of nanostructured TiO_2 electrodes

Other reported methods for the preparation of nanostructured TiO_2 electrodes include the sol-gel technique (Burnside et al. 1998, Li et al.1999, Srikanth et al. 2001), sputter deposition (Gómez et al. 1999, 2000), spray pyrolysis (Okuya et al. 2001), and a pressing technique (Lindström et al. 2001a, see Chapter 5.2.2). Cell efficiency of about 1.4% was reported for the sol-gel method (Li et al.1999), 3.2% for the spray pyrolysis (Okuya et al. 2001), and about 7% (at 10 mW/cm^2) for the sputter deposition, which is already comparable to the efficiencies reached by the colloidal solution deposition method.

The sol-gel technique used by Burnside et al. (1998) should also be mentioned. With this method rod-like TiO_2 nanocrystals were prepared that self-organized into a porous structure with the nanorods perpendicular to the substrate. This structure could offer desired directionality for the electron transport in the TiO_2 electrode, which could result in a faster photoresponse and higher electron collection efficiencies.

4.3 Sensitizer dyes

As discussed above, the absorption of incident light in the DSSCs is realized by specifically engineered dye molecules placed on the semiconductor electrode surface. To achieve a high light-to-energy conversion efficiency in the DSSC, the properties of the dye molecule as attached to the semiconductor particle surface are essential. Such desirable properties can be summarized as:

1. *Absorption:* The dye should absorb light at wavelenghts up to about 920 nanometers, i.e. the energy of the exited state of the molecule should be about 1.35 eV above the electronic ground state corresponding to the ideal band gap of a single band gap solar cell (Green 1982 p. 89).
2. *Energetics:* To minimize energy losses and to maximize the photovoltage, the exited state of the adsorbed dye molecule should be only slightly above the

conduction band edge of the TiO_2, but yet above enough to present an energetic driving force for the electron injection process. For the same reason, the ground state of the molecule should be only slightly below the redox potential of the electrolyte. See Chapter 3.2.2.

3. *Kinetics:* The process of electron injection from the exited state to the conduction band of the semiconductor should be fast enough to outrun competing unwanted relaxation and reaction pathways. The excitation of the molecule should be preferentially of the MLCT-type. See Chapters 3.2.1 and 3.2.5.
4. *Stability:* The adsorbed dye molecule should be stable enough in the working environment (at the semiconductor-electrolyte interface) to sustain about 20 years of operation at exposure to natural daylight, i.e. at least 10^8 redox turnovers (Hagfeldt & Grätzel 2000).
5. *Interfacial properties:* good adsorption to the semiconductor surface
6. *Practical properties:* e.g. high solubility to the solvent used in the dye impregnation.

These can be considered as the prerequisites for a proper photovoltaic sensitizer. However, the factors that actually make the dye-sensitization work efficiently and yield good photovoltaic performance in the practical cell are much more complicated with all the details not even fully understood at the moment (See Chapter 3.2).

Absorption of light by other cell components such as the TiO_2 and the electrolyte is undesirable, because it on one hand does not lead to current generation and reduces thereby the efficiency, and on the other hand may induce side reactions with possibly degrading effects on the cell performance in the long term.

Dyes

The breakthrough in the dye-sensitization of semiconductor electrodes for solar cells was made at EPFL laboratories at the Grätzel group by the use metallo-organic ruthenium complexes along with nanostructured TiO_2 electrodes. For example dyes having the general structure $ML_2(X)_2$, where L stands for 2,2´-bipyridyl-4,4´-dicarboxylic acid, M for ruthenium or osmium and X for halide, cyanide, thiocyanate, or water have been found promising (Hagfeldt & Grätzel 2000, Sauvé et al. 2000). Among these the *cis*-$RuL_2(NCS)_2$, also called the N3 dye has shown superior performance and has been the top choice for dye-sensitized solar cells for long.

Recently, the tri(cyanato)-2,2´,2´´-terpyridyl-4,4´,4´´-tricarboxylate)ruthenium(II) named black dye (Nazeeruddin et al. 1997), has exceeded the performance of the N3

dye extending the spectral response further to the infrared wavelenghts and yielding the record cell efficiency of 10.4% (Hagfeldt & Grätzel 2000). (See Figure 9 and Figure 11).

Dye impregnation of the electrodes

The dye molecules are adhered onto the nanostructured TiO_2 electrode by immersing the sintered electrode into a dye solution, typically $2 \cdot 10^{-4}$ M in alcohol (Kalyanasundaram & Grätzel 1998), for a long enough period to fully impregnate the electrode. During the impregnation process the electrode is sensitive to water (e. g. Hagfeldt et al. 1994). To minimize water vapor content inside the pores of the electrode, the electrode should be warm upon immersion to the dye solution. The impregnation process lasts from one to several hours depending on the TiO_2 layer thickness and whether the dye solution is heated or kept in room temperature (Solaronix 2000).

4.4 Electrolytes

The electrolyte used in the DSSCs consists of iodine (I^-) and triiodide (I_3^-) as a redox couple in a solvent with possibly other substances added to improve the properties of the electrolyte and the performance of the operating DSSC.

I^-/I_3^- redox couple

Wolfbauer et al. (2001) have listed the ideal characteristics of the redox couple for the DSSC electrolyte:

1. Redox potential thermodynamically (energetically) favorable with respect to the redox potential of the dye to maximize cell voltage;
2. High solubility to the solvent to ensure high concentration of charge carriers in the electrolyte;
3. High diffusion coefficients in the used solvent to enable efficient mass transport;
4. Absence of significant spectral characteristics in the visible region to prevent absorption of incident light in the electrolyte;
5. High stability of both the reduced and oxidized forms of the couple to enable long operating life;
6. Highly reversible couple to facilitate fast electron transfer kinetics;
7. Chemically inert toward all other components in the DSSC.

Since the discovery of the DSSC about ten years ago (O'Regan & Grätzel 1991) no redox couple preceding the performance of the I^-/ I_3^- couple in the DSSC has been discovered (Wolfbauer et al. 2001). The I^-/ I_3^- redox electrolyte is prepared by adding I_2 to the solvent together with some iodine salt such as KI (O'Regan & Grätzel 1991), LiI (Hagfeldt et al. 1994), alkyl methylimidazolium iodide (Deb et al. 1998) and methyl-hexylimidazolium iodide MHImI (Chmiel et al. 1998).

A resent report by Wolfbauer et al. (2001) clearly highlights the importance of the cation of the iodine salt to the performance of the DSSC. The photocurrent output was found to increase linearly with decreasing cation radius, the smallest cations Li^+ and K^+ showing the best performance. The results also showed that the relative concentration of I_3^- to I^- in the electrolyte is an important factor to the cell performance.

Solvent

Stanley et al. (1998) have given a number of criteria for a suitable solvent for a high efficiency liquid electrolyte DSSC:

1. The solvent must be liquid with low volatility at the operating temperatures (-40°C - 80°C) to avoid freezing or expansion of the electrolyte, which would damage the cells;
2. It should have low viscosity to permit the rapid diffusion of charge carriers;
3. The intended redox couple should be soluble in the solvent;
4. It should have a high dielectric constant to facilitate dissolution of the redox couple;
5. The sensitizing dye should not desorb into the solvent;
6. It must be resistant to decomposition over long periods of time;
7. And finally from the point of view of commercial production, the solvent should be of low cost and low toxicity

Examples of the solvents used in the electrolytes in DSSCs are: acetonitrile (O'Regan & Grätzel 1991), methoxyacetonitrile (Ferber et al. 2000), methoxypropionitrile (Rijnberg et al. 1998), glutaronitrile (Kohle et al. 1997), butyronitrile (Kay & Grätzel 1996), ethylene carbonate (O'Regan & Grätzel 1991) and propylene carbonate (Smestad et al. 1994).

The solvent used already in the early DSSCs, acetonitrile, seems to be still the best choice when the cell efficiency is to be maximized. However, with respect to the preferred solvent properties listed above, acetonitrile immediately fails at least in two

points. Firstly, it is highly volatile with boiling point of 82°C, which is about the maximum temperature that a roof-top solar cell can reach at full sunlight (Kay & Grätzel 1996), and due to the high volatility it easily escapes from the cell through the sealing. Secondly, acetonitrile is highly toxic and carcinogenic chemical and cannot be used in the commercial DSSCs (Chmiel et al. 1998). The choice of solvent is thus always a trade-off between low viscosity with better ion diffusion properties and high viscosity with ease of manufacturing and less stringent sealing requirements (Papageorgiou et al. 1996).

Papageorgiou et al. (1996) have demonstrated the excellent properties of room temperature molten salts, such as MHImI, functioning both as a high viscosity solvent and iodine salt for the electrolyte. These molten salt electrolytes are good candidates for low power DSSC applications due to their demonstrated long-term stability in sealed cells (Papageorgiou et al. 1996).

Among all other solvents methoxypropionitrile seems arise as a potential candidate for the commercial DSSCs. In contrast to acetonitrile and propionitrile it is nontoxic and has a boiling point of 160°C (Chmiel et al. 1998). Indeed, it also seems to be the solvent chosen by the Sustainable Technologies International (STI)[19].

Additives

The performance and stability of the DSSC can be enhanced to some extent by adding specific compounds to the electrolyte.

One example is the optical properties of the electrolyte. Triiodide absorbs light below 500 nm, so the triiodide concentration in the electrolyte must not be too high. This filtering effect can be avoided by using a base, e.g. tetrabutylammoniumhydroxide (TBAOH), which converts the light absorbing I_3^- complexes into colorless IO^- ions, which are reduced to $I^- + OH^-$ at the counter-electrode. The use of TBAOH often leads to improved cell efficiencies. (Kay & Grätzel 1996).

Another important purpose of the modification of the electrolyte composition is to enhance the long-term stability of the cells under operation (see Chapter 5.1.2). All in all the chemical composition and properties of the electrolyte plays a significant role in the operating and performance of DSSCs (Rensmo et al. 1996, Hara et al. 2001b).

[19] See http://www.sta.com.au/sol_cell.htm

4.5 Counter-electrode catalysts

For sufficiently fast reaction kinetics for the triiodide reduction reaction at the TCO coated cathode, a catalyst coating is needed.

Platinum

As a traditional and usually most efficient catalyst, platinum has been used almost exclusively in the literature. However, the performance of the catalyst layer depends on the method by which the Pt is deposited onto the TCO surface. Platinum catalyst coating has been performed for example electrochemically (e.g. Hagfeldt et al. 1994, Smestad et al. 1994), by sputtering (Nazeeruddin et al. 1993), pyrolytically (Chmiel et al. 1998) or by spin coating (Lee et al. 2001). Electrochemically (Papageorgiou et al. 1997) and vapor deposited (Olsen et al. 2000) Pt has been however found unstable in the presence of the iodide electrolyte.

Papageorgiou et al. (1997) developed an alternative Pt catalyst coating method called "platinum thermal cluster catalyst". This catalyst provided superior kinetic performance with respect to conventional platinum deposition methods, chemical and electrochemical stability in practical cells, low platinum loading of 5-10 $\mu g/cm^2$ leading to cost reduction, mechanical stability of the counter-electrode surface and optical transparency of the counter-electrode due to the low platinum content (Papageorgiou et al. 1997). The thermal Pt catalyst method also seems to be chosen for the DSSC modules by Sustainable Technologies International (STI)[20].

Carbon

While shoving excellent catalytic action, platinum has the disadvantage of being very expensive. Kay and Grätzel (1996) have developed a cell design, which is very interesting with this respect. The design utilizes a porous carbon counter-electrode as a catalyst layer. This carbon electrode is made from a mixture of carbon black, graphite powder and nanocrystalline TiO_2 particles. A high conductivity (sheet resistance of 5 Ω/sq for a 50 μm thick layer) is obtained due to the carbon black particles connecting together separate graphite flakes, while the TiO_2 particles are used as a binder to the structure. It is claimed that thanks to the very high surface area of these electrodes, caused by the carbon black, these electrodes are as active for triiodide reduction as the conventional Pt electrodes. (Kay & Grätzel 1996).

[20] See http://www.sta.com.au/sol_cell.htm

4.6 Electrical contacts

Similarly to the amorphous silicon and the other thin film solar cells deposited on TCO coated glass, the design of dye cells and modules is affected by the limited conductivity of the TCO layer. To keep the resistive losses in the TCO layer reasonably low, the longest distance from a photoactive point to a current collector should not exceed about 1 cm (Kay & Grätzel 1996, McEvoy et al. 1998). For example silver paint and adhesive copper tape (Hagfeldt et al. 1994) can be used to extend the contact area of the current collector to fulfill this geometric requirement. In test cells alligator clips can be easily attached to these conductor strips.

A iodine based electrolyte is highly corrosive attacking most metals, such as silver, aluminum, copper, nickel and even gold, and can thus be particularly problematic when it comes to designing an electrical contacting of single cells in an integrated DSSC module (Kay & Grätzel 1996, Chmiel et al. 1998).

4.7 Sealing

Sealing the DSSCs has long been a difficult question because of the corrosive and volatile liquid iodide electrolyte used in the cells. Being directly related to the long-term stability of the cells it seems to be one of the main technological challenges of the DSSC technology (Pettersson & Gruszecki 2001). A suitable sealing material should at least

1. be leak-proof to the electrolyte components and impermeable to both ambient oxygen and water vapor,
2. be chemically inert towards the electrolyte and other cell components, and
3. adhere well to the glass substrate and TCO coating.

Several sealing materials have been used, such as epoxy glue (e.g. Kohle et al. 1997, Grünwald & Tributsch 1997), water glass (sodium silicate) (e.g. Kay & Grätzel 1996), an ionomer resin Surlyn® (grade 1702) from Du Pont (e.g. Kohle et al. 1997, Deb et al. 1998), aluminum foil laminated with polymer foil (Kay & Grätzel 1996, Burnside et al. 2000), a vacuum sealant Torr Seal® (e.g. Krüger et al. 2001), or a combination of these. Especially for research purposes sealing techniques based on O-rings (Späth et al. 1997, Wolfbauer et al. 2001) and glass soldering (e.g. Späth et al. 1997) have been developed.

One important question when selecting the sealant is the tolerance of the sealing material towards iodide and triiodide in the electrolyte. Interestingly, despite the fact

that the often used sealant, the Surlyn® ionomer resin from Du Pont, has been classified by the manufacturer as not resistant towards iodine (in KI solution) in long term exposure[21], stable long term operation has been demonstrated for DSSCs utilizing Surlyn® sealing with iodide electrolyte (e.g. Kohle et al. 1997).

At the moment a new sealing technique for low-power indoor DSSC applications is being patented and waiting to be published (Pettersson & Gruszecki 2001).

[21] See http://www.dupont.com/industrial-polymers/surlyn/E-78676-3.html

5 Performance and applications of the dye-sensitized solar cells

5.1 Performance of the dye-sensitized solar cells

5.1.1 Energy conversion efficiency

The high energy conversion efficiencies performed by the dye-sensitized solar cells has naturally been one of the reasons for the rapidly expanded interest in the DSSC research. Several published results are listed in Table 1. The Grätzel's group have reported the highest efficiencies (Green 2001, Grätzel 2000, Nazeeruddin et al. 1993, O'Regan & Grätzel 1991), and in the sort of Hall of Fame of photovoltaic cells, The Solar Cell Efficiency Tables (Green 2001), a top efficiency of 11±0.5% has been recorded as measured at FhG-ISE in 1996.

An efficient charge transfer sensitizer dye is prerequisite for high efficiency in the DSSCs, as discussed in Chapter 4.3. While the dyes developed at the Grätzel group hold the state-of-the-art, it is interesting to notice that also natural dyes extracted from berries has been demonstrated in DSSCs with 0.56% cell efficiency (Cherepy et al. 1997).

Attempts to replace the TiO_2 with some other large band-gap semiconductor, such as In_2S_3/In_2O_3 (Hara et al. 2000b), SnO_2 (Fungo et al. 2000), ZnO (Bedja et al. 1997, Rensmo et al. 1997, Hara et al. 2000a), Nb_2O_5 (Sayama et al. 1998), CdS and CdSe (Hodes et al. 1992), has in general not been very successful (Table 2). There is however at least one significant exception. Tennakone et al. (1999) reported 8% efficiency measured at 90 mW/cm^2 direct sunlight for a DSSC utilizing a mixture of ZnO and SnO_2 as the nanostructured photoelectrode sensitized with the N3 dye.

Table 1. Some of the best or otherwise interesting performance results from the dye-sensitized nanostructured TiO_2 solar cells (laboratory scale) shoving the used dye, the cell efficiency, the reported area of the cell and the used illumination in the efficiency measurement.

Semi-conductor	Dye	η (%)	area (cm^2)	illumination (mW/cm^2)	reference
TiO_2	?	11	0.25	100 (AM1.5)	Green 2001
TiO_2	Black Dye	10.4	?	100 (AM1.5)	Grätzel 2000
TiO_2	N3	10.0	0.3	96 (AM1.5)	Nazeeruddin et al. 1993
TiO_2	N719[22]	9.2	1.5	? (AM1.5)	Deb et al. 1998
TiO_2	$RuL_2(\mu\text{-}(CN)Ru(CN)L''_2)_2$	7.1	0.5	75 (AM1.5)	O'Regan & Grätzel 1991
		7.9		8 (AM 1.5)	
TiO_2	N3	6	1	100 (ELH lamp)	Hagfeldt et al. 1994
		7.3		11.5 (ELH lamp)	
TiO_2	A Ru -phenantroline derivative	6.1	0.44	100 (AM 1.5)	Yanagida et al. 2000
TiO_2	a coumarin derivative	5.6	?	100 (AM1.5)	Hara et al. 2001a
TiO_2	Cu-2-α-oxymesoisochlorin	2.6	0.5	100 ("white light")	Kay & Grätzel 1993
TiO_2	A natural cyanin-dye	0.56	0.9	100 (AM1.5)	Cherepy et al. 1997

L = 2,2'-bipyridyl-4,4'-dicarboxylic

L'' = 2,2'-bipyridine

Table 2. Some results reported using other semiconductors than TiO_2 in the DSSC shoving the used dye, the cell efficiency, the reported area of the cell and the used illumination in the efficiency measurement.

Semi-conductor	Dye	η (%)	area (cm^2)	illumination (mW/cm^2)	reference
SnO_2/ZnO	N3	8	1.9	90 ("direct sunlight")	Tennakone et al. 1999
		15		10 ("diffuse daylight")	
ZnO	mercurochrome	2.5	0.09	100 (AM1.5)	Hara et al. 2000a
		1.4	0.25		
Nb_2O_5	N3	2	0.5	100 (AM1.5)	Sayama et al. 1998
ZnO	N3	2	0.25	56 ("solar simulator")	Rensmo et al. 1997

[22] N719 is equal to the N3 having two additional tetrabutylammonium (TBA) groups (http://www.solaronix.ch/products/ruthenium535tba.html)

5.1.2 Long term stability

To become economically viable and commercially feasible technology, the dye-sensitized solar cells should be capable of maintaining non-degrading performance in operating conditions over several years, preferentially tens of years. However, the question of long-term stability of the dye-sensitized solar cells seems to remain unsolved for the time being.

The long term stability of the dye cells can be divided into at least following components:

1. Inherent photochemical stability of the sensitizer dye adsorbed onto the TiO_2 electrode and in interaction with the surrounding electrolyte.
2. Chemical and photochemical stability of the electrolyte.
3. Stability of the Pt-coating of the counter-electrode in the electrolyte environment.
4. Quality of the barrier properties of the sealing of the cell against intrusion of oxygen and water from the ambient air, and against loss of electrolyte solvent from the cell through the sealing.

The interaction of these factors and possibly those not yet discovered makes the situation in the dye cell very complex. The chemical composition of the electrolyte has been observed to change over time by formation of decomposition products of the electrolyte species (Hinsch et al. 2001a) and the dye (Grünwald & Tributsch 1997). These products may furthermore interact with the dye molecules or other species at the TiO_2 - electrolyte interface with deleterious effects to the cell performance in the long term.

Potential sources of degradation in the cell are for example (Hinsch et al. 2001a):

1. photo-chemical or chemical degradation of the dye (e.g. desorption of the dye, or replacement of ligands by electrolyte species or residual water molecules),
2. direct band-gap excitation of TiO_2 (holes in the TiO_2 valence band act as strong oxidants),
3. photo-oxidation of the electrolyte solvent, release of protons from the solvent (change in pH),
4. catalytic reactions by TiO_2 and Pt,
5. failure or inadequate barrier properties of the sealing material,
6. changes in the surface structure of the TiO_2,

7. dissolution of Pt from the counter-electrode, and
8. adsorption of decomposition products onto the TiO_2 and TCO surfaces.

As may be expected, the stability of the dye-sensitized solar cells depends greatly on the designed chemical composition and the materials of the cell as well as on any unwanted impurities possibly included during the preparation of the cells. This is probably the main reason why different research groups have reported somewhat inconsistent stability results in the literature.

High stability for a Ru-based dye was reported already by O'Regan and Grätzel (1991) together with the presentation of the high efficiencies of the dye cell. Grünwald and Tributsch (1997) on the other hand detected the N3 dye unstable in their in-situ IR-spectroscopy studies, and also reported number of other difficulties in the long-term stability of the cells, such as sealing problems and decomposition of the electrolyte. This work was soon criticized by the Grätzel group (Kohle et al. 1997), claiming the reported instability of the dye was due to inadequate conditions for regeneration of the dye, i.e. too low iodide concentration employed in the electrolyte. In addition, measurements showing non-degraded operation of the DSSC after more than 7000 hours of continuous illumination at 1000 W/m^2 light intensity, corresponding to about 6 years of outdoor illumination in central Europe, were reported for cells with efficiencies in the range 1.0-1.5% (Kohle et al. 1997).

Since then the long term stability of the DSSCs has been investigated extensively in an EU-project LOTS-DCS in collaboration between ECN Solar Energy, Freiburg Materials Research Center FMF, Solaronix SA, and Institut für Angewandte Photovoltaik INAP (Hinsch et al. 2000, Ferber et al. 2000). In these studies focussed on the intrinsic chemical stability of the cells, visible light, UV light and temperature were used as stress factors. The main results of these studies are collected in Table 3. The efficiency of the cells studied was around 5% (Hinsch et al. 2001a). The degradation of the cell performance, when observed, was assigned to the degradation of the electrolyte (e.g. methoxyacetonitrile) instead of to the degradation of the dye (Ferber et al. 2000).

From these results it has been concluded that visible light soaking with no or little UV does not affect the cell performance. UV light degrades the cell performance in long term, but tailoring the electrolyte composition (e.g. by adding MgI_2) can reduce this effect significantly. Thermal stability on the other hand can be obtained by choosing the electrolyte solvent correctly (e.g. purified propionitrile). Thermal tests at higher temperatures are however difficult because of sealing problems.

Table 3. Degradation factors and their effects to the cell performance as reported in the literature. Stable means here roughly: "no significant permanent decrease in performance observed".

Temperature	Visible light soaking	UV exposure
Stable power in over 2000 h in the dark at 60°C with purified propionitrile (Hinsch et al. 2001a). 30% decrease in efficiency after 875 h at 85°C with glass frit sealing (Hinsch et al. 2001a). Methoxyacetonitrile unstable above 45°C (Hinsch et al. 2001a). Instability in thermal cycling test with acetonitrile as solvent (Hinsch et al. 2001b)	Stable I_{sc} in over 4000 h at 45 °C and 1000W/m^2 (Meyer et al. 2001). Stability depends on solvent: methoxyacetonitrile unstable, propionitrile more stable with 15% decrease in efficiency after 3400h 1 sun at 45°C (Hinsch et al. 2001a).	Unstable efficiency with 26% decrease after UV dose in 960 h equivalent to 5 years outdoor exposure (Meyer et al. 2001). UV shielding effect by additives such as MgI_2 and CaI_2 (Hinsch et al. 2001a). Also partial recovery of the cell performance observed after UV treatment (Meyer et al. 2001).

Certain chemicals were found to enhance the stability of the cells. Specifically 4-tert-butylpyridine (TBP) was found to increase the tolerance towards water in the electrolyte (Rijnberg et al. 1998), while MgI_2 and CaI_2 increased the tolerance towards UV light (Hinsch et al. 2001a). Pure nitrile based solvents such as acetonitrile and propionitrile were found most stable, and the importance of high chemical purity of the solvent and inert handling was emphasized (Hinsch et al. 2001a).

Exchange of the thiocyanato SCN^- ligands of the dye complex by iodide ions has been observed at extremely high light intensities in resonance Raman scattering measurements, and the stabilizing effect of 4-tert-butylpyridine in the electrolyte has been suggested to be due to suppressing this effect in normal operation conditions (Greijer et al. 2001).

Since UV light may degrade the cell performance in long term operation, the transmittance of the glass plates in the UV region should be checked and the UV light blocked, if necessary, by coating the glass plates for example with an UV absorbing polyester film (Pettersson & Gruszecki 2001). On the other hand UV illumination has also caused significant increase in cell performance (Ferrere & Gregg 2001). It is not yet clear whether this effect has practical importance to the long-term operation of the cells.

Recently elegant degradation studies have been performed at the Hahn-Meitner-Institut in Berlin, Germany (Turrión et al. 1999, Macht et al. 2001). Using spatially

resolved imaging techniques producing photocurrent maps by laser scanning and exposing only defined areas of the cells to light soaking, the light induced degradation of the cells could be separated from the other factors. This method will certainly be useful in further stability and degradation studies. Recently Tributsch (2001) formulated the operation the dye cell analytically covering especially the degradation kinetics of the dye. Based on photodegradation experiments (the referred results not yet published), extrapolated lifetimes of about 2.3 years (defined for 50% of the sensitizer degraded, and calculated for average continuous illumination of 200 W/m^2) were reported for the dye-sensitized solar cells.

In general, it is believed that the long-term stability is not an intrinsic problem of the technology, but can be improved by engineering of the chemical composition of the cells (Hinsch et al. 2001a). While the stability results obtained thus far (Table 3) has to be considered promising, there is still a lot of work left.

The biggest remaining question seems to be the stability at the elevated temperatures to which the cells can be exposed in operation. At these temperatures, perhaps up to 80°C, not only the intrinsic stability of the electrolyte but also the stability of the sealing materials is important. Problems may also arise from increased vapor pressure of the electrolyte, especially with low boiling point solvents generally needed for high efficiencies in the cells. This is also why the development of alternatives for the electrolyte is important for the practical utilization of the dye solar cell technology (see Chapter 5.2.3).

Finally, it has to be mentioned that dye cells are also designed specially for low-power indoor applications where the lifetime requirements are not as stringent as in the outdoor solar module applications, and also the operating conditions are easier. Sufficient stability may be therefore expected for low-efficiency cells, and the first emerging commercial products are expected to be for indoor use (Pettersson & Gruszecki 2001).

5.2 Progress towards applications

5.2.1 Cell and module architectures

Sandwich structure

The standard way of preparing the DSSC in the laboratory is sandwiching the different cell layers between two glass plates, the substrate and the superstrate, the latter being the side through which the cell is to be illuminated, which is usually the

TiO_2 electrode. In this case both glass plates are TCO coated, one supporting the TiO_2 electrode and the other performing as the platinized counter-electrode (Figure 13a). The edges of the cell are sealed with a sealant material (see Chapter 4.7) and the electrical contacts are placed close to the sealant rim to minimize distance from the active electrode area.

To build a module of series connected sandwich cells several issues have to be considered. Due to the limited conductivity of the TCO layer, the width of the cell should not exceed about 1 cm, while the length of the cell is limited only by practical reasons. To minimize manufacturing costs in mass production, the single cells should be prepared between one common glass plate with large surface area, as is already done in commercial thin film modules. In this case both the sealing and the electrical interconnection of the single cells would have to be made by single material as can be seen in Figure 13a. The problem then is to find easily processed material with good barrier properties toward I^- and I_3^- ions[23], high electrical conductivity and resistance to the corrosive electrolyte at the same time. Different interconnection materials (the composition of which were not specified) have been successfully developed and tested by Chmiel et al. (1998) and used to prepare sandwich modules with 7.0% efficiency and over 100 cm^2 active area.

According public information, also the dye solar cell modules of the Sustainable Technologies International STI have the standard sandwich structure, and "coated Ag tracks" are used for the electrical interconnection of the cells[24].

Monolithic structure

To further adapt to the processing benefits of the thin film solar cell technology, and in particular the commercialization of the DSSCs in mind, Kay & Grätzel (1996) developed a three layer monolithic cell structure (Figure 13b). The benefit of the monolithic structure is that all the layers of the cell can be deposited on top of each other on a single TCO coated glass plate, while the opposite glass plate without TCO coating serves merely as a protective barrier and encapsulation. In this invention the counter-electrode is a porous carbon electrode (See Chapter 4.5 for details) separated from the TiO_2 electrode by a porous insulating rutile TiO_2 (Kay & Grätzel 1996) or ZrO_2 (Burnside et al. 2000) interlayer with the electrolyte inside the pores. The TCO layer, contacting the carbon electrode of one cell and the TiO2 electrode of the adjacent cell accomplishes the electrical series connection of the cells.

---

[23] The interconnection-barrier material may be permeable to the electrolyte solvent, but not to the ions, to avoid short circuiting adjacent cells.

[24] See http://www.sta.com.au/sol_cell.htm and http://www.sta.com.au/download/eupres.pdf

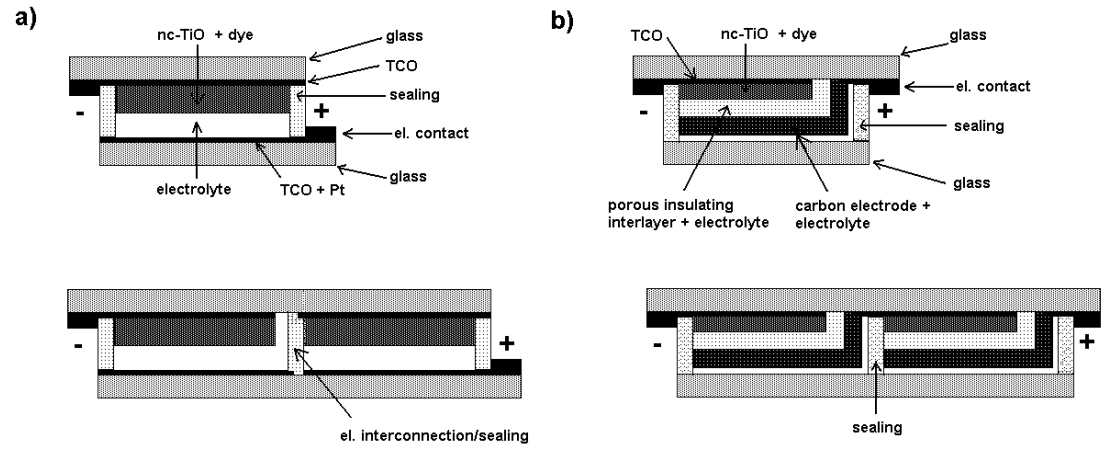

Figure 13. Schematic picture representing the two main DSSC cell (upper) and module (lower) architectures: a) the sandwich structure b) the monolithic structure. The shown module structures require segmentation of the TCO coating and suitable interconnection of the neighboring cells as described in the text. Electrically conducting materials are marked with black and dark color in the picture.

Kay and Grätzel (1996) reported 6.67% efficiency for a single monolithic cell and 5.29% for a small monolithic module. Furthermore, the monolithic cell design has been demonstrated to be suitable for manufacturing DSSC modules by screen-printing for indoor applications, such as for powering electronic price tags for supermarket shelves, successfully competing in performance with the commercially available amorphous silicon cells currently used for this purpose (Burnside et al. 2000).

The monolithic module design has been adopted by Petterson and Gruszecki for low power applications, and has been investigated also by Hinsch et al. (1998).

Finally to mention, He et al. (2000) have demonstrated also a tandem cell structure with a dye-sensitized photocathode and Rousar et al. (1996) have studied the optimization of the geometrical arrangement of a DSSC module.

Table 4. Performance results from DSSC modules with different architectures.

Cell-type	η (%)	area (cm^2)	ill. (mW/cm^2)	comments	reference
sandwich	7	112	?	Module of 12 cells	Chmiel et al. 1998
monolithic	6.7	0.4	100	Single cell	Kay & Grätzel 1996
	7.2		35		
monolithic	5.3	20	100 (AM1.5)	Module of 6 cells	Kay & Grätzel 1996
?	4.7	141.4	100 (AM1.5)	By INAP	Green 2001

5.2.2 DSSCs on plastic substrates

Considering mass production, the use of flexible transparent plastic substrates could offer an advantage over glass substrates. Flexible substrates could be used in continuous roll-to-roll process, making it possible to produce photovoltaic cells in large quantities and at high throughput, and thereby at substantially lower costs. In addition to this, plastic substrate based cells would be lighter, thinner and easier to handle and transport than cells sandwiched between glass substrates.

When replacing the glass substrates in the DSSC by polymer foils, several issues arise.

TCO-coating of the polymer foil

Because polymers cannot stand high temperatures SnO_2:F cannot be used as TCO coating. Instead, ITO can be deposited at low temperatures, e. g. by room temperature sputtering (Sommeling et al. 2000) and is a suitable TCO-coating for the plastic substrates.

Sintering of the TiO_2 film

For the same reason as above, the normal high temperature (450-500 °C) sintering of the nanostructured TiO_2 films has to be replaced by a low-temperature sintering method. The purpose of the high temperature treatment of TiO_2 films is to both sinter the nanoparticles together and to remove surfactants or any other organic additives present in the colloidal TiO_2 solution. The surfactants and additives, for one, are used to render the TiO_2 colloid viscous and easy to deposit, and in some cases to control the porosity of the sintered TiO_2 film.

Pichot et al. (2000a) studied the effect of low temperature (100 °C) sintering of the TiO_2 colloids without using any organic surfactants. TiO_2 films prepared without surfactants could adsorb larger a dye content (due to a larger inner surface area of the films) and adhered better to the SnO_2:F coated glass than those prepared with surfactants (giving possible implications to long term stability issues). Omitting surfactants and sintering at lower temperatures resulted however in reduced performance: a cell with a 1 μm thick TiO_2 film prepared without surfactants and sintered at 100°C was reported to have efficiency of 1.22% under 1 sun illumination (Pichot et al. 2000a).

Pt-catalyst coating

Instead of the usual thermal platinization process of the counter-electrode at 385 °C (Papageorgiou et al. 1997) other platinization methods has to be used, such as galvanic processes and room temperature sputtering (Sommeling et al. 2000). An alternative to this is pressing carbon or platinized SnO_2 powder onto the conducting plastic substrate (Lindström et al. 2001a, 2001b).

Properties of polymer substrates

The polymer substrate used in DSSCs in resent studies has been ITO-coated poly(ethylene terephalate) (PET) (Sommeling et al. 2000, Lindström et al. 2001a, 2001b). However, using polymers as substrate material in DSSC present several problems:

1. Polymers are usually permeable to oxygen and water vapor, which are detrimental substances to the DSSCs (Sommeling et al. 2000).
2. While ITO is the only suitable TCO-material for polymer foils, its exact behavior in the DSSC is uncertain (Sommeling et al. 2000), since almost exclusively SnO_2:F (on glass) has been used in experimental studies.
3. The polymer itself may be unstable in the presence of the electrolyte and release undesirable compounds into the electrolyte (Sommeling et al. 2000).
4. Galvanically deposited Pt may degrade under cell operation (Sommeling et al. 2000, Olsen et al. 2000)

Sommeling et al. (2000) reported that the performance of DSSCs with plastic substrates degraded during time, and attributed it to the degradation of the ITO-coating on PET rather than to the other factors listed above.

A new manufacturing method for nanostructured electrodes on plastic substrates has been introduced and patented by Lindström et al. (2001a, 2001b) in Uppsala University. In this method plastic DSSCs are prepared either by a static or dynamic (roller mill) compression of TiO_2 powder suspension for working electrodes and platinized SnO_2 or carbon powder suspensions for counter-electrodes onto ITO-coated PET-based substrates. A 4.9% efficiency at low illumination level (10 mW/cm^2) with a cell area of 0.19 cm^2 and about 3% efficiency at 1 sun illumination (100 mW/cm^2) was reached with this preparation procedure (Lindström et al. 2001b), and the current baseline efficiency is claimed to be 5 % under 1/10 sun

illumination[25]. An especially important feature of this preparation method is that no heat treatment is needed for the once compressed films. Furthermore, the continuous roller mill compression method could potentially be easily transferred to a large-scale roll-to-roll production line.

5.2.3 Solid state DSSCs

The use of a liquid electrolyte in the dye-sensitized solar cell is problematic for the long-term stability of the cells, because the volatile solvent of the electrolyte leaks easily out of the cell through possible holes or cracks in the sealant. Replacement of the liquid hole transport medium by a solid-state analogue could solve this problem. To avoid significant cell performance losses, the solid electrolyte should at the same time preserve, or successfully replace, the crucial functions of the liquid I^-/I_3^- redox electrolyte. These are fast reduction of the oxidized dye molecules at the TiO_2-electrolyte interface (adequate energy level positioning with respect to the redox potential of the dye), sufficient hole (ion) conductivity, intimate contact to the inner surfaces of the dye-sensitized nanostructured electrode, transparency, stability, and chemical compatibility with the other cell components.

The replacement of the liquid electrolyte in the DSSC by different solid or gel-like electrolytes has been reported in the literature, and a review of the results is presented in Table 5[26]. Tested materials include both true hole conductors, such as p-type inorganic semiconductors and p-type semiconducting polymers, and ionic conductors, such as elastomeric or gel-like electrolytes containing iodine.

Results with true hole conductors have been relatively poor and only recently a moderate efficiency of 2.56% were reported by Krüger et al. (2001) using a spirobifluorene derivative named OMeTAD.

A more successful approach seems to be gelatination of the liquid electrolyte. Cao et al. (1995) reached cell efficiencies of 3-5% by using a polymer gel electrolyte in a standard DSSC configuration (Degussa P-25 TiO_2 powder, N3 dye). The electrolyte was a mixture of polyacrylonitrile, ethylene carbonate, propylene carbonate, acetonitrile, NaI, and I_2, and was said to be flexible and retain its shape, and did not

---

[25] See http://www.asc.angstrom.uu.se/nsc/nsceng.htm

[26] An extensive literature exists describing photovoltaic devices with heterojunctions of variety different materials, some of which could also be considered to have "sensitized photoelectrodes". Table 5 however presents devices with only the electrolyte replaced in the standard nanostructured DSSC cell other components remaining essentially unchanged, i.e. also the dye-layer (usually the N3 dye).

Table 5. Literature review of the results of (quasi-) solid-state DSSCs using different hole transport materials.

Hole transport medium	η (%)	Illum. (mW/cm^2)	area (cm^2)	reference
Organic hole conductors				
Polypyrrole	0.1	22 (Xe lamp)	-	Murakoshi et al. 1998
4CuBr 3S$(C_4H_9)_2$	0.6	100 (≈ AM1.5)	1	Tennakone et al. 2000
Poly(3-octylthiophene) P3OT	0.15	60 ("white light")	0.05	Gebeyehu et al. 2001
OMeTAD	0.74	9.4 ("white light")	-	Bach et al. 1998
OMeTAD	2.56	AM1.5	1	Krüger et al. 2001
Gel or elastomeric electrolytes				
Elastomeric electrolyte*	0.22	120 ("white light")	1	Nogueira & De Paoli 2000
Polymer solid electrolyte**	0.49	100	-	Matsumoto et al. 1996
Polymer gel electrolyte	3-5	30 ("white light")	-	Cao et al. 1995
Polymer gel electrolyte	3.0	100 (AM1.5)	-	Kubo et al. 1998
Polymer gel electrolyte	5.91	100? (AM1.5)	0.25	Kubo et al. 2001
Polymer gel electrolyte	7.3	100 (AM1.5)	-	Mikoshiba et al. 2000
P-type inorganic semiconductors				
p-CuSCN	1.5	100 (AM1.5)	-	O'Regan et al. 2000

* Poly(epi-chlorohydrin-co-ethylene oxide) + NaI/I_2

** Oligoethylene glygol methacrylate + ethylene glygol and LiI

exhibit any significant loss of conductivity (4.5×10^{-3} $\Omega^{-1}cm^{-1}$) after extended exposure to air. Kubo et al. (1998) used amino acid derivatives as low molecular gelators to prepare quasi-solid state DSSCs with 3.0% efficiency and demonstrated, that the gelation successfully suppressed vaporization of the electrolyte solvent. Recently, the same research group further increased the efficiency of the gel electrolyte cell to 5.91% (Kubo et al. 2001).

The state of the art quasi-solid state DSSC has been prepared by Toshiba Corporation, who reported 7.3% cell efficiency for a polymer gel electrolyte cell consisting of imidazolium derivatives, iodide and gelators, the composition of which were not published. The electrolyte had low viscosity before gelation and could penetrate into the pores of the TiO_2 electrode. The gelation was induced by placing the cell in an 80°C oven for 18 minutes, after which the gelation was irreversible up to over 120°C. (Mikoshiba et al. 2000).

While the gelatination of the standard iodide containing electrolyte seems to be a successful direction of development, another interesting approach in the molecular level is to use direct molecular wiring between dye molecules and semiconducting polymers. Murakoshi et al. (1998) demonstrated this principle by synthesizing a dye with ligand groups designed to function as attachment groups for the polymer chains in the polymer hole transport material. It remains to be seen whether this can be done without severely affecting the absorption and charge injection properties of the dye.

5.2.4 Industrial and commercial activities

There are in total eight license holders for the Grätzel patents in the world for the core technology of the DSSCs: INAP (Institut für Angewandte Photovoltaik GmbH), Lechlanché (Greatcell Solar SA), Solaronix SA, Swatch/Asulab, Toyota/IMRA, Solterra SA, Glas Trösch, and Sustainable Technologies International STI (Bossert et al. 2000).

At the time of completing the present study Sustainable Technologies International, STI (former Sustainable Technologies Australia, STA) is preparing to bring the dye-sensitized solar cell technology commercially available. According to a newsletter (SolarAccess 2001b), a first application of the STI technology is planed to be a wall in the new Australian Commonwealth Scientific & Industrial Research Organization (CSIRO) in Newcastle, New South Wales.

Figure 14 shows prototype DSSCs from the STI production line. The STI titania solar wall panel uses 24 series connected 10 cm by 17 cm solar cell tiles (Figure 14 left) encapsulated in transparent insulated polymer and laminated between two glass plates with total panel area of 90 cm by 60 cm and installed rating of 40 W_p per m^2 (STI 2001). An interesting question is whether, or how, the STI has been able to defeat the stability problems generally associated with the technology (see Chapter 5.1.2).

Another visible actor in the field is Solaronix SA, the manufacturer of DSSC materials, especially sensitizer dyes and TiO_2 pastes, and the active developer of the technology. Otherwise however, there is very little public information about the activity towards commercialization of the technology by the other patent licensees.

Due to a good performance in low illumination levels and diffuse light conditions, DSSCs are believed to enter the market first in low-power indoor applications, such as self-powered bathroom scales (Grätzel 1994), light powered watches, or electronic labels for supermarkets shelves.

Figure 14. Left picture: Dye-sensitized solar cell tile from the STI production line (Source: http://www.sta.com.au/newimages/hhtp12.jpg). Right picture: a demonstration of an architectural use of DSSCs by STI (Source: http://www.sta.com.au/images/nz1.jpg). Pictures courtesy of STI. Copyright STI 2001.

5.2.5 Cost estimates and comparison with other photovoltaic technologies

Cost estimates for the DSSC technology

Only little information on the estimated costs for dye-sensitized solar cells is available in the literature, and the given estimates tend to vary a lot. Grätzel (1994) refers to a cost estimate commissioned from the Research Triangle Institute (USA) predicting a module cost of US \$0.60/W_p. No background information for this figure was given. Hanke (1999) on the other hand refers to calculations by INAP estimating manufacturing costs of 1.5-3.8 DM/W_p (about US \$3.2-8.3/W_p).

Smestad et al. (1994) and Solaronix SA (Meyer 1996) have presented more detailed estimates for the manufacturing costs of DSSC modules, and the data from these two studies is collected in Table 6 for a comparison. Solaronix estimated manufacturing costs of about 2.2 \$/W_p for a 5% efficient modules, while Smestad et al. ended up to a lower cost of about 1-1.3 \$/W_p[27]. However, as can be seen by inspection of Table 6, the data given by the two authors differ from each other quite substantially. In fact, some ambiguity seems to exist. For example the over \$30/m^2 cost for protective overcoats and connections estimated by Solaronix is very much higher than estimated by Smestad et al. (\$2-\$3/m^2).

[27] The original cost estimated by Smestad for 8-10% efficient cells is scaled here for 5% cell efficiency for comparison.

Table 6. Estimated manufacturing costs for DSSCs (Smestad et al. 1994, Meyer 1996).

Smestad et al. 1994	**US $/ m^2**	**Solaronix SA (Meyer 1996)[28]**	**US $/m^2**
TiO_2 (10g/m^2)	0.03	Anatase screen printable paste	5.0
Ru-dye (100 mg/m^2 adsorbed)	7-10	Ru-dye	10.0
Pt catalyst (3 monolayers)	0.01	Pt catalyst	1.7
Electrolyte and iodide (50 ml/m^2)	0.1-1	Electrolyte and iodide salt	0.5
SnO_2:F Glass (10 Ω/sq)	30	SnO2:F Glass (10 Ω/sq)	30.0
Encapsulation and sealing	2-3	Sealant (primary + plugs)	3.0
Frame and electrical interconnections	2	Interconnect + contacts	5.0
Protective glass cover and Tedlar backing	2-3	Protective overcoats and connections	33.3
Materials subtotal	**43-49**	**Materials subtotal**	**88.5**
Production overhead	5-7	Rent floor space	0.9
Labor (100 people)	0.3-0.5	Labor (12 people)	13.2
Profit, Interest due top loans	0-8	Depreciation (20%)	8.0
Total module cost ($/m2)	**48-64**	**Total module cost ($/m2)**	**110.6**
Module efficiency	8-10 %	Module efficiency	5 %
Cost ($/Wp)	0.48-0.80		
Cost per W_p at 5% eff. ($/Wp)	**0.96-1.28**	**Cost ($/Wp)**	**2.2**

From the material costs some conclusions can yet be made: the most significant cost factor is the SnO2:F coated glass, which is needed for both electrodes in the standard DSSC. Today the cost of tin oxide coated glass is about \$10/m^2 (Zweibel 1999), suggesting \$20/m^2, or \$0.40/W_p at 5% module efficiency, for the mere TCO glass costs for a sandwich type DSSCs today. The Ru-dye is also a significant cost factor with about \$10/m^2. The simple Ru content of the dye is estimated to contribute only \$0.07/m^2 (Grätzel 1994). TiO_2 paste, sealants and interconnects are potentially the next expensive components in the DSSC module costing together \$5-\$13/m^2.

Comparison with other PV technologies

In the end, the question of market penetration of the dye-sensitized solar cells boils down to the cost competitiveness (in terms of \$/W_p) of the dye-sensitized solar cells against other thin film solar cell technologies and the standard crystalline silicon technology, the present market leader. It is therefore instructive to make a comparison on the basis of what can be learned from the manufacturing costs of the competing PV technologies and what could potentially be the benefits, and on the other hand, drawbacks of the DSSC technology with respect to these.

[28] The original data by Meyer (1996) was in US cents per module, and is here converted to US \$/m^2 using the rated module power 3 W_p (5% cell efficiency).

Table 7 presents a comparison of the estimated DSSC module manufacturing costs and projected costs of thin film (CdTe) and multi-crystalline silicon modules based on the above mentioned studies by Smestad et al. (1994) and Meyer (1996) for the DSSC modules, Zweibel (1999, 2000) for the CdTe thin film modules, and Little & Nowlan (1997) for the multi-crystalline (cast) silicon modules. It should be however kept in mind, that the data are not directly comparable for several reasons. Firstly, the DSSC manufacturing technology has been rather immature at the time of the referred reports and there are most likely differences in the elaborateness of the studies. Secondly, the DSSC cost estimates are for a future technology, while the CdTe and mc-Si estimates are near term projections from an existing technology.

Some observations can however be made based on the figures in Table 7. The manufacturing costs ($/m^2) for DSSC modules could be significantly less than what has been projected for mc-Si modules and about equal or possibly less than projected cost of CdTe modules. The material costs are more significant factor (%) in the total manufacturing costs for DSSCs than for CdTe and mc-Si. The cost of active materials ($/m^2) could be somewhat higher for DSSC modules than what has been projected for CdTe modules but significantly less than the active material costs for mc-Si modules.

On the $/$W_p$ basis Smestad et al. (1994) estimates for 5% efficient DSSC module a total cost that is less than the projected cost of 15% efficient mc-Si modules and about equal to that of 8% efficient CdTe modules. Meyer (1996) on the other hand estimates cost exceeding both of these. In other words the estimates by Smestad et al. and Meyer indicate no clear cost advantage for the glass based DSSC technology over CdTe or mc-Si technology. The validity of these estimates is however difficult to assess and compare for the above mentioned reasons.

5.3 Discussion and outlook

The top laboratory efficiency today among the DSSCs is 10.4% for a TiO_2 cell using the "black dye". This means an increase of about 3.3 efficiency units from the first results obtained in 1991 or increase of 0.4 efficiency units from the 1993 results obtained with the N3 dye. The use of an efficient sensitizer dye and a successful control of the morphology and properties of the nanostructured film are perhaps the most important factors for reaching high efficiencies in DSSCs.

Table 7. Comparison of the estimated DSSC module manufacturing costs and projected costs of thin film (CdTe) and multi-crystalline silicon modules. The portion of the material costs and the active material costs are shown both in US $/m^2 and as a percentage of the total manufacturing costs. The cost per peak watt is calculated using typical production scale efficiency for the technologies. No correction for depreciation or conversion for present value has been made for the reported cost values (values are shown as reported, or converted, when necessary, between $/$W_p$ and $/m^2 using the given efficiency).

Technology	DSSC (1)		DSSC (2)		CdTe (3)		mc-Si (4)	
Manufacturing costs (US $/m^2)	48-64		111		90		267	
Material costs (US $/m^2)	43-49	(77-89%)	89	(80%)	48	(53%)	152	(57%)
Active material costs [29] (US $/m^2)	7-11	(15-17%)	17	(15%)	5	(6%)	110	(41%)
Representative module efficiency	5%		5%		8%		15%	
Cost per peak watt (US $/$W_p$)	1.0-1.3		2.2		1.1		1.78	

(1) Smestad et al. 1994 (estimated DSSC module costs at 5-10 MW_p/year production)

(2) Meyer 1996 (estimated DSSC module costs at 4 MW_p/year production)

(3) Zweibel 1999, Zweibel 2000 (projected near term costs for a CdTe modules at 20 MW_p/year production)

(4) Little & Nowlan 1997 (projected near term costs for a mc-Si modules at 25 MW_p/year production)

(For comparison: Current direct manufacturing costs have been estimated to be $2.45/$W_p$ for sc-Si, $2.10/$W_p$ for mc-Si, $2.70/$W_p$ for a-Si, $2.30/$W_p$ for CdTe and $2.25/$W_p$ for CIS modules (Frantzis et al. 2000).

The DSSC technology seems to be rather well established at the moment and is based mostly on the work done in the Professor Grätzel's laboratory at the EPFL. The key materials of the standard technology include the nanostructured TiO_2 electrodes (and its preparation methods), Ru based dyes (e.g. N3 dye), nitrile based I^-/I^-_3 redox electrolytes, thermal platinum catalyst coating of the counter-electrode and 4-*tert*-butylpyridine as a surface passivation agent.

One of the major advantages of the DSSC technology over other PV technologies is the relatively simple manufacturing processes and the inexpensive equipment and

[29] To yield active material costs in DSSCs the cost of TiO_2 paste, electrolyte, dye, and Pt catalysts are summed. For mc-Si modules, material costs for wafer and cell production steps are taken as representative active materials costs. The active material costs in CdTe were taken as reported and was mostly due to semiconductor and interlayer materials, as well as metal back contacts.

facilities needed. In the DSSC manufacturing old-fashioned screen printing machines can be used compared to the expensive vacuum deposition machines needed in the other thin film technologies[30]. Also the very expensive clean room facilities invariably needed for semiconductor processing are not prerequisite for the manufacturing of the DSSCs. Cost effective dye solar cell production may thus be possible in production lines with smaller capacities (MW/year) than with the other PV technologies.

The standard DSSC technology is based on a multi stage batch process including a slow dye impregnation step. This may restrict the production speed of the DSSCs and make it difficult to utilize all the possibilities behind the simple manufacturing method. Excluding some possible niche markets arising from the good performance of the DSSCs under low light intensities and diffuse light[31], the glass based DSSC module technology has the existing silicon module technology as a direct competitor. In the glass based module technologies other than active material costs are generally dominant in the total material costs (See Table 7). It is therefore questionable whether the manufacturing of DSSCs with the batch process onto glass can be made cheap enough to compete with other PV technologies in terms of €/W_p in the end.

As already pointed out in Chapter 2.1.4 significant manufacturing cost reductions could be achieved if solar cells could be manufactured in a continuous roll-to-roll process from low-cost materials for example on large area flexible polymer foils. With this respect the DSSC technology offers interesting advantages. The standard DSSC technology described in Chapter 4 already includes solution processing steps such as the screen printing of the TiO_2 layer and the thermal platinum catalyst deposition, which could be suitable for continuos processing.

Realization of a transition from the glass substrates and module manufacturing based on the batch process to continuos processing onto flexible polymer foils requires modification and development of the electrode preparation method, the dye-impregnation method, the electrolyte composition and the electrical interconnection techniques. The use of solid or gelatinous electrolytes for example could be advantageous with continuos processing and polymer substrates by making the sealing and manufacturing of the cells somewhat easier.

The pressing technique adapted from the paper manufacturing technology and developed for DSSCs in the Ångström Solar Center in Uppsala University

[30] See e.g. Bossert et al. (2000)

[31] See http://www.sta.com.au/sol_cell.htm

(Lindström et al. 2001a) is the first significant step towards continuous processing of the DSSCs. An interesting scenario along this road would be further application of existing industrial continuous coating processes, such as paper coating, for the manufacture of DSSCs.

Further interesting future directions of development from the starting point of the standard technology are listed in Table 8. Another direction besides the manufacturing oriented material development is the improvement of the fundamental photovoltaic processes in the cell by new materials and preparation methods in order to raise the energy conversion efficiency of the cells. Here the control of the photoelectrochemical kinetics by molecular level engineering of the nanocrystal/dye/electrolyte interface plays a significant role. A lot of basic research needs to be done to relate the nature of the electron transport in the nanostructured TiO_2 film to the properties of the dye layer and surrounding electrolyte and to the performance and degradation behavior of the cell in operation conditions.

Other perspectives for the research include for example the development of new dyes with enhanced absorption properties, purely organic dyes, dye cocktails, semiconductor quantum dot dyes, UV and IR absorbing dyes for transparent photovoltaic windows, new oxide materials for the nanostructured electrodes and well as new redox pairs for the electrolyte (Grätzel 2000).

The research around the DSSC is booming. Going through the literature cited in this thesis and other literature not discussed here, a rough estimate for the number of different research groups in the world having published research with varying contributions directly concerning the DSSCs amounts to seventy, the actual number being likely much bigger.

The bulk of the research is done in Europe, especially in Austria, Switzerland, Germany, Netherlands, United Kingdom and Sweden. Research in the United States and Australia should also be mentioned. The research interest toward molecular photovoltaic materials is growing especially fast in Japan and an interesting question is whether the Europe can hold its original leading position in the dye-sensitized solar cell technology in the future.

Table 8. Summary of the materials of the DSSCs: the standard technology and the new directions of development. See the text for further information and references. The comments with a question mark are ideas and perspectives absorbed from the literature.

	Standard technology	**New directions of development**
Substrate	Glass	Polymer foil, metal foil?
TCO	SnO_2:F on glass	ITO on polymer foils. New low-temperature TCOs?
Counter-electrode catalyst	Thermal platinization, conventional Pt coating methods	Porous carbon, compressed platinized SnO_2 or carbon powder
Electrolyte	Liquid with I^-/I^-_3 couple and additives (e.g. 4-*tert*-butylpyridine) in nitrile solvent	Solid hole conductive polymers, Gelatinized I^-/I^-_3 -electrolytes, molten salts, direct molecular linking between polymer electrolyte and dye
Dye	Metallo-organic Ru-complexes (e.g. the N3 dye)	Purely organic dyes, hydrophobic dyes?, dye cocktails?
Nanoparticle electrode	TiO_2	Rod-like TiO_2 nanocrystals, ZnO, SnO_2, composites of different metal oxides
Electrical contacts	Silver paint, copper tape in small area single cells	Coated Ag tracks or combined interconnection - sealing materials in the modules
Sealing	Epoxy glues, Surlyn 1702, Al/polymer foils, Sodium silicate, Torr Seal, O-rings, glass soldering	Lamination in polymer foils?
Cell and module processing	A multi step batch process	Continuous roll-to-roll processes (on flexible substrates), material development for continuos processing

6 Organic solar cells

Synthetic organic materials such as plastics are used literally everywhere in our daily life in coatings and packing materials and in form of plastic consumer products, cloth fibers, coatings, paints, etc. It is therefore not a big surprise, that ever since the discovery of semiconducting polymers, great possibilities and new avenues have been foreseen for the replacement of the inorganic semiconductors, the core materials of the present electronics, with their organic counterparts. One of the possible future applications of these new organic electronic materials is an organic solar cell.

The potential of organic solar cells is related to the idea of low-cost photovoltaic materials such as polymers (plastics), which could be easily manufactured as large area films, cut from rolls and installed onto permanent structures. Inspired by the significant progress in solar cell efficiencies with some organic materials such as dyes in the case of dye-sensitized solar cells and the discovery of efficient charge transfer between certain organic electron donor and acceptor molecules, the research on organic photovoltaic materials has grown rapidly during the last decade and is very active at the moment.

Organic materials used presently in solar cells include for example conducting polymers, dyes, pigments, and liquid crystals. Among these, the conductive polymers are perhaps the best known for their photophysical properties, and some reviews have published on the subject (Wallace et al. 2000, and Brabec & Sariciftci 2001c, Brabec et al. 2001b).

6.1 Conductive polymers

Plastics are lightweight, cheap to produce and generally known to be excellent insulators, and therefore used for example to cover electric wires. However, in 1977 MacDiarmid, Shirikawa and Heeger showed that conjugated polymers could be made electrically conductive by suitable doping. The discovery and the subsequent development of the conducting polymers resulted in Nobel Prize of Chemistry to these authors in 2000. Today conductive polymers are used for example in sensors, biomaterials, light-emitting diodes and corrosion protection agents (Wallace et al. 2000).

Conjugated polymers are organic molecules with repeating structural units attached to each other by alternating single and double carbon-carbon (sometimes carbon-

nitrogen) bonds. The single bond is so-called σ-bond, while the double bond contains a σ-bond a π-bond. In this alternating chain of single and double bonds, the molecular p_z orbitals constituting the π-bonds are actually overlapped and spread over the entire molecule, and the electrons in this molecular orbital are respectively delocalized along the whole molecular chain[32].

The polymers can be made conductive by doping; they can be oxidized to produce p-doped materials or reduced to produce n-doped materials. Especially p-doped polymeric materials have found applications such as electrochromic devices, rechargeable batteries, capacitors, membranes etc., while n-doped materials have shared less attention (Wallace et al. 2000). Upon p-doping electrons are removed from the polymer leaving holes in the π-electron orbitals. The holes can be filled by π-electrons hopping from the nearby molecules, this way presenting electrical conductivity in the polymer material.

6.2 Photovoltaic effect in conjugated polymers

The Photovoltaic properties of crystalline inorganic semiconductor solar cells can be described by energy band models. The situation in molecular or polymeric organic solar cells is however much more complex because of the absence of three-dimensional crystal lattice, different intramolecular and intermolecular interactions, local structural disorders, amorphous and crystalline regions, and chemical impurities (Wöhrle & Meissner 1991). The photophysics of organic materials is not yet fully understood (Petritsch 2000b) nor are there any comprehensive theoretical models explaining the organic thin film photovoltaic device characteristics from the basis of molecular properties of the materials (Meissner & Rostalski 2000). The subsequent discussion of the photovoltaic effect in conductive polymers, adapted from the literature, is therefore necessarily highly simplified. In fact, to gain qualitative understanding the operation of the organic solar cells is usually discussed in the framework and terminology of classical inorganic pn-junction solar cells.

The basic steps of photovoltaic conversion, i.e. light absorption, charge separation, and charge transport and collection, has to be fulfilled also in the organic photovoltaic materials.

Light absorption

[32] See e.g. Alonso & Finn 1968, p. 208

In conjugated polymers the delocalized p_z orbitals constituting the π-bond actually produce two orbitals: a lower bonding (π) orbital and a higher antibonding (π*) orbital. The difference between the energies of these states corresponds to the energy gap of the semiconducting polymer material, and as a rule of thumb is the smaller the longer is the conjugation length of the molecule. The absorption of light with energy equal to or above the band-gap energy generates an electron in the π* level and a hole in the π level. In contrast to the inorganic semiconductors, where photogenerated electrons and holes are free in the conduction and valence band respectively, the generated electron and hole in conductive polymer are loosely bound together by Coulombic force. This electron-hole pair is called exciton and it moves within the material as a one entity. The diffusion length of excitons is typically in the order of 10 nm (Wallace et al. 2000).

Charge separation

The operation of a polymer photovoltaic cell requires splitting of the excitons before their recombination, that is, within about 10 nm from the site of the light absorption. The excitons can be dissociated by charge transfer at interfaces such as the interface between a metal and the polymer material or interface between molecules of different electron donating and accepting properties. The electron is accepted by material (electron acceptor) with larger electron affinity and the hole by material (electron donor) with lower ionization potential. The excitons can also be dissociated simply in an electric field strong enough to overcome the Coulomb attraction between the electron and the hole in the exciton.

In donor-acceptor molecular junctions, the charge separation process can be further separated to an excitonic step, where a sort of charge transfer exciton is formed with an electron in the acceptor side and a hole in the donor side of the junction, and to an electronic step, where the electron and hole are separated by thermal dissociation or ionization in an electric field (Yoshino et al. 1997).

Charge collection

In most of the organic solar cells, the separated electrons and holes are transported to the opposite electrodes in an internal electric field created by asymmetry of the electrodes (different work functions) or in built in potentials (Yoshino et al. 1997). In order to reduce recombination, the electrons and holes are preferentially transported in different materials or phases. For example in the case of donor-acceptor device (See Chapter 6.5.2), an acceptor material with good electron conductivity and a donor material with good hole conductivity is ideal. Good non-blocking contacts between the molecular materials and the electrodes of the cell are

essential for efficient charge collection. In some cases an additional material layer may be needed between the metal and organic layer to facilitate good ohmic contact, such as LiF between MDMO-PPV - PCMB blend and aluminum (Shaheen et al. 2001a, Brabec et al. 2001b).

6.3 Organic photovoltaic materials

Detailed study of the electronic and photophysical properties of the organic semiconductors is beyond the scope of this work. Useful insight can however be gained by categorizing the materials according to their processing properties, since they are important for the practical device preparation and especially viewed against the possibility of large-scale industrial utilization in the future.

According to Petritsch (2000b) the current organic solar cell materials can be divided into three different categories according to their mechanical or processing properties: insoluble, soluble or liquid crystalline (Figure 15). They may be further divided into molecules with few (oligomers) or single (monomer) structural repeat units, and molecules (polymers) with more than about 10 repeat units. Oligomers and monomers that absorb in the visible light are also called chromophores and are referred to as dyes if they are soluble or pigments if they are not.

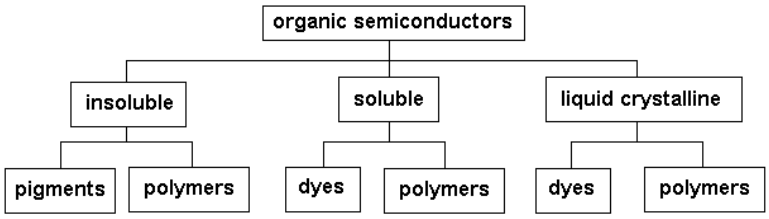

Figure 15. Organic semiconductors can be categorized according to their mechanical or processing properties as insoluble, soluble or liquid crystalline. They may be further divided into monomers (pigments and dyes) or polymers. (Petritsch 2000b).

Pigments

Examples of different organic photovoltaic pigments and their basic molecular structures are shown in Figure 16. Especially perylene, or perylenetetracarboxylic acid diimide, and phthalocyanine, or different metallo-phthalocyanines, give the structural back-bone to many molecules recently used in efficient pigment and dye based organic solar cells (see Table 9). Also fullerene (C_{60}) and pentacene are insoluble to most solvents, and as such should be considered as pigments (Petritsch 2000b).

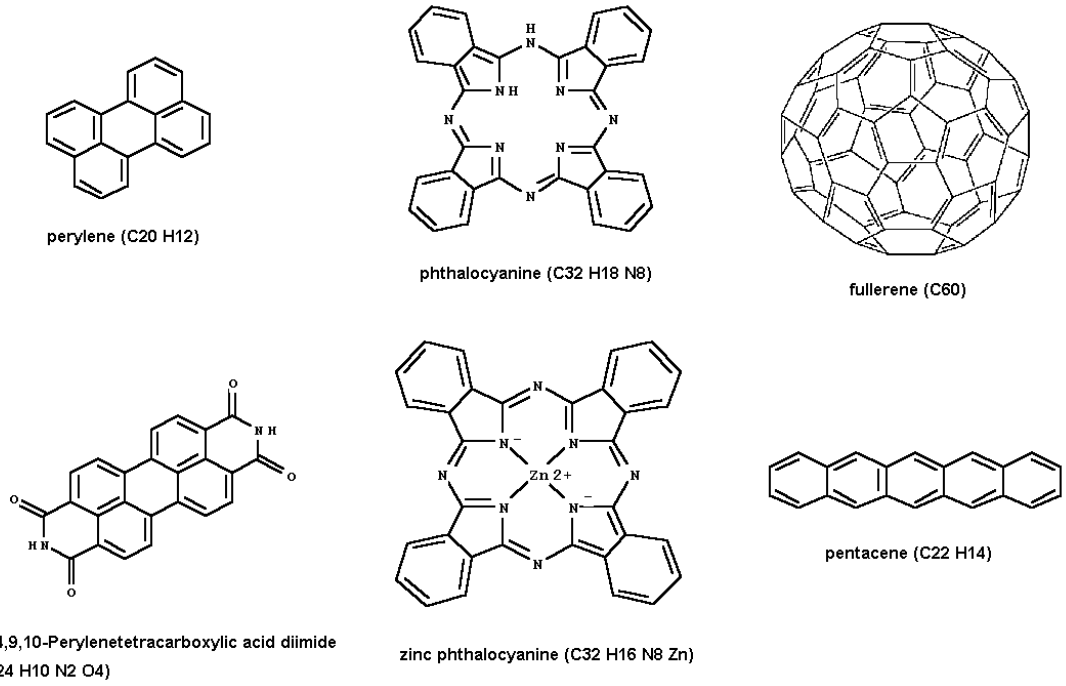

Figure 16. Examples of the molecular structures of different organic pigments used in efficient organic solar cells (see Table 9). Pigments like these can be made soluble by synthesizing suitable side chains to the molecules.

Dyes

Processing the pigment based organic solar cells requires deposition of the organic layers by high vacuum evaporation methods, which is both time consuming and complicated, and cannot be easily scaled up for manufacturing of large surfaces at high throughput. Fortunately, pigments can be synthesized soluble by adding suitable side chains to the molecules, as demonstrated by Petritsch et al. (2000a) for perylenetetracarboxylic acid diimide and phthalocyanine. This way also soluble fullerene derivatives, such as the PCBM (Figure 17), can be synthesized and used in spin-coated organic solar cells (Figure 17).

Polymers

Depending on their molecular structure and chemical composition polymers can in principle be soluble, insoluble or liquid crystalline, and they can be used as either electron donor or acceptor materials in the organic solar cells. Figure 17 shows the molecular structure of the common semiconductor polymers as well as acceptor-type fullerene and one of its soluble derivatives used in organic solar cells. Other polymers studied in the organic photovoltaic cells are for example polythiophenes (e.g. Too et al. 2001) and poly(*para*-phenylene vinylene) (PPV) (Jenekhe & Yi 2000).

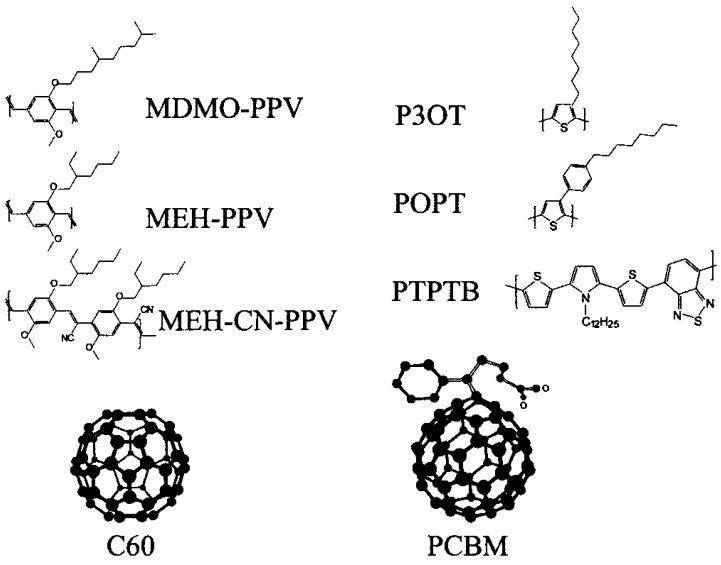

Figure 17. Common conjugated polymers and macromolecules used in organic photovoltaic cells. Picture from (Brabec et al. 2001b).

Liquid crystals

Liquid crystals have emerged only recently as a new organic solar cell material category, offering high charge carrier mobility and long (a few 100 nm) exciton diffusion lengths, which could be beneficial for organic solar cells (Petritsch et al. 1999). For a certain temperature range these materials exhibit a phase with properties somewhere in between those of liquids and solids. The liquid crystalline molecules tend to arrange or self-assemble in an ordered structure like crystalline solids but exhibit the mechanical properties of liquids, i.e. they are soft in a sense.

High external quantum efficiency (EQE[33]) of over 34% at 490 nm was reported for a self-organized liquid crystal organic solar cell by Schmidt-Mende et al. (2001), who used bilayer of liquid crystalline hexaphenyl-substituted hexabenzocorone (HBC-PhC_{12}) as an electron donor and a perylene dicarboxylic acid diimide derivative as an electron acceptor in the active layer of the cell. The HBC-PhC_{12} has a disc-like structure and forms in room temperature liquid crystalline phase, a discotic liquid, where the molecules self-organize into a columnar structure (Figure 18). This structure forms, because the flat shape of the molecules allows the molecular π-orbitals sticking out of the plane of each molecule to form a firm bonds between molecules in adjacent layer in the same fashion as in the graphite structure.

[33] EQE = IPCE, incident photon to current efficiency or spectral response

Spin-coating a blend of the perylene derivative and HBC-PhC_{12} onto an ITO surface and drying in ambient air resulted in a bilayer film, which was interpreted as perylene and HBC-PhC_{12} layers on top of each other, formed possibly due to solubility differences of the blend constituents. Furthermore, the high EQE of the device was thought to be partly result of a high internal surface area within the spontaneously formed bilayer structure and partly due the high exciton diffusion lengths in the separated liquid crystalline and perylene regions (Schmidt-Mende et al. 2001). This result can be summarized as a novel example of organic solar cell processed from a single blend solution of organic photovoltaic materials spontaneously assembling themselves to a nanoscale structure with desirable photovoltaic properties.

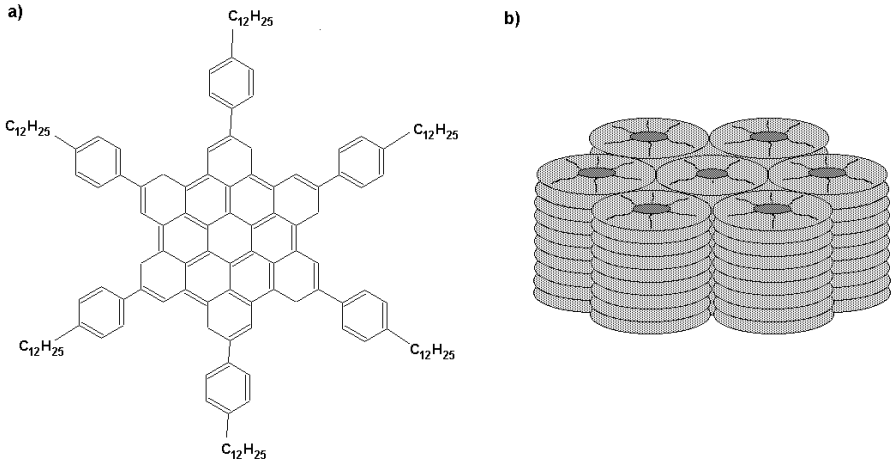

Figure 18. a) Molecular structure of the hexaphenyl-substituted hexabenzocorone (HBC-PhC_{12}) used by Schmidt-Mende et al. (2001) as a liquid crystalline material in organic solar cell. b) In the liquid crystal phase the discotic HBC-PhC_{12} molecular self-assemble in an ordered columnar structure.

6.4 Processing of organic solar cells

The processing method for the active layer(s) in the organic solar cells depends on the solubility of the materials. High vacuum deposition (thermal sublimation) is needed for depositing pigment layers (e.g. Meissner & Rostalski 2000, Tang 1986, Wöhrle et al. 1995, Peumans et al. 2000, Peumans & Forrest 2001). Crystalline pigment layers on the other hand can be produced by physical vapor growth (e.g. Schön et al. 2000b). Dyes and soluble polymers can be processed into active layers of the cells by spin coating (e.g. Chen et al. 2000, Shaheen et al. 2001a, Petritsch et al. 2000a), doctor blading (Neugebauer et al. 2000), screen printing (Shaheen et al. 2001b), or laminating spin-coated films together (Granström et al. 1998), or

electrochemically (Zaban & Diamant 2000). Inkjet printing has been used to manufacture organic light emitting devices (LEDs) (Chang et al. 1999), but demonstrations of organic solar cells prepared by this method has not yet emerged.

The organic active layers are usually deposited onto ITO coated glass plates or ITO coated plastic films. The counter-electrode, usually aluminum, is deposited by vacuum evaporation on top of the organic layer. Whenever a metal electrode other than the transparent ITO layer is needed in both sides, one of the electrodes is prepared semitransparent. It should be noted that vacuum evaporation of the metal electrodes, which is needed for good a electrical contact between the metal and the organic material, may be in contradictory with the ultimate goal of the organic solar cells, i.e. processing of large surfaces at high speed and volumes. While at the early stage of development this is certainly not an acute question, more convenient methods needs to be developed in the future for the processing the electrical contacts of the organic solar cells.

6.5 Organic solar cell architectures and review of performance results

The organic solar cells reported in the literature can be categorized by their device architecture as having single layer, bilayer, blend, or laminated structure (Figure 19). The reasoning behind the development of these structures seems to be more or less universal for all organic photovoltaic materials, i.e. obtaining higher cell efficiencies by enhancing charge separation and collection processes in the molecular materials.

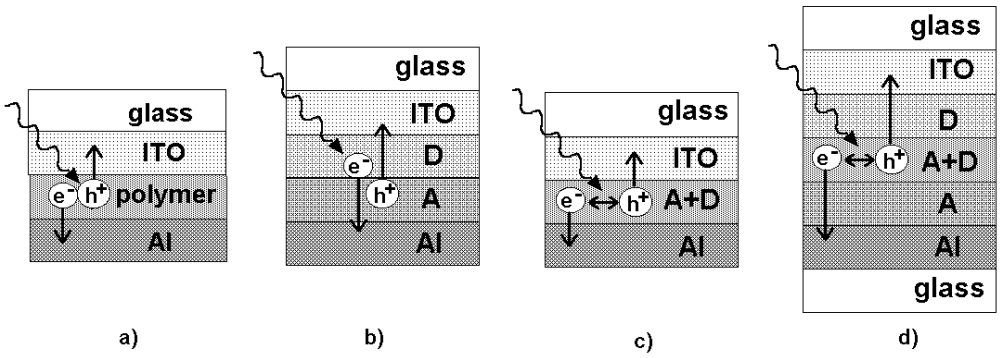

Figure 19. Schematic presentation of the different organic photovoltaic device architectures. A) Single layer, b) donor-acceptor bilayer, c) donor-acceptor bulk heterojunction (or blend) and d) laminated donor-acceptor structure. Here ITO and aluminum are chosen as representatives of high and low work function electrodes respectively. The thickness of the organic layers ranges typically from tens to few hundreds of nanometers.

6.5.1 Single layer devices

In the first generation of the conjugated polymer photovoltaic devices a single layer of pure conjugated polymer, for example poly(*para*-phenylene vinylene) (PPV), were sandwiched between electrodes with different work functions, such as ITO and Al (Brabec & Sariciftci 2001c). The dissimilarity of the work functions of the electrodes in these devices is essential. Upon short-circuiting the device, electrons move from the low work-function electrode (Al) to the high work-function electrode (ITO) creating an electric field across the polymer layer.

This behavior can be described to some extent with the so-called metal-insulator-metal (MIM) tunnel diode model (Figure 20a). The existing external electric field works to dissociate the excitons and to transport the charge carriers to the opposite electrodes, thus creating current. It should however be noted that the behavior of the single layer device depends on the impurity densities (or free carrier concentration) of the polymer. Behavior according to the MIM model is expected at low impurity concentration (low carrier concentration), whereas at high impurity concentrations (high carrier concentrations) better understanding of the device operation is obtained in terms of the so-called Schottky diode model (Brabec et al. 2001b).

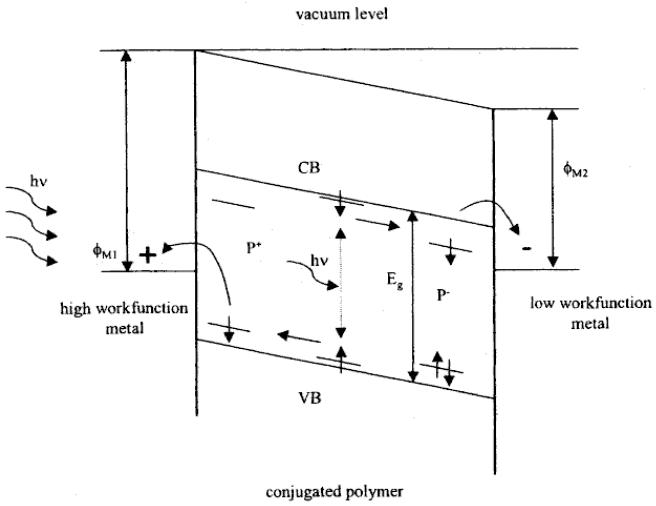

Figure 20. Energy diagram according to the MIM model of a single layer conjugated polymer photovoltaic device under short circuit conditions. Symbols in the picture: VB valence band, CB conduction band, E_g band gap energy, P^+, P^-, positive and negative polarons respectively. Picture from (Brabec et al. 2001b).

While these single layer polymer diodes can have significant current rectifying characteristics, the operation in the photovoltaic mode, that is without an external bias voltage, is limited by the fact that the electrical field available in the polymer layer is caused only by the work function difference of the electrodes. In most cases

(such as ITO and Al) this potential difference and thus the electric field is not high enough for efficient exciton dissociation in the polymer (Brabec et al. 2001b). Furthermore, in the single layer device both the electrons and the holes travel in the same material and recombination losses are generally high. In Schottky type devices the photoactive region is usually very thin (low total absorption of light) and close to one of the two electrodes, while the rest of the bulk of the organic layer is inactive and works merely as an optical filter if the cell is illuminated from the inactive side (Petritsch 2000b). Because of these limitation, the energy conversion efficiencies of these photovoltaic devices have usually remained low, typically around 0.1% (Brabec & Sariciftci 2001c).

Doped pentacene crystal based single layer organic solar cells (Schön et al. 2000b) present however an important recent exception to this pattern reaching already 4.5% standard solar efficiency (Schön et al. 2000a). The pentacene single crystals are grown by horizontal physical vapor transport in a stream of hydrogen in 200-300°C (Schön et al. 2000b) and also thin film deposition of pentacene requires vapor deposition (Schön et al. 2000a). This may be considered a drawback compared to the organic solar cells deposited from solutions in room temperature.

6.5.2 Donor-acceptor bilayer devices

To enhance the exciton splitting process, devices with electron accepting and electron donating molecules have been developed. In these so-called donor-acceptor bilayer devices (Figure 20b), the excitons can be dissociated at the donor-acceptor interface due to a relative energy level difference of the donor and acceptor molecules (Figure 21). The donor and acceptor molecules can be for example conjugated polymers (e.g. Jenekhe & Yi 2000), organic macromolecules (e.g. Meissner & Rostalski 2000), pigments (e.g. Tang 1986) or dyes (e.g. Petritsch et al. 2000a).

The bilayer structure is more advantageous than the single layer structure for several reasons: exciton splitting is enhanced by the D-A interface, the active region is extended to both the donor and the acceptor sides of the junction thereby roughly doubling its width to about 20 nm, and the transport of electrons and holes is separated into different materials reducing the recombination losses. In addition to this, by using two different semiconductors, the band gaps can in principle be tuned to match better the solar spectrum. (Petritsch 2000b).

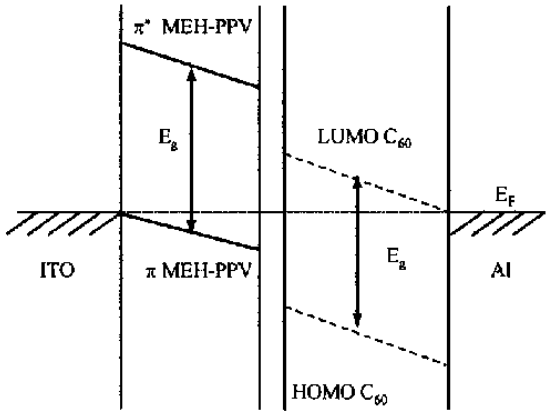

Figure 21. Schematic energy diagram of a bilayer donor-acceptor device under short circuit conditions. The conjugated polymer MEH-PPV acts as an electron donor, and C_{60} as an electron acceptor. Picture from (Brabec et al. 2001b).

Already in 1986 Tang (1986) reached about 1% solar efficiency with a bilayer organic solar cell consisting of vacuum evaporated copper phthalocyanine (CuPc) and perylene derivative (PV) pigment layers, which has remained as one of the best results among organic solar cells (see Table 9). Recently Petritsch et al. (2000a) repeated the Tang's cell with soluble derivatives (dyes) of CuPc and perylene, but obtained considerably lower cell performance.

Another example of an efficient bilayer organic solar cell is the ZnPc | PTCDIa bilayer device with a 0.43% efficiency by Wöhrle et al. (1995), and an example of a polymer | polymer bilayer device is the cell by Jenekhe & Yi (2000) with a 0.7% efficiency. The hitherto most efficient organic bilayer solar cell to the author's knowledge is however a vacuum evaporated pigment based CuPc | C_{60} device by Peumans & Forrest (2001) with 3.6% efficiency at 150 mW/cm^2 AM1.5 illumination.

6.5.3 Donor-acceptor blend devices

The planar donor-acceptor junction only doubles the active region of the solar cell with respect to the single layer device, which is still usually not enough for efficient light absorption. To overcome this problem and to increase the optical thickness of the film while maintaining efficient current collection at the same time, the concept of interpenetrating network of electron-accepting and electron-donating molecular species was developed (Halls et al. 1995, Yu & Heeger 1995, Yu et al 1995), and demonstrated successfully in number of different so-called donor-acceptor blend devices (Figure 19c).

The thickness of the active exciton dissociation region can be increased by a phase-separated blend of organic donor and acceptor semiconductor materials with domains not larger than twice the exciton diffusion length. While an organic blend layer of this type can easily be made thick enough for efficient light absorption without loosing efficient exciton dissociation, the challenge is to achieve an interpenetrating structure of the donor and acceptor phases instead of a random blend. This is essential since every site within the donor and acceptor phases should be contacted to the opposite electrodes by the respective materials - any isolated domain of either donor or acceptor material would be optically active but electrically inactive, which would decrease the efficiency of the photovoltaic cell.

Granström et al. (1998) designed a laminated polymer donor-acceptor device, which may be considered as an intermediate of the bilayer and the blend device (Figure 20c). The cell consisted of separately prepared films of MEH-CN-PPV : POPT (19:1) blend on aluminum or calcium coated glass substrate and a POPT : MEH-CN-PPV (19:1) blend on ITO or PEDOT coated glass substrate, laminated together by pressing the organic layers together at elevated temperature. The lamination procedure was shown to result in an about 20-30 nm thick interpenetrating layer of the donor and the acceptor type polymer materials. By this way a concentration gradient of the donor and the acceptor materials can be expected to form in the active layer of the cell, which can be beneficial for the operation of the donor-acceptor cells. A solar efficiency of 1.9% at 77 mW/cm^2 AM1.5 illumination was achieved with this laminated organic solar cell.

The highest efficiencies among polymer based organic solar cells to date has been reported for devices with blends of semiconducting polymers and fullerenes as the active layer. Shaheen et al. (2001a) could obtain efficiency as high as 2.5% at 80 mW/cm^2 AM1.5 illumination with a 100 nm thick blend layer of MDMO-PPV polymer as the donor material and soluble fullerene derivative [6,6]-PCBM as the acceptor material (Figure 22). Presently large area devices (> 6 cm × 6 cm) with around 2% efficiency are claimed to be routinely fabricated (Brabec & Sariciftci 2001a).

By carefully selecting the solvents of the polymer solutions, partial dissolution of the bottom layer during spin coating of the upper layer can be used to make diffused donor-acceptor interfaces. Chen et al. (2000) prepared in this way spin coated diffused MDMO-PPV | PCBM device with 0.5% efficiency at 78 mW/cm^2 AM1.5 illumination.

Also pigment-pigment blend layer devices have been studied: Meissner and Rostalski (2000) reached 1.05% efficiency with an organic cell having a vacuum co-

evaporated ZnPc and C_{60} (1:1) blend layer, and Hiramoto et al. (1991) 0.7 % efficiency with a three-layer cell having a vacuum co-evaporated perylene derivative and phthalocyanine blend between pure perylene and phthalocyanine layers.

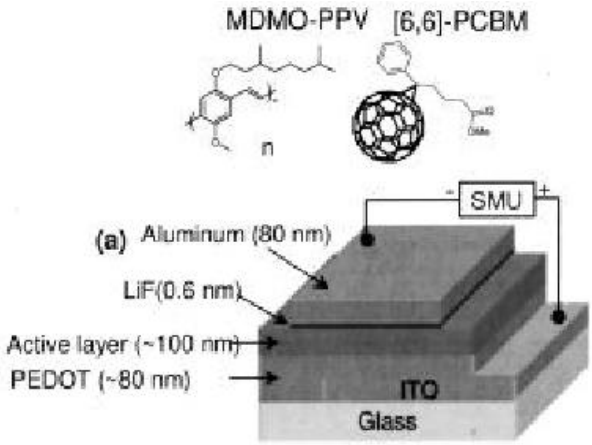

Figure 22. Device structure of a conductive polymer (MDMO-PPV) / fullerene ([6,6]-PCBM) blend solar cell by Shaheen et al. (2001a) having 2.5% efficiency (picture from Shaheen et al. 2001a).

6.5.4 Performance and stability of the organic solar cells

Energy conversion efficiency

The performance results from different organic solar cells already discussed above are shown in Table 9. The only safe conclusion from the state-of-the-art of the organic solar cell materials is that development in this field of research is only at the beginning and no clearly outperforming materials or device concepts have yet emerged.

Stability

Organic materials are generally susceptible to oxidative and UV-light-induced degradation, which usually leads to reduction in physical properties or discoloration. In commercial polymer materials for example, small amounts of stabilizing additives, antioxidants, processing stabilizers, and UV stabilizers are added to increase the lifetime of the materials.

Perhaps because of the early stage of development, the stability of the prepared organic solar cells is not usually reported in the literature. In general the long-term stability of these materials and devices remains an open question.

Table 9. Collection of the best performance results among organic solar cells to date. Only results obtained near standard illumination conditions are accepted for this review. It should be noted that the list is not aimed to be complete at the lower end of the range of efficiencies presented here. Explanations for the abbreviations are given below the Table.

Active layer	η (%)	Illum. (mW/cm^2)	area (mm^2)	reference
Single layer (pigment)				
Doped pentacene (single crystal)	2.4	100 (AM1.5)	2 - 5	Schön et al. 2000b
Doped pentacene (single crystal)	4.5	100 (AM1.5)	4.6	Schön et al. 2000a
Doped pentacene (thin film)	2.2	100 (AM1.5)	10	Schön et al. 2000a
D-A bilayer (pigment | pigment)				
CuPc | C_{60} | BCP	3.6	150 (AM1.5)	?	Peumans & Forrest 2001
CuPc | PTCBI | BCP	1.0	100 (AM1.5)*	?	Peumans et al. 2000
ZnPc | PTCDIa	0.43	100 ("white light")	15	Wöhrle et al. 1995
CuPc | PV	0.95	75 (AM2)	10	Tang 1986
D-A bilayer (polymer | polymer)				
PPV | BBL	0.7	100 (AM1.5)	20	Jenekhe & Yi 2000
D-A blend (pigment : pigment)				
Me-PTC | Me-PTC : H_2PC | H_2PC	0.7	100 ("white light")	?	Hiramoto et al. 1991
MPP | ZnPc : C_{60} (1:1) | ZnPc	1.05	86 (AM1.5)	?	Meissner & Rostalski 2000
D-A blend (polymer : dye)				
MDMO-PPV : [6,6]-PCBM	2.5	80 (AM1.5)	10	Shaheen et al. 2001a
MDMO-PPV | [6,6]-PCBM (diffused)	0.5	78 (AM1.5)	8	Chen et al. 2000
D-A blend (polymer : polymer)				
POPT : MEH-CN-PPV (19:1)| MEH-CN-PPV : POPT (19:1) (laminated)	1.9	77 (AM1.5)	2.5	Granström et al. 1998

* In a concentrating and light confining device configuration

CuPc = copper phthalocyanine

PV = a perylene tetracarboxylic derivative

ZnPc = zinc phthalocyanine

PTCDIa = a 3,4,9,10-perylenetetracarboxylic acid diimide derivative

PTCBI = 3,4,9,10-perylenetetracarboxylic-bis-benzimidazole

BCP = bathocuproine (used as an 'exciton blocking layer' (Peumans et al. 2000))

MPP = N,N-bis-methyl-perylene-3,4,9,10-tetracarboxylic acid diimide

MDMO-PPV = (poly)[2-methyl,5-(3*,7** dimethyl-octyloxy)]-p-phenylene vinylene)

[6,6]-PCBM = [6,6]-phenyl C61 butyric acid methyl ester

POPT = a regioregular phenyl-octyl substituted polythiophene

MEH-CN-PPV = a cyano derivative of poly(p-phenylene-vinylene)

PPV = poly(p-phenylene vinylene)

BBL = poly(benzimidazole-benzophenanthroline ladder)

Me-PTC = a perylene tetracarboxylic derivative

H_2PC = metal-free phtalocyanine (same as in Figure 16)

Some stability results have however been reported on the conjugated polymer based plastic solar cells. Stability of these devices under ambient conditions without any protection is very poor, but can be enhanced to some extent by protection against oxygen or adding fullerenes to the polymer matrix (Brabec et al. 2001b). A shelf life of more than 150 days were reported for polymer-fullerene plastic solar cells prepared under ambient conditions and sealed thereafter without any actions taken to remove possibly adsorbed residual oxygen from the cells (Brabec et al. 1999, Neugebauer et al. 2000).

The protection and sealing techniques could in principle be similar to those developed for other photovoltaic elements, as well as for light emitting diodes (LEDs). It is therefore encouraging to know that LEDs based on conjugated polymers can already have a good stability and a long operating life (e.g. Yu & Heeger 1997), implying that also durable organic photodiodes and photovoltaic cells can be expected in the future.

6.6 Discussion and outlook

Organic materials could offer several advantages for photovoltaic cells such as low production costs by large scale production, possibility to produce large area light weight flexible devices, tunability of the band gap and other properties by chemical synthesis or blending with dopants or other additives. However, despite the promising development so far the efficiencies of the organic solar cells are still low, and a lot of research has to be done before organic solar cells became serious competitors against the inorganic ones today at the market.

There is still a lot of room for optimization in the photophysical properties of the organic solar cell materials. For instance, the majority of semiconducting polymers have band gaps higher than 2.0 eV, which limits the absorption to about 30%, compared with 77% for silicon solar cells with a band gap of 1.1 eV (Petritsch 2000b). Also reflection losses of the organic films may be significant, but has not been investigated much to date (Petritsch 2000b).

Another place for optimization is the device physics as a whole. The choice of metal electrodes should be optimized to achieve good ohmic contacts to the organic materials (Brabec et al. 2001b), and the donor-acceptor pairs should be chosen so that their energy levels match favorably for both the exciton dissociation and the generation of photovoltage.

Considering the random molecular structure of the most organic materials, it becomes clear that besides optimal material properties also certain nanoscale

ordering may be needed for efficient charge generation, separation and transport in the organic solar cells. The general problem in the organic solar cell materials is the low exciton diffusion lengths of these materials compared to the layer thickness needed to absorb a major part of the incoming light. Variety of methods have been developed to increase the active internal junction area of the cells by molecular mixing and to facilitate efficient charge collection by controlling the morphology of the phase segregation. Efforts in this direction will most likely accelerate in the future due to the promising results obtained so far.

Another interesting approach is to separate the tasks of light absorption and charge transport to different materials by using an additional dye layer between the donor and acceptor materials for example in a polymer/dye/polymer structure (Yoshino et al. 1997). In this way the dye molecules could be selected to optimize the light absorption and charge separation properties, while the donor and acceptor materials could be optimized for good hole and electron conductivity respectively. Also internal electric fields could be established by selective doping of the donor and acceptor materials to enhance charge collection (Yoshino et al. 1997, Takahashi et al. 2000).

The principle of self-assembly (Soten & Ozin 1999), demonstrated in the organic solar cells only recently (Schmidt-Mende et al. 2001, Durstock et al. 2001)[34], could provide a useful tool for processing of optimized organic nanoscale structures for photovoltaic cells in a simple manner. The fascinating idea of solar converter molecules self-organizing themselves into an active layer of solar cell when poured onto a flat surface has already received keen attention (Gorman 2001, Nelson 2001, SolarAccess 2001a, UANews 2001).

In the same way that the development of the silicon solar cells has been able to take advantage of the rapid development of the semiconductor technologies for electronic industry, also the organic solar cells can benefit significantly from the existing mature technologies. Such enabling technologies are the polymer technology and the xerography in the case of the dye and pigment development, and plastic film processing and paper coating in the case of device manufacturing. Also liquid crystal displays, polymer LEDs, and other organic optoelectronic devices have similarities with the organic solar cells and could offer tried technical solutions for their development.

[34] See discussion of liquid crystals in Chapter 6.3

7 Experiences from the DSSC preparation

In addition to the literature survey on the dye-sensitized nanostructured and organic solar cells, this work included also an experimental part, in which dye-sensitized solar cells were prepared according to the information gathered from the research reports in the literature. The results from the experimental work are presented in this Chapter.

7.1 Demonstrating the photosensitization effect with a natural dye

As a first step in the experimental part of this work, experience from the dye cell preparation was gathered by demonstrating the dye-sensitization by a natural dye. The materials and the preparation of the natural dye cells followed closely those described in the literature by Smestad and Grätzel (1998) or Smestad (1998).

The TiO_2 electrodes were prepared from a commercial titanium(IV)oxide powder (Merck) onto ITO coated glass plates by the so-called *tape casting* method. The TiO_2 powder solution was prepared as described by Smestad (1998). The desired active electrode area on the TCO glass substrate was framed with Scotch Magic ™tape (having measured thickness of about 65 μm) with a rectangular opening cut to it, and tightly attached to the glass substrate. Cut sufficiently long, the strip of tape also fastened the glass plate to the paper-covered table at the same time. Drop of the prepared TiO_2 powder solution was then spread over the framed area by sliding a glass rod over the tape.

The deposited TiO_2 layer was sintered by firing at 450°C in a convection oven for about 30 min, after which the white TiO_2 electrodes were stained by soaking the electrodes overnight in crushed raspberries slightly diluted with water. The staining rendered the electrodes faintly red. The counter-electrode was prepared by rubbing the ITO surface of the glass plate with a graphite rod to deposit loose visible graphite particles, followed by firing at 450°C for few minutes. The dyed TiO_2 electrode and the graphite coated counter-electrode were washed in isopropanol and let to dry in air. The cell was assembled by placing the electrodes little offset opposite to each other to expose contact areas for alligator clips and by pressing them together by paper clamps. An electrolyte (0.5 M potassium iodide and 0.05 M iodine in ethylene glygol) was then added between the plates by capillary action.

Figure 23 shows measured I-V curves of the raspberry dye-sensitized solar cells and a cell with naked (not dyed) TiO_2 electrode. The photosensitization effect is clearly visible in this very simple experiment. The dye-sensitized TiO_2 electrode produced short circuit photocurrents almost a hundred times greater than the naked TiO_2 electrode. The small amount of photocurrent with the naked TiO_2 electrode may be attributed to the direct band gap excitation of the TiO_2 in the UV part of the light, which on the other hand was only a tiny fraction of the total intensity of the light (Figure 26). Furthermore, the direct band gap excitation was not enough to build up a significant photovoltage in the cell with the naked TiO_2 electrode.

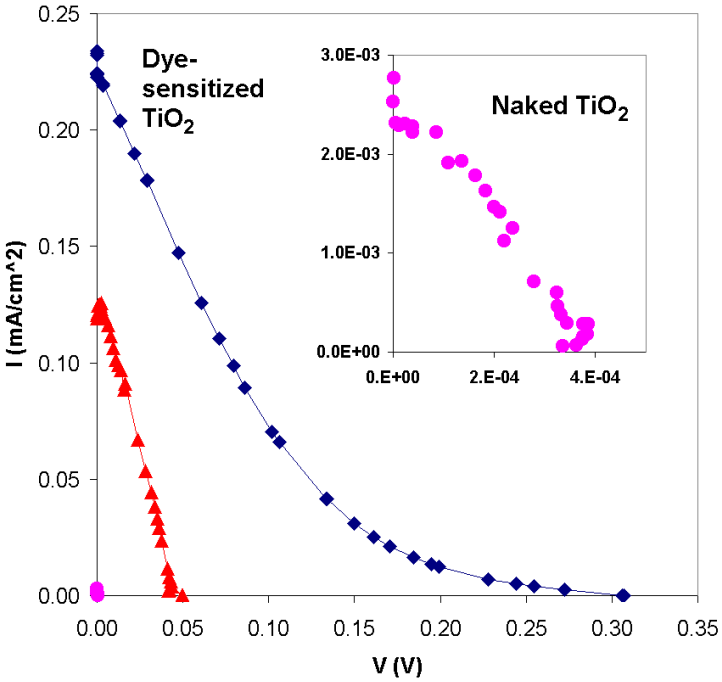

Figure 23. Current-voltage (I-V) curves of raspberry dye-sensitized solar cells. The inset showing the I-V curve of a cell with a naked (not dyed) TiO2 electrode, is a magnification close to the origin of the larger graph. The cells were illuminated by standard overhead projector lamp and the current and voltage were recorded with HP 34970 Data Acquisition/Switch Unit using HP 34901A 20-Channel Multiplexer and a manual variable load.

7.2 Results from ruthenium dye based dye-sensitized solar cells

A more serious goal of the experimental part of this work was to gather hands-on experience from the preparation of ruthenium dye based Grätzel-cells according to the procedures published in the literature. The experimental work was preceded by a literature survey on the art of DSSC preparation, the essential results of which are

presented in Chapter 4. In this Chapter the preparation of the test dye cells and the performance results obtained are presented.

7.2.1 Materials and cell preparation

Substrates

Soda-lime float glass with 600 nm thick ITO coating (sheet resistance <5Ω/sq, transmittance > 85% in visible light) or Pilkington K glass (SnO_2:F coated, sheet resistance unknown[35]) were used as the transparent conducting glass substrates for the electrodes. Before preparation of the electrodes, the glass substrates were washed with ethanol or isopropanol, wiped clean with a lint-free cloth and let to dry in air.

Deposition of the TiO_2 electrodes

Ti-Nanoxide T purchased from Solaronix SA was used as received as the colloidal paste for the TiO_2 electrode preparation. The tape casting method described above was used to deposit TiO_2 paste onto the conducting glass plate.

It was found typical for this tape casting method, that if a drop of Ti-Nanoxide T was let to stay on the glass for even seconds, a visible trace of the edges of the drop could be clearly seen afterwards in the film. It appeared as if the TiO_2 particles were concentrating to the edges of the drop thereby producing a thicker layer of TiO_2 on those sites on the glass plate. To prevent this, the paste was distributed to the entire masked area quickly by the tip of the glass rod, immediately followed by a quick spreading by sliding the glass rod. It was also noticed that the most uniform TiO_2 films were obtained with a single pull of the glass rod: if a desired film result was not obtained for the first pull, additional pulling usually made it only worse.

The deposited TiO_2 film was let to dry in air, which rendered the TiO_2 layer transparent and very faintly yellowish. After complete drying, the tapes were removed and the TiO_2 electrode was ready for sintering.

Sintering of the TiO_2 electrodes

Sintering of the TiO_2 electrodes was performed at 450 °C for about 30 minutes in a convection oven. A typical temperature profile in the sintering process is shown in Figure 24. When the oven had reached 450 °C, the cover piece of the oven was opened and the temperature of the air was let to drop for example to 250 °C before

[35] Two point resistance measured with a multimeter was about four times higher for the Pilkington K glass than for the ITO coated glass.

the electrodes were placed inside and the oven was closed. This procedure was needed to ensure at the same time a low starting temperature and a reasonably fast temperature rise in the oven having large thermal mass due to its size unnecessarily big (inner volume about 40 liters) for this purpose. After about 30 minutes at 450 °C the cover piece was opened, and the temperature was let to drop, after which the electrodes were taken out of the oven to room temperature. The actual effect of the sintering temperature profile to the final electrode performance in the DSSCs could not be studied within this work. However, high heating and cooling rates may in principle affect the structure of the TiO_2 electrodes for example as peeling of the film especially with thick TiO_2 layers. Peeling of the TiO_2 film was indeed observed in some cases.

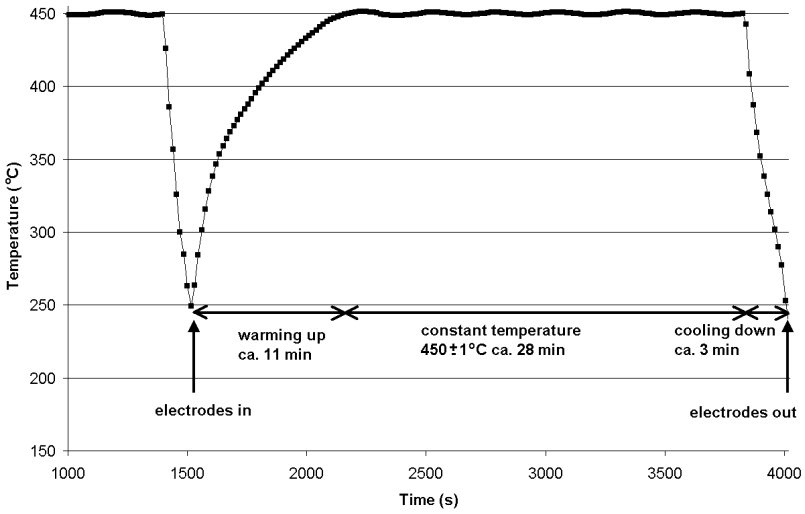

Figure 24. A typical temperature profile of the convection oven during the sintering of the TiO2 electrodes.

Platinum catalyst coating of the counter-electrode

The platinization of the counter-electrode followed the "thermal cluster catalyst" procedure reported by Papageorgiou et al. (1997). About 5 mM $PtCl_4$ (Aldrich 206113) was dissolved in isopropanol (Merck P156) to prepare a platinum solution. One to two drops of the platinum solution were dropped onto a TCO coated glass plate and let to cover the surface and finally evaporate to air. The coated plates were then fired in the convection oven at about 385 °C for about 15 minutes. After the firing small black spots with varying size were visible on the glass, possibly indicating formation of platinum black aggregates. Sometimes the spots seemed to have concentrated to the area, typically one side or corner of the glass plate, from where the very last amounts of platinum solution had evaporated away. Perhaps

surface tension was keeping the platinum particles to some extent inside the evaporating and receding sheet of solution.

Staining the TiO_2 electrodes with the N3 dye

For the sensitization of the sintered TiO_2 electrodes the N3 dye, *cis*-bis(isothiocyanato)bis(2,2'-bipyridyl-4,4'-dicarboxylato)-ruthenium(II) (product name Ruthenium 535), from Solaronix SA was used. A dye solution was prepared by dissolving $3 \cdot 10^{-4}$ M of the dye in pure ethanol (>96%). The result was a dark purple solution, which was stored in a non-transparent bottle.

The staining of the TiO_2 electrodes were performed by heating the electrodes to about 70 °C with a hot air gun and immersed immediately into the room temperature dye solution. This was done in order to remove any water possibly deposited from the ambient air to the TiO_2 film. Alternatively, the electrodes were immersed to the dye solution directly after the sintering process, when the electrodes were still warm. In the latter case a few small bubbles were sometimes seen on the glass surface indicating that the temperature of the electrodes had been somewhat above the boiling point of dye solution (79 °C for ethanol).

The TiO_2 electrodes were kept in the dye solution in the dark to the next day, which rendered the electrodes purple red. At this point, undesired variations in the thickness of the TiO_2 layer could be easily seen as areas darker or lighter than the rest of the film. The stained electrodes were stored in the dark under ethanol in a closed bottle until being used to assemble the cell.

Assembling the cell

The stained TiO_2 electrode and the platinum catalyst coated counter-electrode were washed in ethanol and let to dry in air. For the sealing of the cell, strips were cut from 65 μm thick film of DuPont Surlyn® 1702[36], washed in isopropanol and de-ionized water and pressed dry with paper. The Surlyn® strips were placed around the stained TiO_2 electrode leaving small channels to the opposite sides of the cell for filling the cell with electrolyte, and the counter-electrode was placed on the top of this. The cell was then firmly pressed together with paper clamps and heated in air stream of a hot air gun to over 82 °C for the Surlyn® to melt and adhere to the glass substrates. Melting of the Surlyn® film could be observed both visually through the glass and by toughing any excess film on the edges of the cell. The melted Surlyn® 1702 is highly viscous at least in normal sealing temperatures and does not spread

[36] DuPont Sverige AB kindly donated the samples of Surlyn® for this work.

much between the glass plates even under the pressure of the paper clamps, yet it adheres well to the glass substrates and is thus ideal for precise cell sealing. When cooled down, the Surlyn® edge sealing was ready.

The electrolyte, Iodolyte TG-50 purchased from Solaronix SA and used as received, was applied to the cell from one of the two holes in the Surlyn® gasket. The electrolyte filled the space between the electrodes by capillary action and pushed the air out through the opposite hole. Due to the capillary action the electrolyte was kept in all positions well inside the cell in the thin gap between the electrodes.

Any excess electrolyte was removed from the edges of the cell and from the vicinity of the filling ports with a paper and a lint-free clothe dampened with acetone. And finally, the filling ports were sealed with a two component sealant glue Amosil 4 (Solaronix SA, used as received), which were let to dry in room temperature for about 24 hours, after which the cell was completely sealed and ready for measurements.

Figure 25 shows a picture of a sealed test cell. The cell has a nanostructured electrode with two layers of Ti-Nanoxide T separately deposited and sintered on top of each other. Cells with a single tape cast TiO_2 layer were more transparent than those with double TiO_2 layer, implying that the dye could adsorb also to the underlying TiO_2 layer. As seen in the picture, bubbles of air get easily trapped in the corners of the gasket, which however, according to the information given by Solaronix (2000), should not affect the performance of the cell.

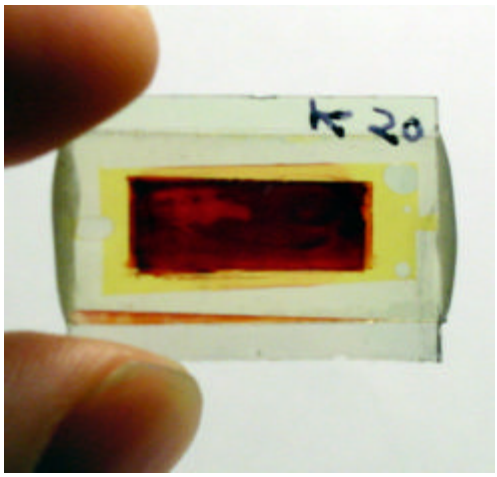

Figure 25. A N3 dye-sensitized solar cell with an electrode area of 0.6 $\times$ 1.6 cm^2 prepared using ITO coated glass substrates, Ti-Nanoxide T as the TiO_2 paste deposited in two overlapping layers by tape casting, Iodolyte TG-50 as the electrolyte, Ruthenium 535 (N3 dye) as the sensitizer dye and Surlyn® 1702 and Amosil 4 as the sealants.

7.2.2 Testing the dye solar cells

The performance (efficiency and I-V curve) of a solar cell depends on the spectral distribution ($Wm^{-2}\mu m^{-1}$) and total irradiance power (Wm^{-2}) of the illumination, as well as on the environmental conditions (first of all on the temperature). To obtain comparable and reliable performance data the solar cells are usually measured in research laboratories at standard conditions with solar simulators imitating the standard solar spectrum. For the present study, a commercial solar simulator was not available in the laboratory. On the other hand, because of the preliminary nature of the experiments, exact imitation of the standard solar spectrum and standard conditions in the measurements was not given the highest priority. Instead, the effort was concentrated to the preparation of the solar cells in order to gather valuable experience, and it was decided to postpone the building of an advanced experimental instrumentation to the stage when dye solar cells with of an acceptable quality and performance could be routinely made.

The test equipment used for the measurements reported in this work, included an overhead projector[37] as the light source, LI-1800 portable spectroradiometer (LI-COR Inc.) with a cosine light receptor for spectral irradiance measurements in the range 300-1100 nm. HP 34970 Data Acquisition/Switch Unit using HP 34901A 20-Channel Multiplexer and a manual variable load connected in series with the cell was used for measuring the I-V curves. At the measurements the cells were placed on top of the spectroradiometer, which ensured same distance between the lamp and the cell, as was between the lamp and the light receptor of the spectrophotometer at the irradiance measurements.

Figure 26 shows the spectral irradiance ($Wm^{-2}\mu m^{-1}$) of the projector lamp measured with the spectrophotometer as well as the AM1.5 (1000 Wm^{-2}) global spectrum in the same units and a typical spectral response (IPCE) curve of a N3 dye-sensitized solar cell in arbitrary units for comparison. From the figure it can be seen that the spectral profile of the projector lamp light is not even close to that of AM1.5 spectrum, but yet has a reasonable spectral power content in the active range of a typical N3 dye-sensitized solar cell, and thus can be used to activate the cells for the I-V characterization.

Heating of the cells was observed during the measurements under the intense illumination. To decrease the infrared content of the light a TCO coated glass plate

[37] the type of where light is directed downwards towards a mirror level for the slides

(same material as used for the cells) was placed in front of the cells. As seen in Figure 26 this shaped the spectral irradiance at 300-1100 nm a little.

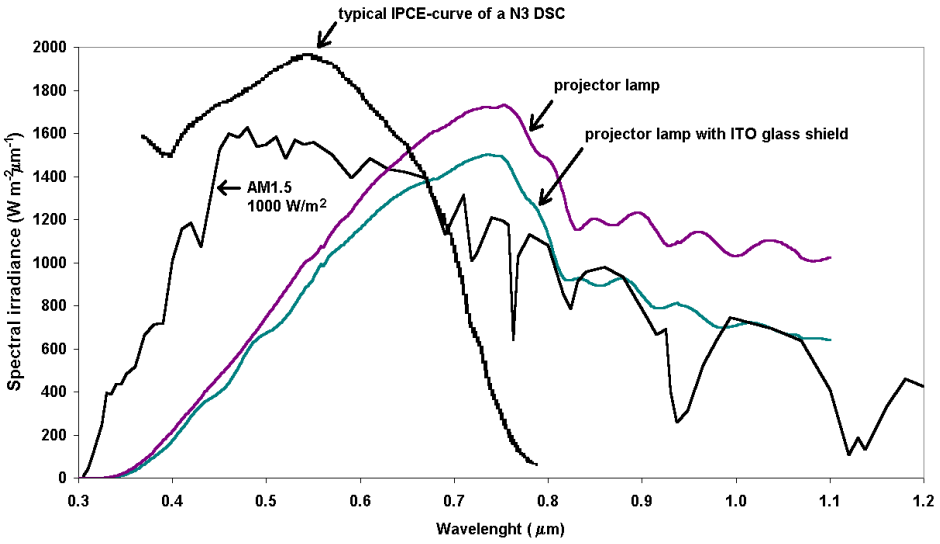

Figure 26. Spectral irradiance ($Wm^{-2}\mu m^{-1}$) of the projector lamp compared with the Air Mass (AM) 1.5 global spectrum with total energy content of $1000W/m^2$ (source: http://www.pv.unsw.edu.au/am1.5.html). Also a typical incident photon to current efficiency (IPCE) curve of a N3 dye-sensitized solar cell (source: http://dcwww.epfl.ch/icp/ICP-2/solarcellE.html) is shown in arbitrary units to indicate the effective spectral operating region of the measured dye solar cells.

To calculate a nominal efficiency value for the cells in these measurements, the measured spectral irradiance (Figure 26) was integrated over the 300-1100 nm range to yield a nominal input light power value (W/m^2) for the cells. The maximum power from the I-V curve (MPP) was then divided with this input light power to yield the efficiency. This efficiency value was naturally not a true sunlight to electricity conversion efficiency of the cells, since the irradiance above 1100 nm was missed by the spectrophotometer, and the spectrum of the projector lamplight differed from the solar spectrum. Instead it served only as a characteristic for mutual comparison of the individual cells.

Examples of measured I-V curves of experimental N3 dye-sensitized solar cells are shown in Figure 27. The maximum efficiency that was reached was 1.4% as calculated for the shielded projector lamp illumination in 300-1100 nm.

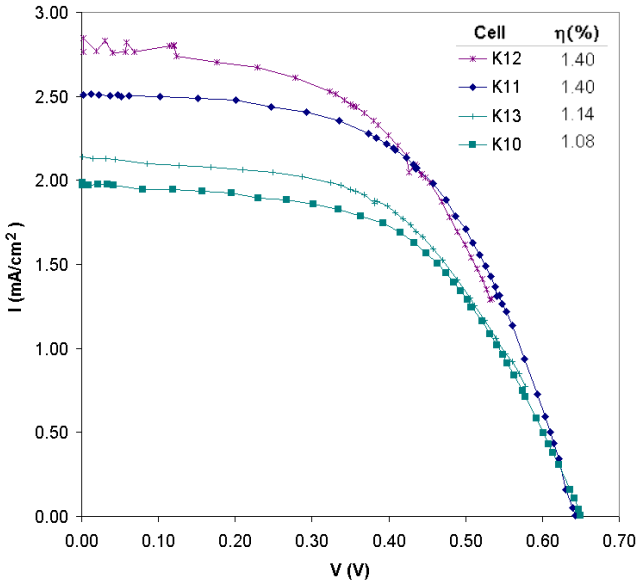

Figure 27. Current-Voltage (I-V) curves of experimental N3 dye-sensitized solar cells measured under projector lamp illumination directly after the assembly of the cells. The cells were sealed with a Surlyn® gasket, but the electrolyte filling ports were let open. The efficiencies in the inset were calculated using the integrated spectral irradiance (300-1100 nm) measured with a spectroradiometer (with shielding ITO glass).

To obtain a more realistic efficiency for the cells, outdoor measurements were performed. In this case the solar irradiance on horizontal plane was continuously monitored with a Kipp&Zonen CM11 pyranometer while measuring the I-V curves of the cells placed on a horizontal surface leveled with a bubble level.

The results of the outdoor measurements are shown in Figure 28. Highest efficiencies obtained were about 0.6%. All the measured cells were completely sealed with Surlyn® gasket and Amosil 4 glue. The time between the assembly and the outdoor measurement of the cell was one day for the cells K19 and K20, eight days for the cells K14 and K15, and 19 days for the cell K7, and 20 days for the cell K6.

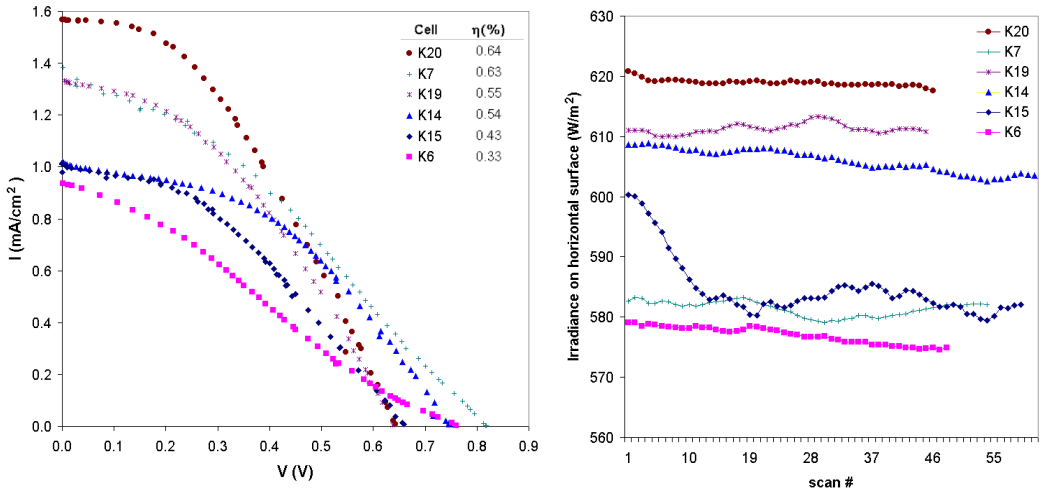

Figure 28. Left picture: Current-Voltage (I-V) curves of experimental N3 dye-sensitized solar cells measured in clear daylight at 29.8.2001 on the roof of the HUT physics department (the labels in the inset are in order of decreasing I_{SC}). Right picture: The global irradiance on horizontal surface measured with Kipp&Zonen CM11 pyranometer for each point in the I-V curves. As can be seen, the irradiance on the horizontal surface staid relatively constant during the measurements with only slight decrease due to descending sun and a thin cloud passing the sun during the measurement of the cell K15. For the efficiency calculations the measured irradiance was averaged over each cell measurement period.

7.3 Discussion and conclusions from the cell preparation

Fully sealed dye-sensitized solar cells using the N3 dye impregnated nanostructured TiO_2 electrodes was successfully prepared. The measured sunlight to electricity conversion efficiencies were however quite low compared to the published efficiencies obtained with similar materials and methods. On the other hand, no systematic optimization of the cell preparation or the cell material properties was done in this work, and mostly materials purchased from Solaronix SA were used.

According to the information given by Solaronix (2000) a single deposition of Ti-Nanoxide T by tape casting with a single strip of Scotch Magic ™tape gives 2-3 µm thick TiO_2 layers, and in order to achieve an electrode thickness of about 8 µm, two layers of tape are required. Cells with fully dye impregnated 8-10 µm thick TiO_2 electrodes are said to be able to produce short circuit currents between 8 to 12 mA/m^2 at full (1000 W/m^2) light (Solaronix 2000), while thickness as high as 14 µm may be needed to optimize the light collection in the dyed TiO_2 electrode (Meyer et al. 2001). In this work, some test cells with double tape cast TiO_2 layers were prepared (cells K14, K15, K19, and K20 in Figure 28), yet no improvement of the low photocurrents was observed. On the other hand, the typical open circuit voltage

of cells prepared from these materials is between 0.6V to 0.7V according to the information by Solaronix (2000). Values in this range were routinely obtained in the tested cells.

Several reasons for the low performance of the test cells are possible:

1. While most of the key components of the cell were purchased from Solaronix SA (dye, TiO_2 paste, electrolyte, sealant glue) and used as received, the platinum catalyst coating of the counter-electrode was made in the laboratory according to method reported in literature (Papageorgiou et al. 1997). The performance of the deposited catalyst was not confirmed by electrochemical measurements. These measurements should be performed to see whether low catalytic activity of the counter-electrode was limiting the cell efficiencies.
2. Sealing the cell with the Surlyn® strips was done by heating the assembled cell above 82 °C. Partial dye degradation may have occurred during this step, for example due to combined effect of water residues and elevated temperature. This effect can be studied by omitting the sealing step and assembling and measuring the cells as soon as possible after removing the TiO_2 electrode from the dye solution.
3. Despite the fact that the cell preparation in principle does not need clean room conditions and can be performed in an ordinary chemistry laboratory under ambient conditions, the effect of impurities cannot be totally cancelled out here. More attention is perhaps needed to exclude any unwanted substances and dust particles during the preparation.

It is apparent that a more systematic approach to the dye cell preparation is needed in the future. Variation of the properties of the cell components such as the electrolyte composition, counter-electrode catalyst, TiO_2 paste composition and morphology of the nanostructured TiO_2 electrode, together with physical and chemical characterization of the essential performance related properties of these components is a long way to go.

Despite the fact that the obtained solar cell efficiencies were quite low the manufacturing of the DSSCs in the quite simple laboratory conditions was found to be feasible. In fact the author believes that significant improvement of the cell efficiencies should be achievable by means of more careful cell preparation and re-evaluation of the used materials and methods.

8 Summary

Photovoltaics is a rapidly growing renewable energy technology today. The market growth has been between 15% and 20% in the last decade and the production of PV panels has exceeded 280 MW per year. Despite the development of materials and manufacturing methods over decades strongly assisted by the growth of the semiconductor industry, the cost of the solar cells has remained high.

During the 1990s new photovoltaic materials have been developed, which could enable production of low-cost solar cells in the future. These so-called molecular photovoltaic materials include for example different types of synthetic organic materials and inorganic nanoparticle systems.

The objective of this study was to make a comprehensive literature review on the new molecular solar cells, i.e. the dye-sensitized nanostructured and the organic solar cells and to gather experimental experience on the preparation of the dye-sensitized solar cells in standard laboratory conditions.

In Chapter 2 the general issues of photovoltaic energy conversion were discussed. The world's PV market has been forecasted to surpass 350 MW per year in 2001 with the grid-connected PV systems as the dominant application. Photovoltaics is a viable energy technology: The energy payback time of the present-day grid connected roof-top installations is substantially less than their expected lifetimes, the CO_2 emissions over their life cycle is significantly less than those of fossil fuel power plants, and the technology for recycling the solar cells already exists.

The profitable PV module costs are about US \$3.50/W_p at present. The total cost of grid-connected PV systems being at least twice as much, the PV electricity is generally many times more expensive than electricity produced by other means. The need for the cost reduction of solar cells thus remains as the driving force for the photovoltaic material development. The cost reduction of solar cells could in principle be pursued via two different strategies giving emphasis either to the high cell efficiencies or to the low manufacturing costs, the molecular PV materials discussed in this study belonging in the first place to the latter strategy.

The dominant photovoltaic cell technologies are single-crystal and polycrystalline silicon. Thin film solar cell materials, such as amorphous silicon, CdTe, CIS and thin film silicon are actively developed. From the other conventional photovoltaic cells the III-VI semiconductor cells are generally too expensive for terrestrial applications

and the standard photoelectrochemical solar cells have remained in the laboratory level due to photocorrosion problems.

The standard silicon solar cell is based on a semiconductor pn-junction. In this solar cell the light absorption occurs in the bulk of the semiconductor, charge separation in the internal electric field of the pn-junction and charge collection by transport of electrons and holes through the bulk of the semiconductor to the electrical contacts of the cell.

The dye-sensitized solar cell (DSSC) introduced in Chapter 3 is an electrochemical solar cell. In the DSSC light absorption occurs by dye molecules attached to a nanostructured TiO_2 electrode, charge separation in the TiO_2 - dye interface and charge transport by electron transport in the TiO_2 electrode and ion diffusion in the electrolyte. The operation of the DSSC is closely related to the nanometer scale morphology of the TiO_2 electrode and the molecular nature of the dye - TiO_2 - electrolyte interface.

The standard DSSC technology was introduced in Chapter 4 through a systematic literature review on the materials and essential preparation methods of the cell. The standard DSSC technology is based on a sintered nanostructured TiO_2 electrode deposited by screen printing or tape casting of colloidal TiO_2 solution onto SnO_2:F coated glass, a Ru-based metallo-organic dye, a liquid nitrile-based I^-/I^-_3 redox electrolyte, a thermal platinum catalyst of the counter-electrode and some chemical additives used to improve the cell performance.

The current status and important directions of development of the DSSC technology were reviewed in Chapter 5. The highest reported laboratory scale efficiency in a DSSC is 10.4% obtained with the black dye. Good stability of over thousands of hours has been reported in light soaking experiments for cells using the N3 dye, but stability in elevated temperatures seems to remain as a problem.

Two different cell and module architectures were identified and discussed: the sandwich structure and the monolithic structure. The former is the standard structure used for basic research in laboratories, but has also been demonstrated in DSSC modules with 7.0% efficiency and over 100 cm^2 active area. The geometry of latter structure is adapted from the thin film solar cells and is used to design DSSCs for low power indoor applications.

Transition from the batch process using glass substrates to a continuous process using flexible plastic foils can be seen as an important direction of development for the DSSC technology. With plastic substrates ITO has to be used instead of SnO_2:F

as the TCO material, and the standard sintering and platinization methods has to be replaced by low-temperature processes. As an interesting alternative a unique room temperature pressing technique adapted from the paper industry has been developed in Uppsala University. This method can be considered as the first step towards continuous roll-to-roll processing of DSSCs.

An important direction is also the development of solid state electrolytes. Gelatination of the standard iodide electrolyte seems to be a successful strategy with a 7% cell efficiency recently reached by Toshiba Co. Solid state organic hole conductors is another group of interesting alternatives for the liquid electrolyte but have shown only moderate success in practice thus far.

Research to improve the fundamental photovoltaic processes in the cell by new materials and preparation methods also continues, the control of the phoelectrochemical kinetics by molecular level engineering of the nanocrystal/dye/electrolyte being the most important issue.

The glass-based DSSC technology is on the verge of commercialization by the Australian company Sustainable Technologies International and the manufacturing cost estimates for the technology are close to the projected costs of CdTe and multi-crystalline silicon technologies. The simple manufacturing process and the relatively inexpensive equipment and facilities needed are the main advantages of the DSSCs technology over the other PV technologies.

The purely organic solar cells were discussed individually in Chapter 6. Organic solar cells are based on organic semiconductor materials that have a π-electron orbital configuration resembling the band structure of the inorganic semiconductors. In these materials light absorption generates electron-hole pairs called excitons that can be dissociated at interfaces between materials with different electron affinities and ionization potentials or in an internal electric field introduced by work function difference of the opposite electrodes of the cell. The electrons and holes are then transported to the electrodes in the internal electric field.

Organic solar cell materials include different polymers, dyes, pigments and liquid crystalline materials. Vacuum evaporation of pigments has been the traditional way of preparing organic solar cells, whereas solution processing of dyes and soluble polymers can be considered as a more advantageous method for practice. The organic solar cells can be categorized by their device architecture to have either single layer, bilayer or blend structure. The highest efficiency thus far among organic solar cells, 4.5%, has been reached with a single layer cell using a doped pentacene

crystal, whereas efficiency of 2.5% has been demonstrated with donor-acceptor cell using a blend of semiconducting polymer and fullerene dye.

As a whole, the development of organic PV materials is only at an early stage and no clearly outperforming materials or device concepts have yet emerged. Research efforts are needed to improve the materials' photophysical properties, device physics of the cells and control of the nanometer scale morphology of the donor-acceptor blend materials.

In the experimental part of the study the dye-sensitization effect was demonstrated with a DSSC using a natural dye from raspberries. After this a series of Ru-dye based DSSCs were successfully prepared and characterized by current - voltage measurements. Energy conversion efficiency of 0.6% at about 600 W/m^2 solar illumination was obtained in outdoor measurements without optimization of the materials and methods.

The new molecular PV materials can be considered as interesting future alternatives for the conventional PV materials. Incorporation of these materials with existing large scale manufacturing processes could open new directions for the development of low-cost solar cells in the future.

9 Suggestions for further research

The research of dye-sensitized solar cells has concentrated almost exclusively to the glass substrate based technology, which has already been pushed close to commercialization. Also the basic research of physical and chemical phenomena in the DSSC has been done using the standard glass based cells. A sidetrack from the mainstream would therefore be a study of DSSCs on plastic or metal foil substrates. An interesting topic would be for example examination of the suitability of different manufacturing methods for the preparation of the nanostructured TiO_2 electrodes onto plastic sheets concentrating on the study of mechanical and electrical properties of the interface between the TiO_2 film and the ITO coated plastic sheet.

The dye-sensitized solar cell research is quite interdisciplinary involving different areas of expertise such as photoelectrochemistry, electrochemistry of the electrolytes and catalysts, electroanalytical chemistry, quantum chemistry, colloid science, semiconductor physics, laser spectroscopy, synthetic organic chemistry, computational modeling etc. A combination of researchers with a background in different areas is evidently needed for a successful basic research with the DSSCs.

The ease of manufacturing dye cells in basic laboratory conditions should however enable successful work also in a smaller research group, if the research problems were selected with care and close collaboration with other research groups were established. While the major part of the DSSC research involves different areas of electrochemistry, special topics with an emphasis in physics could be for example the semiconductor properties of the TiO_2 electrodes and especially the role of surface traps in the processes at the TiO_2 / dye / electrolyte, the electron transport in the TiO_2 electrode and the electrical properties of the TiO_2 / TCO interface.

In this work the first steps were taken in manufacturing DSSCs in the laboratory. The work should be continued by a re-evaluation of the used materials and methods and with a systematic progression to raise the efficiency of the cells. The thickness of the TiO_2 film is an essential parameter in the cell. The transparency of the dyed film can be adjusted and evidently the efficiency of the cell optimized by changing the film thickness. This is however difficult with the tape casting method because not only the thickness of the framing tape and the concentration of the TiO_2 solution but also the speed of the glass rod is likely to affect the obtained film thickness. A screen printing machine is therefore essential for the systematic optimization of the TiO_2 film thickness.

Also an adequate solar simulator should be built or purchased for the current - voltage characterization of the cells. For routine comparative measurements of sample cells the quality of the lamp spectrum is not the most important question and for example the standard projector lamp used in this study would do, but the measurement system should be designed for fast measuring and repeatable results.

The acquirement of other measurement equipment should of course be decided on the basis the research problem and the availability of suitable equipment in the co-operating laboratories.

10 Bibliography

Alonso, M., Finn, E. J., 1968, Fundamental University Physics, Volume III, Quantum and Statistical Physics, Addison-Wesley

Alsema, E. A., Nieuwlaar, E., 2000a, Energy viability of photovoltaic systems, Energy Policy, 28, 14, 999-1010

Bach U., et al., 1998, Solid-state dye-sensitized mesoporous TiO_2 solar cells with high photon-to-electron conversion efficiencies, Nature, 395, 8 October

Barbé, C. J., et al., 1997, Nanocrystalline Titanium Oxide Electrodes for Photovoltaic Applications, J. Am. Ceram. Soc., 80, 12, 3157-71

Bedja I., et al., 1997, Photosensitization of Nanocrystalline ZnO Films by Bis(2,2'-bipyridine)(2,2'-bipyridine-4,4'-dicarboxylic acid)ruthenium(II), Langmuir, 13, 2398-2403

Bossert, R.H., et al., 2000, Thin-film Solar Cells, Technology Evaluation and Perspectives, Novem

Brabec, C. J., et al., 1999, Realization of Large Area Flexible Fullerene - Conjugated Polymer Photocells: A Route to Plastic Solar Cells, Synth. Met., 102, 861-864

Brabec, C. J., Sariciftci, S. N., 2001a, Recent Developments in Conjugated Polymer Based Plastic Solar Cells, Monatshefte für Chemie, 132, 421-31

Brabec, et al., 2001b, Plastic Solar Cells, Adv. Funct. Mater., 11, 1, 15-26

Brabec, C. J., Sariciftci, S. N., 2001c, Conjugated Polymer Based Plastic Solar Cells, in: Semiconducting Polymers, ed. Hadziioannou, G., van Hutten, P. F., WILEY-VHC Verlag Gmbh, D-69469 Weinheim (Federal Republic of Germany)

Burnside S. D., et al., 1998, Self-Organization of TiO_2 Nanoparticles in Thins Films, Chem. Mater., 10, 2419-2425

Burnside S. D., et al., 2000, Deposition and characterization of screen-printed porous multi-layer thick film structures from semiconducting and conducting nanomaterials for use in photovoltaic devices, J. Mater. Sci.: Mater. Electron., 11, 355-362

Cahen D., et al., 2000, Nature of Photovoltaic Action in Dye-Sensitized Solar Cells, J. Phys. Chem. B, 104, 2053-2059

Cao, F., et al., 1995, A Solid State, Dye Sensitized Photoelectrochemical Cell, J. Phys. Chem., 99, 17071-3

Chang, S., et al., 1999, Multicolor Organic Light-Emitting Diodes, Adv. Mater., 11, 9, 734-7

Chen, L., et al., 2000, Polymer Photovoltaic Devices from Stratified Multilayers of Donor-Acceptor Blends, Adv. Mater., 12, 18, 1367-70

Cherepy, N. J., et al., 1997, Ultrafast Electron Injection: Implications for a Photoelectrochemical Cell Utilizing an Anthocyanin Dye-Sensitized TiO_2 Nanocrystalline Electrode, J. Phys. Chem B, 101, 9342-9351

Chmiel, G., et al., 1998, Dye sensitized solar cells (DSC): Progress towards application, 2nd World Conference and Exhibition on Photovoltaic Solar Energy Conversion, 6-10 July Vienna Austria

Deb, S. K., et al., 1998, Photochemical Solar Cells Based on Dye-Sensitization of Nanocrystalline TiO_2, National Energy Laboratory, Presented at the 2nd World Conference and Exhibition on Photovoltaic Solar Energy Conversion; 6-10 July 1998, Austria, NREL/CP-590-250-25056

Durstock, M. F., et al. 2001, Electrostatic self-assembly as a means to create organic photovoltaic devices, Synthetic Metals, 116, 373-377

Ferber, J., et al., 1998, An electric model of the dye-sensitized solar cell, Solar Energy Materials and Solar Cells, 53, 29-54

Ferber, J., et al., 2000, Investigation of the long-term stability of dye-sensitized solar cells, Proceedings of the 12th Workshop on Quantum Solar Energy Conversion - (QUANTSOL 2000), March 11-18, 2000, Wolkenstein, Südtirol, Italy

Ferrere, S., Gregg, B. A., 2001, Large Increases in Photocurrents and Solar Conversion Efficiencies by UV Illumination of Dye Sensitized Solar Cells J. Phys. Chem. B, 105, 7602-7605 (*)

Frantzis, L., et. al., 2000, Opportunities for Cost Reductions in Photovoltaic Modules, 16th European Photovoltaic Solar Energy Conference, 1-5 May, Glasgow, UK

Fthenakis, V. M., 2000, End-of-life management and recycling of PV modules, Energy Policy, 28, 14, 1051-1058

Fungo, F., et al., 2000, Photosensitization of Thin SnO_2 Nanocrystalline Semiconductor Film Electrodes with Metallodiporphyrin, J. Phys. Chem. B, 104, 7644-51

Gebeyehu, D., et al., 2001, The interplay of efficiency and morphology in photovoltaic devices based on interpenetrating networks of conjugated polymers with fullerenes, Synthetic Metals, 118, 1-9

Gómez M., et al., 1999, Photoelectrochemical studies of dye-sensitized polycrystalline titanium oxide thin films prepared by sputtering, Thin Solid Films, 342, 148-152

Gómez, M. M., et al., 2000, High efficiency dye-sensitized nanocrystalline solar cells based on sputter deposited Ti oxide films, Solar Energy Materials & Solar Cells, 64, 385-392

Goetzberger, A., Hebling, C., 2000, Photovoltaic materials, past, present, future, Solar Energy Materials & Solar Cells, 62, 1-19

Gordon, R. G., 2000, Criteria for Choosing Transparent Conductors, MRS Bulletin, Aug., 52-57

Gorman, J., 2001, New method light path for solar cells, Science News, Vol 160, August 11

Granström M., et al., 1998, Laminated fabrication of polymeric photovoltaic diodes, Nature, 395, 17 September, 257-260

Green, M. A., 1982, Solar Cells, Operating Principles, Technology, and System Applications, Englewood Cliffs, N.J., Prentice-Hall, Inc., 276 s., ISBN 0-13-822270-3

Green, M. A., 2000a, Photovoltaics: technology overview, Energy Policy, 28, 14, 989-998

Green, M. A., 2000b, The future of crystalline silicon solar cells, Prog. Photovolt. Res. & Appl., 8, 1, 127-139

Green, M. A., 2001, Solar Cell Efficiency Tables (Version 18), Prog. Photovolt. Res. Appl., 9, 287-93

Greijer, H., et al., 2001, Resonance Raman Scattering of Dye-Sensitized Solar Cell: Mechanism of Thiocyanato Ligand Exchange, J. Phys. Chem B, 105, 6314-20

Grünwald R., Tributsch H., 1997, Mechanism of Instability in Ru-Based Sensitization Solar Cells, J. Phys. Chem. B, 101, 2564-2575

Grätzel M., 1994, Highly Efficient Nanocrystalline Photovoltaic Devices, Platinum Metals Rev., 38, 4, 151-159

Grätzel M., 2000, Perspectives for Dye-sensitized Nanocrystalline Solar Cells, Prog. Photovolt. Res. Appl. 8, 171-185

Guha, S., et. al., 2000, Amorphous silicon alloy photovoltic research – present and future, Prog. Photovolt. Res. & Appl., 8, 1, 141-150

Gutschner, M., Nowak, S., 2001, Potential and implementation of building-integrated photovoltaics on the local level - case studies and comparison of urban and rural areas in Switzerland, 16th European Photovoltaic Solar Energy Conference, 1-5- May, Glasgow, UK

Hagfeldt A., et al., 1994, Verification of high efficiencies for the Grätzel-cell. A 7% efficient solar cell based on dye-sensitized colloidal TiO_2 films, Solar Energy Materials & Solar Cells, 31, 481-488

Hagfeldt A., Grätzel M., 1995, Light-Induced Redox Reactions in Nanocrystalline Systems, Chem. Rev., 95, 49-68

Hagfeldt A., Grätzel M., 2000, Molecular Photovoltaics, Acc. Chem. Res., 33, 5, 269-277

Hague S. A., et al., 1998, Charge Recombination Kinetics in Dye-Sensitized Nanocrystalline Titanium Dioxide Films under Externally Applied Bias, J. Phys. Chem. B, 102, 1745-1749

Halls J.J.M., et al., 1995, Efficient photodiodes from interpenetrating polymer networks, Nature, 376, 10 August, 498-500

Hanke, K. P., 1999, Upscaling of the Dye Sensitized Solar Cell, Zeitschrift für Physikalische Chemie, 212, 1, 1-9

Hara, K., et al., 2000a, Highly efficient photon-to-electron conversion with mercurochrome-sensitized nanoporous oxide semiconductor solar cells, Solar Energy Materials & Solar Cells, 64, 115-134

Hara, K., et al., 2000b, Semiconductor-sensitized solar cells based on nanocrystalline In_2S_3/In_2O_3 thin film electrodes, Solar Energy Materials & Solar Cells, 62, 441-447

Hara, K., et al., 2001a, A coumarin-derivative dye sensitized nanocrystalline TiO_2 solar cell having a high solar-energy conversion efficiency up to 5,6%, Chem. Commun., 569-70

Hara, K., et al., 2001b, Influence of electrolytes on the photovoltaic performance of organic dye-sensitized nanocrystalline TiO_2 solar cells, Solar Energy Materials & Solar Cells, 70, 151-161

He, J., et al., 2000, Dye-sensitized nanostructured tandem cell – first demonstrated cell with a dye-sensitized photocathode, Solar Energy Materials & Solar Cells, 62, 265-273

Hinsch A., et al., 1998, The performance of dye-sensitized solar cells with a one-facial, monolithic layer built-up prepared by screen printing, 2nd World Conference and Exhibition on Photovoltaic Solar Energy Conversion, 6-10 July Vienna Austria

Hinsch A., et al., 2000, Long-term stability of dye sensitized solar cells for large area power applications (LOTS-DSC), 16th European Photovoltaic Solar Energy Conference and Exhibition, Glasgow 2000

Hinsch A., et al., 2001a, Long-term stability of dye sensitized solar cells, Prog. Photovolt: Res. Appl., 9, 425-38

Hinsch A., et. al., 2001b, Long-term stability and efficiency of dye-sensitized solar cells, ECN report [ECN-RX--01-020], ftp://ftp.ecn.nl/pub/www/library/report/2001/rx01020.pdf, available on 11.1.2001

Hiramoto, M., et al., 1991, Three-layered organic solar cell with a photoactive interlayer of codeposited pigments, Appl. Phys. Lett., 58, 10, 1062-1064

Hodes G., et al., 1992, Nanocrystalline Photoelectrochemical Cells; A New Concept In Photovoltaic Cells, J. Electrochem. Soc., 139, 11, 3136-3140

Huang S. Y., et al., 1997, Charge Recombination in Dye-Sensitized Nanocrystalline TiO_2 Solar Cells, J. Phys. Chem. B, 101, 2576-2582

Jenekhe S. A., Yi, S., 2000, Efficient photovoltaic cells from semiconducting polymer heterojunctions, Appl. Phys. Lett., 77, 17, 2635-7

Kallioinen, J., et. al., 2001, Transient absorption studies of the $Ru(dcbpy)_2(NCS)_2$ excited state and the dye cation on nanocrystalline TiO_2 film, Chemical Physics Letters, 340, 217-21

Kalyanasundaram, K., Grätzel, M., 1998, Applications of functionalized transition metal complexes in photonic and optoelectronic devices, Coordination Chemistry Reviews, 177, 347-414

Kavan, L., et al., 1993, Preparation of TiO_2 (anatase) films on electrodes by anodic oxidative hydrolysis of $TiCl_3$, J. Electroanal. Chem., 346, 291-307

Kay A., Grätzel M., 1993, Artificial Photosynthesis. 1. Photosensitization of TiO_2 Solar Cells with Chlorophyll Derivatives and Related Natural Porphyrins, J. Phys. Chem., 97, 6272-6277

Kay, A., Grätzel, M., 1996, Low cost photovoltaic modules based on dye sensitized nanocrystalline titanium dioxide and carbon powder, Solar Energy Materials & Solar Cells, 44, 99-117

Kazmerski, L. L., 1997, Photovoltaics: A review of cell and module technologies, Renewable and Sustainable Energy Reviews, 1, 1, 71-170

Kohle, et al., 1997, The Photovoltaic Stability of Bis(isothiocyanato)ruthenium(II)-bis-2,2´-bipyridine-4,4´-dicarboxylic Acid and Related Sensitizers, Adv. Mater., 9, 11, 904-6

Krüger, J., et al., 2001, High efficiency solid-state photovoltaic device due to inhibition of interface charge recombination, Appl. Phys. Lett., 79, 13, 2085-7

Kubo, W., et al., 1998, Fabrication of Quasi-sold-state Dye-sensitized TiO_2 Solar Cells Using Low Molecular Weight Gelators, Chemistry Letters, 1241-2

Kubo, W., et al., 2001, Quasi-Solid-State Dye-Sensitized TiO2 Solar Cells: Effective Charge Transport in Mesoporous Space Filled with Gel Electrolytes Containing Iodide and Iodine, J. Phys. Chem. B, 105, 51, 12809-12815.

Lee, S., et al., 2001, Modification of electrodes in nanocrystalline dye-sensitised TiO_2 solar cells, Solar Energy Materials and Solar Cells, 65, 193-200

Levine, I. N., 1978, Physical Chemistry, International student edition, McGraw-Hill, ISBN 0-07-066388-2

Li, Y., et al., 1999, Titanium dioxide films for photovoltaic cells derived from a sol-gel process, Solar Energy Materials & Solar Cells, 56, 167-174

Lindström H., et al., 2001a, A New Method for Manufacturing Nanostructured Electrodes on Plastic Substrates, Nano Letters, 1, 2, 97-100

Lindström, H., et al., 2001b, A new method to make dye-sensitized nanocrystalline solar cells at room temperature, J. Photochem. Photobiol., A, 145(1-2), 107-112

Little, R. G., Nowlan, M. J., 1997, Crystalline Silicon Photovoltaics: The Hurdle for Thin Films, Prog. Photovolt. Res. Appl., 5, 309-15

Macht, B., et al., 2001, Patterns of efficiency and degradation in dye sensitized solar cells measured with imaging techniques, Solar Energy Materials and Solar Cells, in press, available on-line via ScienceDirect®, Elsevier Science

Matsumoto, M., et al., 1996, A dye sensitized TiO_2 photoelectrochemical cell constructed with polymer solid electrolyte, Solid State Ionics, 89, 3-4, 263-7

Matthews, D., et al., 1996, Calculation of the photocurrent-potential characteristic for regenerative, sensitized semiconductor electrodes, Solar Energy Materials & Solar Cells, 44, 119-155

Maycock P., 2000, The World PV market 2000: shifting from subsidy to 'fully economic'?, Renewable Energy World, 3, 4, Jul-Aug., 59-74

McEvoy, A. J., Grätzel, M., 1994, Sensitization in photochemistry and photovoltaics, Solar Energy Materials & Solar Cells, 32, 3, 221-227

McEvoy, A. J., et al., 1998, Dye-sensitized nanocrystalline semiconductor photovoltaic devices, 2nd World Conference and Exhibition on Photovoltaic Solar Energy Conversion, 6-10 July Vienna Austria

Meissner, D., 1999, Solar Technology - Photoelectrochemical Solar Energy Conversion, Ullmann's Encyclopedia of Industrial Chemistry, Sixth Edition, Electronic Release

Meissner, D., Rostalski, J., 2000, Highly efficient molecular organic solar cells, Proceedings of the 16th European photovoltaic solar energy conference, Glasgow

Meyer, T., 1996, Solid state nanocrystalline titanium oxide photovoltaic cells, Thèse N° 1542, École Polytechnique Fédérale de Lausanne

Meyer, T. B., et al., 2001, Recent Development in Dye-Sensitized Solar Cell Technology, Proceedings of SPIE, 4108, Organic Photovoltaics, 8-16

Mikoshiba, S., et al., 2000, Highly efficient photoelectrochemical cell with novel polymer gel electrolytes, 16th European Photovoltaic Solar Energy Conference, 1-5 May Glasgow UK

Motiva, 2001, http://www.motiva.fi/tietopankki/asuminen/asu-kul-sahko.html, available on 16.12.2001

Murakoshi, K., et al., 1998, Fabrication of solid-state dye-sensitized TiO_2 solar cells combined with polypyrrole, Solar Energy Materials & Solar Cells, 55, 113-125

Nazeeruddin M. K., et al., 1993, Conversion of Light to Electricity by cis-X_2Bis(2,2'-bipyridyl-4,4'-dicarboxylate)ruthenium(II) Charge-Transfer Sensitizers (X = Cl^-, Br^-, I^-, CN^- and SCN^-) on Nanocrystalline TiO_2 Electrodes, J. Am. Chem. Soc., 115, 6382-6390

Nazeeruddin M.K., et al., 1997, Efficient panchromatic sensitization of nanocrystalline TiO_2 films by a black dye based on a trithiocyanato-ruthenium complex, Chem. Comm., 1705

Nelson, J., 2001, Solar Cells by Self-Assembly?, Science, VOL 293, 10 August, 1059-60

Neugebauer, H., et al., 2000, Stability and photodegradation mechanisms of conjugated polymer/fullerene plastic solar cells, Solar Energy Materials & Solar Cells, 61, 35-42

Nogueira, A. F., De Paoli, M.-A.,2000, A dye sensitized TiO_2 photovoltaic cell constructed with an elastomeric electrolyte, Solar Energy Materials & Solar Cells, 61, 135-41

Okuya, M., et al., 2001, Porous TiO_2 thin films synthesized by a spray pyrolysis deposition (SPD) technique and their application to dye-sensitized solar cells, Solar Energy Materials & Solar Cells, 70, 4, 425-35

Oliver, M., Jackson, T., 2000, The evolution of economic and environmental cost for crystalline silicon photovoltaics, Energy Policy, 28, 14, 1011-1021

Olsen, E., et al., 2000, Dissolution of platinum in methoxy propionitrile containing Li/I_2, Solar Energy Materials and Solar Cells, 63, 267-273

O'Regan B., Grätzel M., 1991, A low cost high-efficiency solar cell based on dye-sensitized colloidal TiO_2 films, Nature, 353, 24 October, 737-740

O'Regan B., et al., 2000, Electrodeposited Nanocomposite n-p Heterojunctions for Solid-State Dye-Sensitized Photovoltaics, Adv. Mater., 12, 17, 1263-7

Papageorgiou, N., et al., 1996, The Performance and Stability of Ambient Temperature Molten Slats for Solar Cell Applications, J. Electrochem. Soc., 143, 10, 3099-3108

Papageorgiou, N., et al., 1997, An Iodine/Triiodide reduction Electrocatalyst for Aqueous and Organic Media, J. Electrochem. Soc., 144, 3, 876-84

Park, N.-G., et al., 1999, Dye-Sensitized TiO_2 Solar Cells: Structural and Photoelectrochemical Characterization of Nanocrystalline Electrodes Formed from the Hydrolysis of $TiCl_4$, J. Phys. Chem. B, 103, 3308-14

Park, N.-G., et al., 2000, Comparison of Dye-Sensitized Rutile- and Anatase-Based TiO_2 Solar Cells, J. Phys. Chem. B, 104, 8989-94

Peippo, K., 1992, Aurinkosähköjärjestelmien käytön ja mitoituksen perusteita, NEMO-raportti 23, ISSN 0785-644X, ISNB 951-22-1342-7, Teknillinen korkeakoulu, in Finnish

Petritsch, K., et al., 1999, Liquid Crystalline Phthalocyanines in Organic Solar Cells, Synth. Met., 102, 1776-7

Petritsch, K., et al., 2000a, Dye based donor/acceptor solar cells, Solar Energy Materials & Solar Cells, 61, 63-72

Petritsch, K., 2000b, Organic Solar Cell Architectures, PhD Thesis, Technisch-Naturwissenschaftliche Fakultät der Technischen Universität Graz (Austria)

Pettersson, H., Gruszecki, T., 2001, Long-term stability of low-power dye-sensitised solar cells prepared by industrial methods, Solar Energy Materials & Solar Cells, 70, 203-212

Peumans, P., et al., 2000, Efficient photon harvesting at high optical intensities in ultrathin organic double-heterostructure photovoltaic diodes, Applied Physics Letters, 76, 19, 2650-2

Peumans, P., Forrest, R., 2001, Very-high-efficiency double-heterostructure copper phtalocyanine/C_{60} photovoltaic cells, Appl. Phys. Lett., 79, 1, 126-8

Pichot F., et al., 2000a, Low-Temperature Sintering of TiO_2 Colloids: Application to Flexible Dye-Sensitized Solar Cells, Langmuir, 16, 5626-5630

Pichot, F., Gregg, B. A., 2000b, The Photovoltage-Determining Mechanism in Dye-Sensitized Solar Cells, J. Phys. Chem. B, 104, 6-10

Rensmo H., et al., 1996, Photocurrent Losses in Nanocrystalline/Nanoporous TiO_2 Electrodes Due to Electrochemically Active Species in the Electrolyte, J. Electrochem. Soc., 143, 10, 3173-8

Rensmo H., et al., 1997, High Light-to-Energy Conversion Efficiencies for Solar Cells Based on Nanostructured ZnO Electrodes, J. Phys. Chem. B, 101, 2598-2601

Rijnberg, E., et al., 1998, Long term stability of nanocrystalline dye-sensitized solar cells, 2nd World Conference and Exhibition on Photovoltaic Solar Energy Conversion, 6-10 July Vienna Austria

Rousar, I., et al., 1996, Optimization of parameters of an electrochemical photovoltaic regenerative solar cell, Solar Energy Materials & Solar Cells, 43, 249-262

Sauvé, G., et al., 2000, Dye Sensitization of Nanocrystalline Titanium Dioxide with Osmium and Ruthenium Polypyridyl Complexes, J. Phys. Chem. B, 104, 6821-36

Sayama K., et al., 1998, Photoelectrochemical Properties of a Porous Nb_2O_5 Electrode Sensitized by Ruthenium Dye, Chem. Mater., 10,3825-3832

Schlichthörl, G., et al., 1997, Band Edge Movement and Recombination Kinetics in Dye-Sensitized Nanocrystalline TiO_2 Solar Cells: A Study by Intensity Modulated Photovoltage Spectroscopy, J. Phys. Chem. B, 101, 8141-8155

Schmidt-Mende, L., et al., 2001, Self-Organized Discotic Liquid Crystals for High-Efficiency Organic Photovoltaics, Science, VOL 293, 10 August, 1119-22

Schön, J. H., et al., 2000a, Efficient photovoltaic energy conversion in pentacene-based heterojunctions, Appl. Phys. Lett., 77, 16, 2473-5

Schön, J. H., et al., 2000b, Efficient organic photovoltaic diodes based on doped pentacene, Nature, 403, 27 January, 408-10

Shah, A., et al., 1999, Photovoltaic Technology: The Case for Thin-Film Solar Cells, Science, 30 July, 285, 692-8

Shaheen, S. E., et al., 2001a, 2.5% efficient organic plastic solar cells, Applied Physics Letters, 78, 6, 841-3

Shaheen, S. E., et al., 2001b, Fabrication of bulk heterojunction plastic solar cells by screen printing, Appl. Phys. Lett., 79, 18, 2996-8

Smestad, G., et al., 1994, Testing of dye-sensitized TiO_2 solar cells I: Experimental photocurrent output and conversion efficiencies, Solar Energy Materials & Solar Cells, 32, 3, 259-272

Smestad G. P., Grätzel M., 1998, Demonstrating Electron Transfer and Nanotechnology: A Natural Dye-Sensitized Nanocrystalline Energy Converter, J. Chem. Edu., 75, 6, 752-756

Smestad, G., 1998, Education and solar conversion: Demonstrating electron transfer, Solar Energy Materials and Solar Cells, 55, 1-2, 157-178

SolarAccess, 2001a, PV Research Concentrates on Lowering Cost and Thickness, http://www.solaraccess.com/news/story.jsp?storyid=1032, available on 5.12.2001

SolarAccess, 2001b, Sustainable Technologies to Market Solar Panels in November, http://www.solaraccess.com/news/story.jsp?storyid=905, available on 7.12.2001

SolarAccess, 2001c, 2001 PV Production May Surpass 350 MW, http://www.solaraccess.com/news/story.jsp?storyid=1207, available on 7.12.2001

Solaronix, 2000, Dye Solar Cell Assembly, instructions received from Solaronix SA

Sommeling, P. M., et al., 2000, Flexible dye-sensitized nanocrystalline TiO_2 solar cells, [ECN-RX--00-020], ftp://ftp.ecn.nl/pub/www/library/report/2000/rx00020.pdf, available in 8.10.2001

Soten, I., Ozin, G. A., 1999, New directions in self-assembly: materials synthesis over 'all' length scales, Current Opinion in Colloid & Interface Science, 4, 325-37

Späth, M., et al., 1997, New Concepts of Nano-Crystalline Organic Photovoltaic Devices, ftp://ftp.ecn.nl/pub/www/library/report/1997/rx97060.pdf

Srikanth K., et al., 2001, Investigation of the effect of sol processing parameters on the photoelectrical properties of dye-sensitized TiO_2 solar cells, Solar Energy Materials and Solar Cells, 65, 171-177

Stanley, A., et al., 1998, Minimizing the dark current at the dye-sensitized TiO_2 electrode, Solar Energy Materials & Solar Cells, 52, 141-154

STI, 2001, Sustainable Technologies International, Titania Solar Wall Panel, Draft Specification, Model-DSC 54, September 2001, http://www.sta.com.au/download/swpss09_01.pdf, available on 11.12.2001

Takahashi, K., et al., 2000, Three-layer organic solar cell with high-power conversion efficiency of 3.5%, Solar Energy Materials & Solar Cells, 61, 403-16

Tang, C. W., 1986, Two-layer organic solar cell, Appl. Phys. Lett., 48, 2, 183-5

Tennakone K., et al., 1999, An efficient dye-sensitized photoelectrochemical cell made from oxides of tin and zinc, Chem. Comm., 15-16

Tennakone, K., et al., 2000, Highly stable dye-sensitized solid-state solar cell with the semiconductor 4CuBr $3S(C_4H_9)_2$ as the hole collector, Appl. Phys. Lett., 77, 15, 2367-9

Too et al. , C. O., et al., 2001, Photovoltaic devices based on polythiophenes and substituted polythiophenes, Synthetic Metals, 123, 53-60

Tributsch, H., 2001, Function and analytical formula for nanocrystalline dye-sensitization solar cells, Appl. Phys. A, 73, 305-16

Turrión, M., et al., 1999, Imaging Techniques for the Study of Photodegradation of dye Sensitized Solar Cells, Zeitschrift für Physikalische Chemie, 212, 1, 51-57

UANews, 2001, UA Scientists Are Developing 'Self-Assembling' Solar Cells, http://uanews.opi.arizona.edu/cgi-bin/WebObjects/UANews.woa/wa/SRStoryDetails?ArticleID=4088, available on 5.12.2001

Wallace G.G., et al., 2000, Conjugated polymers: New materials for photovoltaics, chemical innovation, 30, 1, 14-22

Wienke, J., et al., 1997, Effect of TiO_2-electrode properties on the efficiency of nanocrystalline dye-sensitized solar cells (nc-DSC) , ftp://ftp.ecn.nl/pub/www/library/report/1997/rx97033.

Wolfbauer, G., et al., 2001, A channel flow cell system specifically designed to test the efficiency of redox shuttles in dye sensitized solar cells, Solar Energy Materials & Solar Cells, 70, 85-101

Wöhrle, D., et al., 1995, Investigation of n/p-Junction Photovoltaic Cells of Perylenetetracarboxylic Acid Diimides and Phtalocyanines, J. Mater. Chem., 5, 11, 1819-29

Wöhrle, D., Meissner, D., 1991, Organic Solar Cells, Adv. Mater., 3, 3, 129

Yoshino, K., et al., 1997, Novel Photovoltaic Devices Based on Donor-Acceptor Molecular and Conducting Polymer Systems, IEEE Transaction on Electron Devices, 44, 8, 1315-1324

Yu, G., et. al., 1995, Polymer Photovoltaic Cells: Enhanced Efficiencies via a Network of Internal Donor-Acceptor Heterojunctions, Science, 270, 1789-91

Yu, G., Heeger, J., 1995, Charge separation and photovoltaic conversion in polymer composites with internal donor/acceptor heterojunctions, J. Appl. Phys., 78, 7, 4510-5

Yu, G., Heeger, J., 1997, High efficiency photonic devices made with semiconducting polymers, Synthetic Metals, 85, 1183-6

Zaban, A., et al., 1997, Electric Potential Distribution and Short-Range Screening in Nanoporous TiO_2 Electrodes, J. Phys. Chem. B, 101, 7985-90

Zaban, A., Diamant, Y., 2000, Electrochemical Deposition of Organic Semiconductors on High Surface Area Electrodes for Solar Cells, J. Phys. Chem. B, 104, 10043-6

Zweibel, K., 1999, Issues in thin film PV manufacturing cost reduction, Solar Energy Materials & Solar Cells, 59, 1-18

Zweibel, K., 2000, Thin film PV manufacturing: Materials costs and their optimization, Solar Energy Materials & Solar Cells, 63, 375-386